Copyright

by

David T. Lodowski

2004

The Dissertation Committee for David Thomas Lodowski Certifies that this is the approved version of the following dissertation:

Structural Basis for the Regulation of GRK2 by Gβγ

Committee:

John Tesmer, Supervisor

Jon Robertus

John Mihic

Kevin Dalby

Edward Marcotte

Structural Basis for the Regulation of GRK2 by Gβγ

by

David Thomas Lodowski, B.S.

Dissertation

Presented to the Faculty of the Graduate School of

The University of Texas at Austin

in Partial Fulfillment

of the Requirements

for the Degree of

Doctor of Philosophy

The University of Texas at Austin

December, 2004

Dedication

I dedicate this work to:

My parents who always encouraged me in all of my endeavors

and

Kerrie, my wife,
who has been there for me ever since we became friends that first year in grad school.
Her love and encouragement has kept me going through this long process.

Acknowledgements

First and foremost, I would like to thank my supervisor, Dr. John Tesmer for his patience, understanding and the guidance that he has provided me during my work in his laboratory. His assistance and encouragement has helped keep me on task even when there were no crystals.

I would like the members of the lab for assistance they have accorded me, without their assistance I would have never succeeded. I would like to thank Jennifer and Brett for being my cold room crystallization/ protein purification lackeys. I would also like to thank Romana, Jeff, Paul and John for assistance in the collection of data during long nights at the beamline.

I would like to especially thank Dr. Robert Lefkowitz and Darrel Capel for providing me GRK2. Without Dr. Lefkowitz's shipments of GRK2, we would have never had enough protein to solve either structure.

I would also like to thank the members of my committee for their input and assistance in this research.

A special thanks to my family who have always encouraged me in my love of science.

Finally, I would like to thank my wife, Kerrie. Without her love and encouragement none of this would have been possible. I look forward to many happy years together.

Structural Basis for the Regulation of GRK2 by Gβγ

Publication No._____

David Thomas Lodowski, PhD

The University of Texas at Austin, 2004

Supervisor: John J. G. Tesmer

The sensations of sight, smell, and taste as well as the regulation of heart rate, blood pressure, and glucose metabolism are all controlled by a family of proteins known as the heterotrimeric G proteins. The heterotrimeric G proteins are made up of a Gα, and a constitutive dimer of Gβ and Gγ. These heterotrimeric G proteins function to transmit a signal generated by the binding of an agonist (hormone) to a G protein-coupled receptor (GPCR) to G protein effector proteins within the cell. This binding event initiates a structural change within the GPCR which triggers a structural change within the Gα subunit and triggers the release of the Gα and Gβγ subunits. This conformational change within the Gα subunit leads an exchange of GDP for GTP and allows the Gα subunit to regulate the activities of downstream signaling proteins such as adenylyl cyclase and other signaling proteins. Upon activation of Gα, the Gβγ subunits also associate with and regulate G protein effectors such as G protein-coupled receptor kinases (GRKs), phospholipases, and signaling proteins. In order that cells can rapidly adapt to changes in their external (extracellular) environments, previously stimulated GPCRs must be quickly desensitized. This process is initiated by GRKs, enzymes that phosphorylate the

cytoplasmic loops of activated GPCRs. This phosphorylation event tags the GPCR for binding by proteins called arrestins, which upon binding block further activation of heterotrimeric G protein subunits and initiates recycling or degradation via clathrin mediated endocytosis.

To gain a better understanding of the role that the GRKs play in the regulation of the signals that are transmitted through GPCRs, we have crystallized and solved the structures of GRK2 alone and in complex with the heterotrimeric G proteins $G\beta_1\gamma_2$. These structures reveal the orientations and interactions of the individual domains within GRK2. Furthermore, the domain structure and the $G\beta_1\gamma_2$ binding surfaces reveal both the mechanism of recruitment to the membrane as well as suggesting possible routes for the allosteric activation of GRK2 by $G\beta_1\gamma_2$ and phospholipids.

Table of Contents

STRUCTURE DETERMINATION

THE GRK2·Gβγ COMPLEX STRUCTURE

LIST OF TABLES

LIST OF FIGURES

GRKs AND THE REGULATION OF CELL SIGNALING

The role of G protein coupled receptor kinases in GPCR signaling

G protein–coupled receptors (GPCRs) are integral membrane proteins that respond to specific extracellular signals by activating G proteins within the cell (Fig. 1) (Pitcher, Freedman et al. 1998). They represent the largest class of receptors in the mammalian genome and play a fundamental role in the sensations of light, smell, and taste and in the regulation of heart rate, blood pressure, and glucose metabolism(Pierce, Premont et al. 2002). For cells to remain responsive to their environment, activated GPCRs must be rapidly desensitized (Fig. 2). The best characterized system for receptor desensitization is that of the GRKs and arrestins (Krupnick and Benovic 1998; Pitcher, Freedman et al. 1998). Activated GPCRs are first phosphorylated by GRKs and are then bound by molecules of arrestin, which block the binding of G proteins, target the receptors for clathrin-mediated endocytosis (Claing, Laporte et al. 2002), and serve as adaptors that link receptors to other signaling pathways such as those of the mitogen-activated protein kinases (MAP) (Perry and Lefkowitz 2002). GRKs may also inhibit G protein signaling in a phosphorylation-independent manner by blocking the interactions of Gα and Gβγ subunits with their effector targets or by playing a direct role in receptor sequestration and internalization (Carman, Parent et al. 1999; Pao and Benovic 2002; Lodowski, Pitcher et al. 2003).

GRKs, G proteins, and arrestins are the only protein families known to specifically recognize the activated form of most GPCRs. Protein kinase C and protein kinase A, kinases which phosphorylate GPCRs among their other cellular targets, lack this specificity (Pitcher, Lohse et al. 1992). Structural studies of these proteins could

therefore provide insights into the mechanism of signal transduction through activated receptors by elucidating the methods by which GRKs interact with activated GPCRs and heterotrimeric G proteins. To date, structures of several members of the G protein family have been determined, but none of any GRK. GRK2 (Benovic, Mayor et al. 1986; Benovic, Strasser et al. 1986; Benovic, DeBlasi et al. 1989), the best characterized GRK, is ubiquitously expressed and can phosphorylate many different GPCRs (Pitcher, Freedman et al. 1998; Rockman, Koch et al. 2002). These include the adenosine, α and β adrenergic, angiotensin, dopamine, histamine, muscarinic, δ-opioid and substance P GPCRs(Pitcher, Freedman et al. 1998). However, the enzyme plays a particularly vital role in the heart, where it regulates the force and rate of muscle contraction by phosphorylating β-adrenergic and muscarinic acetylcholine receptors (Rockman, Koch et al. 2002). Despite its beneficial roles, biochemical and transgenic studies have strongly implicated GRK2 in the progression of cardiovascular disease (Rockman, Koch et al. 2002). Inhibitors of GRK2 may therefore serve as useful therapeutic agents (Iaccarino, Lefkowitz et al. 1999; Iaccarino, Keys et al. 2001).

The Discovery of the GRK family of proteins

In the early 1970s, Kuhn and Bownds observed the light dependant phosphorylation of bovine and frog rhodopsin prepared from rod outer segments (Kuhn, Cook et al. 1973; Bownds and Brodie 1975). The phosphorylation was determined to be dependant on the exposure of the rhodopsin to light but it was not phosphorylated immediately upon exposure to light (Kuhn and Wilden 1982). Although not described as such, this was the first example of homologous desensitization of a G protein coupled receptor. This work was followed by the discovery that a membrane preparation from

rod outer segments was able to reproduce this light dependent activity *in vitro*(Miller and Paulsen 1975). The purification of the rhodopsin kinase from these preparations allowed the study and characterization of substrate specificity and activity (Shichi and Somers 1978). Further work with the purified rhodopsin kinase would determine phosphorylation sites on rhodopsin and the relative level of phosphorylation per rhodopsin molecule (Thompson and Findlay 1984; Palczewski, McDowell et al. 1988).

The discovery that activation-dependent regulation (homologous desensitization) of G protein coupled receptors (GPCRs) occurred even in the absence of protein kinase A, led to the discovery that another protein kinase was responsible for the homologous desensitization of β-adrenergic receptor (βAR) (Stadel, Nambi et al. 1983). This kinase was both purified and characterized, revealing that the kinase had a much higher affinity for the activated agonist occupied GPCR than for the inactive GPCR (Benovic, Strasser et al. 1986). This kinase was termed β adrenergic receptor kinase 1 (βARK-1) for its ability to desensitize the βAR. βARK-1 would be shown to preferentially phosphorylate agonist occupied βAR on serine and threonine residues within the third cytoplasmic loop and carboxyl-terminal tail. This phosphorylation event was found to trigger the binding of β-arrestin which blocked further activation of Gα subunits and begins the process of GPCR recycling or degradation (Ferguson, Downey et al. 1996). Subsequent work would reveal six other homologous kinases which had varying specificities for GPCRs (Pitcher, Freedman et al. 1998). These include the previously characterized rhodopsin kinase, cone opsin kinase, and four other kinases were responsible for all of the desensitization of all GPCRs (Shichi and Somers 1978; Pitcher, Freedman et al. 1998). Because of the promiscuity of these seven kinases for their GPCR targets, a more appropriate name for this family of kinases was coined, the family of G protein coupled receptor kinases (GRKs) (Pitcher, Freedman et al. 1998).

G Protein Coupled Receptors

G protein coupled receptors are a ubiquitous family of proteins found within the body. Every cell contains GPCRs which act to transduce the many varied signal transduction events throughout the body. Of the 29,000 to 34,000 genes identified in the human genome sequence, approximately 950 have been putatively identified as GPCRs (Venter, Adams et al.; Lander, Linton et al. 2001; Wise, Jupe et al. 2004). These 950 GPCRs are responsible for signaling both the sensations of sight, smell, and taste as well as homeostatic processes such as heart rate, blood pressure and glucose metabolism. Of these 950 receptors, 360 have been characterized as sensory GPCRs, and the ligands that activate 210 of the remaining GPCRs have been characterized (Wise, Jupe et al. 2004). Approximately 30 percent of all therapeutic drugs work to modulate, stimulate or block the actions of GPCRs (Wise, Jupe et al. 2004).

All GPCRs share certain common structural motifs and functional similarities (Figure 1). They all consist of seven transmembrane α-helices, which upon stimulation by agonist, transmit a signal through the plasma membrane and impart it onto the "first messenger" proteins, the heterotrimeric G proteins (Gainetdinov, Premont et al. 2004). These "first messengers" are then able to interface with proteins such as AC and phospholipase C (PLC), which then act to produce the "second messengers" such as cAMP, diacylglycerol (DAG), and inositol triphosphate (IP_3). These "second messengers" act to initiate signaling cascades which exert control over many cellular proteins and processes. Some signaling cascades are regulated by feedback inhibition, and this feedback inhibition allows for greater control over the extent and duration of GPCR activation and propagation of signal in the cell (Gainetdinov, Premont et al. 2004).

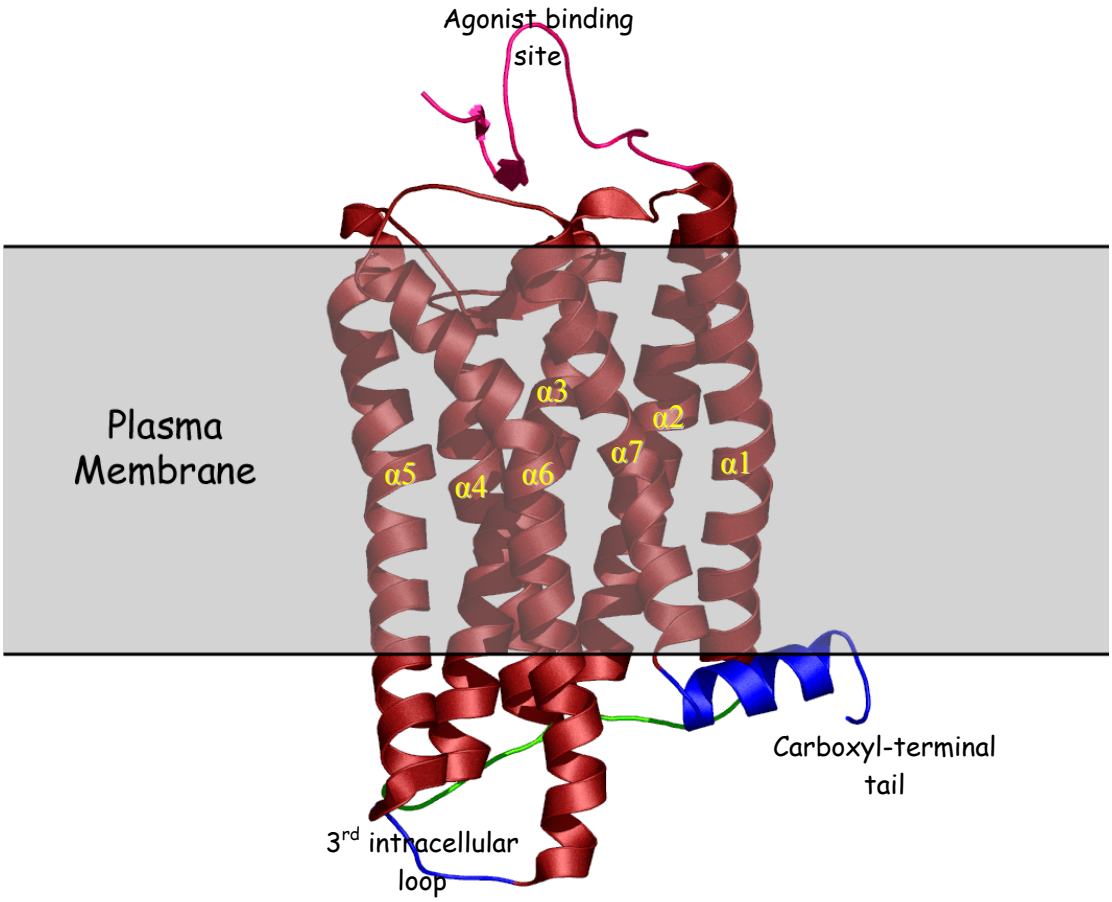

Figure 1. **Rhodopsin: the only GPCR of known structure**. The grey region represents the hydrophobic portion of the plasma membrane. GPCRs are comprised of seven transmembrane α-helices. In rhodopsin, a photon of light induces a conformational change in a retinal group located inside of the cavity formed by the seven transmembrane helices from *cis* to *trans*. In most other GPCRs, the extracellular regions of the GPCR make up the agonist/ligand binding region (shown in pink). After the agonist binds to the extracellular domain, a signal is transmitted through these helices and is imparted to the intracellular cytoplasmic region of the GPCR. It is this cytoplasmic region that is responsible for propagating the signal onto the heterotrimeric G proteins, initiating the cellular signaling cascade. It is also this region that is responsible for the initiation of the desensitization process by GRKs and arrestins. The third intracellular loop and carboxyl-terminal tail which follows the helix denoted in blue contain the GRK phosphorylation sites. The first and second intracellular loops (in lime green) are important for the regulation of the kinase GRK2. (PDB:1GZM). All molecular graphics representations were prepared using PYMOL or MOLSCRIPT/BOBSCRIPT and RENDER3D (Merritt 1994; Esnouf 1997; Esnouf 1999; DeLano 2002).

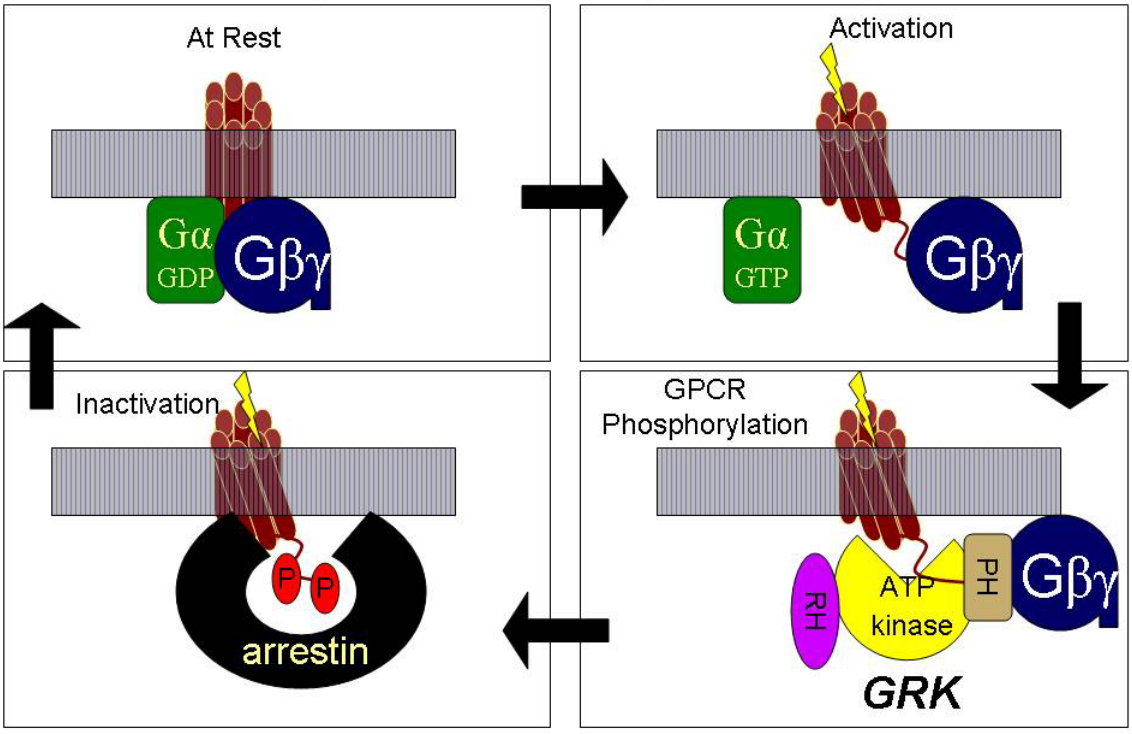

Figure 2. Overview of the cycle of GPCR signaling. A. GPCR at rest and ready to respond to an extracellular signal (agonist). The GPCR is in an inactive state and is unable to activate heterotrimeric G proteins which are also in an inactive state. B. GPCR upon hormone binding. This binding event triggers a structural change within the GPCR which is transmitted through the plasma membrane of the cell. The signal is then imparted onto the Gα subunit of the Gαβγ heterotrimer, and triggers a structural change in the Gα subunit. The change in the Gα subunit causes the exchange of GDP for GTP and release of the Gβγ subunits. The nucleotide exchange activates the Gα subunit for the enervation of cellular effectors such as adenylyl cyclase and phospholipases. C. The recruitment of a GRK to the plasma membrane by Gβγ. After Gβγ is released from the Gα subunit, it binds to various G protein effectors including GRKs. The GRK is recruited to the site of the activated GPCR where it phosphorylates the third intracellular loop and carboxyl terminus of the GPCR, tagging it for binding and inactivation by arrestin. D. Binding of arrestin to the tagged GPCR. The binding of arrestin to the GPCR blocks further activation of Gαβγ heterotrimers and begins the process of clathrin-mediated endocytosis by which the GPCR is either recycled or degraded.

The G protein Coupled Receptor Kinases

The family of GRKs is comprised of seven members. These include rhodopsin kinase which is now referred to as GRK1, β adrenergic receptor kinases 1 and 2 which are now known as GRK2 and GRK3 respectively, GRK4, GRK5 and GRK6 and cone opsin kinase which is called GRK7. All members of the GRK family share a similar domain structure (Fig. 3). Each contains an amino terminal regulator of G protein signaling (RGS) homology (RH) domain (Fig. 4). This RH domain was originally thought to contain nine helices, but with our structures, it is obvious that the RH domain actually contains two additional helices with the protein kinase domain inserted between the ninth and tenth helixes within the RH domain (Fig. 6) (Lodowski, Pitcher et al. 2003). The last helix of the RH domain is followed by a membrane targeting domain. Amino and carboxyl terminal residues play regulatory roles in the recruitment of GRKs to the sites of activated receptor and the kinase activity of GRKs.

The domain structure of GRK2 consists of an amino terminal regulatory region consisting of the first 29 residues in the GRK2 sequence (Fig. 3). This is followed by a RH domain made up of two discontinuous segments, from 29-185 and from 513-548. Located within the two discontinuous segments comprising the RH domain (Fig. 4), a protein kinase domain of the AGC family exists (Fig. 6, residues 186-512). This is followed by a pleckstrin homology (PH) domain which spans residues 553 to 661 (Fig. 5). The final carboxyl residues (662-689) comprise one final regulatory region.

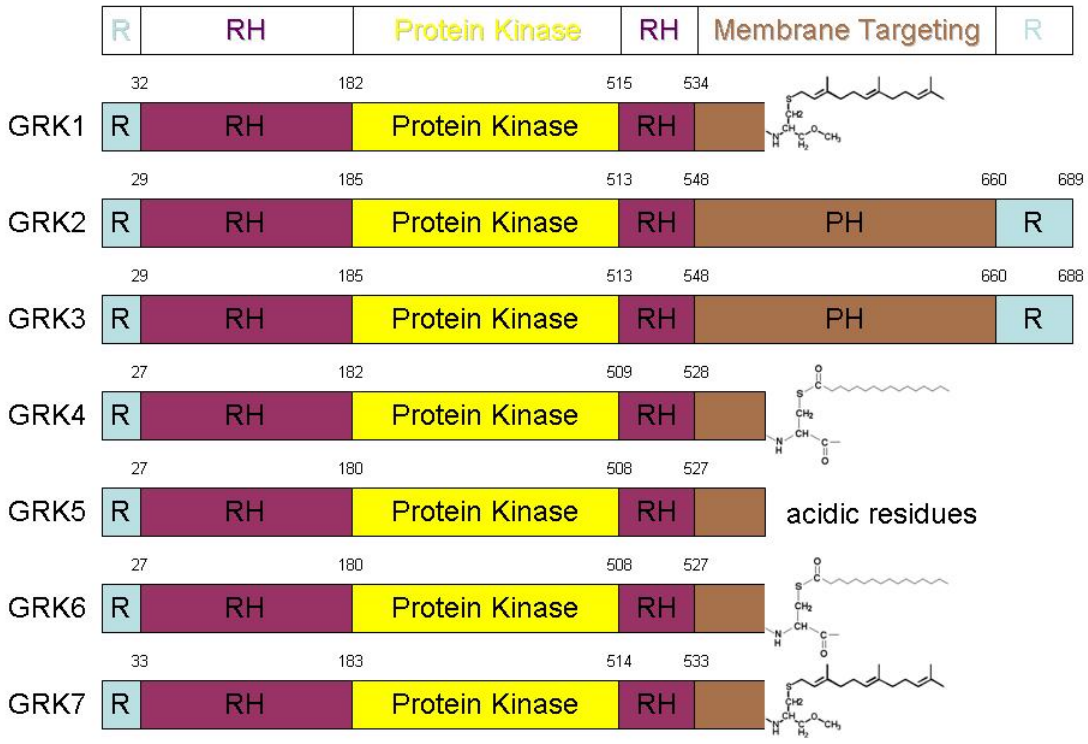

Figure 3. Domain structure and organization of the GRK family. All members contain an amino terminal RH domain which contains a kinase domain as an insertion within. This is followed by a membrane targeting region which is a pleckstrin homology (PH) domain in GRK2 and GRK3. GRK1 and 7 have isoprenyl moieties that tether them permanently to the membrane while GRK4 and GRK6 are reversibly tethered to the membrane via palmitoyl moieties. GRK5 appears to be kept in the vicinity of the membrane through the interactions of acidic residues at its amino and carboxyl terminus with phospholipid headgroups in the plasma membrane (Hisatomi, Matsuda et al. 1998; Pitcher, Freedman et al. 1998; Weiss, Raman et al. 1998; Chen, Zhang et al. 2001).

Regulator of G protein Signaling Domains

All members of the GRK family contain regulator of G protein signaling homology (RH) domains (Koelle 1997; Ross and Wilkie 2000; Zhong and Neubig 2001). All consist of the prototypical nine helix domain which is that is divided into two subdomains, a four helix "bundle subdomain" made up of helixes α4-α7and a five helix "terminal subdomain" made of helixes α1-α3 and α8-α9 (Ross and Wilkie 2000). These first nine helices of the GRK RH domain are ~45% homologous and ~25% identical with that of the RGS family of proteins, but in our structure of the GRK2·Gβγ complex, the RH domain of GRK2 actually contains a further two helices, α10 and α11 (Lodowski, Pitcher et al. 2003) much like that of the structure of p115-rhoGEF (Chen, Wells et al. 2001). It appears from alignments of all of the GRKs that these two helices are present in all members of the GRK family (Fig. 14a).

The RH domains were originally shown to function as GTPase activating proteins (GAPs), intensifying the basal rate of hydrolysis of GTP within activated G-proteins (Siderovski, Heximer et al. 1994; Vries, Mousli et al. 1995; Koelle 1997). The change in rate of GTP hydrolysis is accomplished by stabilizing the switch regions of the G-protein in a conformation that favors the transition state of the hydrolysis of GTP into GDP and inorganic phosphate (Tesmer, Berman et al. 1997). The expression of proteins containing RH domains provides a method by which duration of activity of G proteins may be modulated (Berstein, Blank et al. 1992; Siderovski, Heximer et al. 1994; Koelle 1997).

Although many RH domain proteins bind to the activated (GTP bound) form of specific G proteins to increase their basal rate of GTP hydrolysis, this is not true of the GRKs. The RH domain of GRK2 binds activated $G\alpha_q$ subunits, but does not measurably affect their rate of GTP hydrolysis (Carman, Parent et al. 1999; Sterne-Marr, Tesmer et

al. 2003). This could be physiological, as it would make sense for the enzyme that is performing the desensitization of the GPCR to sequester activated Gα subunits (Lodowski, Pitcher et al. 2003). This sequestration of active Gα subunits would prevent their interactions with cellular effectors and prevent their reactivation by GPCRs that have not yet been desensitized by GRK2 and arrestin. The GRK2·Gβγ complex structure revealed that the RH domain of GRK2 utilizes a novel binding surface to bind $G\alpha_{q/11}$ when compared to the Gα and small-molecular weight GTPase binding surfaces of other RH domains such as RGS4 and p115RhoGEF (Tesmer, Berman et al. 1997; Lodowski, Pitcher et al. 2003; Sterne-Marr, Tesmer et al. 2003). While some RH domains that have had their binding surfaces characterized bind to their cognate G-proteins through a binding surface consisting of the loops between α3-α4 and α5-α6 as well as the α8 helix (Tesmer, Berman et al. 1997), the GRK2 RH domain interacts with $G\alpha_q$ through residues located on the outside of the bundle subdomain on the α5 and α6 helixes (Lodowski, Pitcher et al. 2003; Sterne-Marr, Tesmer et al. 2003). The Gα subunits that interact with the RH domains of other GRK family members have not been determined (Sterne-Marr, Tesmer et al. 2003).

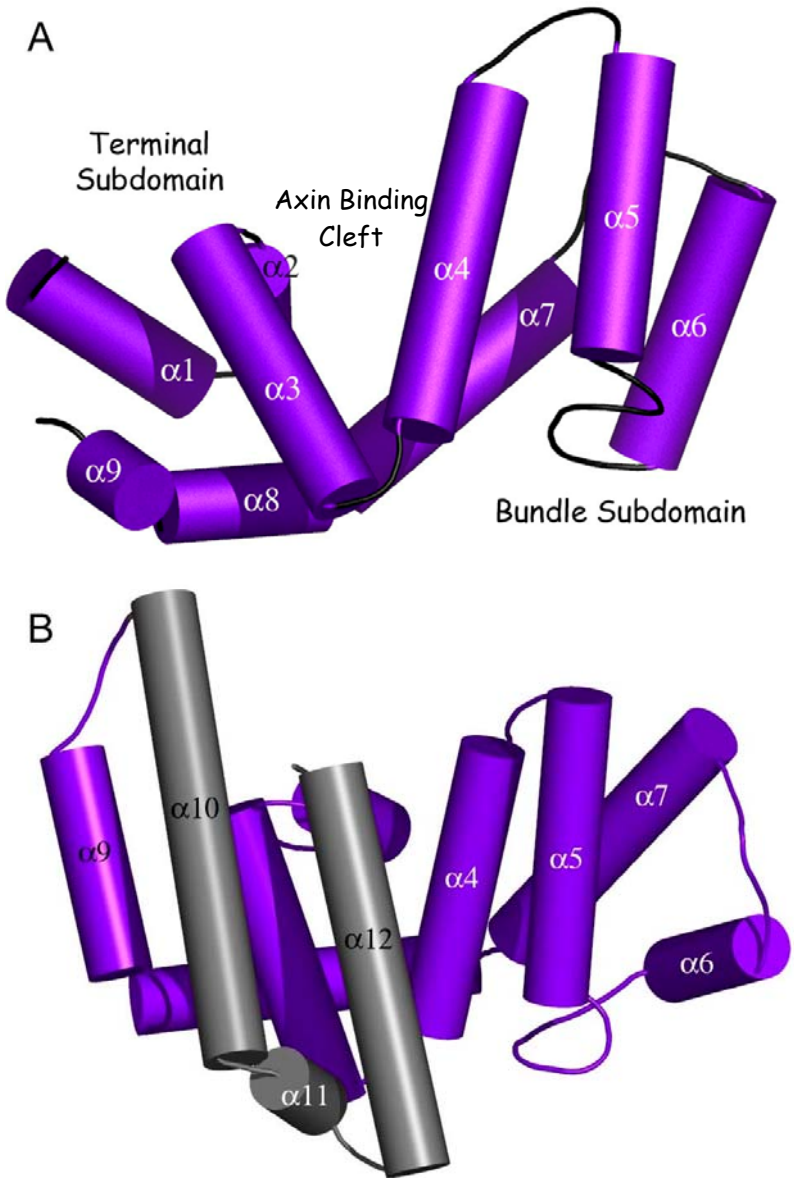

Figure 4. RGS4, a protypical RH domain and p115rhoGEF, a 12 helix RH domain. A. RGS4 is composed of the nine helices that are characteristic of all RGS homology domains. These are divided into subdomains, the terminal subdomain, made up of helices α1-α3 and α8-α9 and the bundle subdomain made of helices α4-α7. The binding surface utilized to bind Gα subunits consists of the loops between α3-α4 and α5-α6 as well as the α8 helix. The RH domain of axin binds peptide across the cleft between the bundle and terminal subdomains. Conversely, the $G\alpha_{q/11}$ binding surface utilized by GRK2 consists of the α5 and α6 helices in the bundle subdomain. B. The RGS domain of GRK2 shares a higher degree of sequence similarity with that of p115rhoGEF. This RH domain contains 12 α helices, and the α10 helix shares some sequence similarity with the α10 helix of GRK2. PDB accession code for RGS4 is 1AGR and p115rhoGEF is 1IAP.

Pleckstrin Homology Domains

Pleckstrin Homology domains were originally discovered when researchers noticed two repeated amino-acid sequences of approximately 100 residues within *p*latelet and *l*eukocyte *C k*inase sub*str*ate prote*in* (pleckstrin) (Haslam, Koide et al. 1993; Mayer, Ren et al. 1993). This repeated motif was determined to be a structural domain when the NMR structures of pleckstrin, β-spectrin and crystal structures dynamin and β-spectrin were solved revealing that this was in fact a structural domain. Proteins containing pleckstrin homology (PH) domains are a diverse and varied group of structurally homologous but share little in the way of sequence similarity. In fact, there is only a single highly conserved tryptophan residue within the whole group of known PH domains (Rebecchi and Scarlata 1998). Nevertheless, all PH domains share certain structural similarities. All PH domains consist of seven β-strands which are arrayed in two semi-continuous anti-parallel sheets that are bent to form a "β-taco" or squashed β-barrel. The β1-β4 strands form one half of this taco, and β5-β7 form the other side. A carboxyl terminal helix packs up against the edge of the β-sheets and the amino and carboxyl termini are both located on the same face of the domain (Rebecchi and Scarlata 1998). The loop regions that exist between the individual β-strands are variable and often form the ligand binding surfaces of the PH domain (Ferguson, Lemmon et al. 1995; Zhang, Talluri et al. 1995).

Many PH domains are also utilized as regulatory binding motifs that provide a binding site for both phospholipids and Gβγ subunits. In phospholipase C-ζ1 the PH domain has been shown to recruit the protein to the plasma membrane. A high affinity PIP_2 binding site within the PH domain orients and recruits the phospholipase catalytic site to the vicinity of the plasma membrane surface where the enzyme cleaves PIP_2 into

inositol (1,4,5)triphosphate [Ins (1,4,5)P_3] and diacylglycerol (DAG) (James, Paterson et al. 1995). Furthermore, the PH domain has been shown to allosterically activate the catalytic domain upon binding to PIP_3 (Bromann, Boetticher et al. 1997). The Bruton's tyrosine kinase (BTK) PH domain binds Gβγ, protein kinase C and phospholipid providing a means for the recruitment of a modular protein to the plasma membrane as well as the allosteric activation of BTK through the binding of the PH domain to inositol phosphates. The association of $G\beta_1\gamma_3$ with the BTK PH domain has been shown to activate the kinase activity of BTK towards both itself (autophosphorylation) and its substrate (Langhans-Rajasekaran, Wan et al. 1995). Furthermore, the PH domain of BTK is intimately associated with an adjacent (btk) motif and could use this interface to transmit allosteric signals that activate the rest of this multidomain protein.

The interactions and concomitant control of the GRK2 through its PH domain have been well characterized, and the NMR solution structure of its PH domain solved (Pitcher, Inglese et al. 1992; Pitcher, Touhara et al. 1995; Fushman, Najmabadi-Haske et al. 1998). The GRK2 PH domain structure revealed the structural similarities of the GRK2 PH domain to other PH domains of known structure, but also revealed two differences. The αCT helix in the GRK2 PH domain was found to be longer and had a much more basic charge distribution than that of the BTK PH domain. It was proposed that these charged residues were partially responsible for the binding to Gβγ subunits, this was backed up with both experimental data as well as our structure of the GRK2·Gβγ complex (Touhara, Koch et al. 1995; Touhara 1997; Lodowski, Pitcher et al. 2003). A role for the almost universally conserved Trp^{643} was assigned; it formed part of the hydrophobic core of the PH domain specifically assisting in the cementing of the β4-β5 loop and β5 strand to the core of the domain. Furthermore, this structure suggested that the site for phosphoinositide binding is located at the β1-β2 loop and amino terminus of

the β2 strand, work that has been confirmed by later mutational analysis (Fushman, Najmabadi-Haske et al. 1998; Carman, Barak et al. 2000). One last observation about the GRK2 PH domain structure was that the pairwise r.m.s.d for the NMR structures was 2.1 Å compared to other PH domains that were solved at the time (Fushman, Najmabadi-Haske et al. 1998).

Figure 5. The structures of the PH domains of PLCδ and GRK2. PH domains are made up of seven antiparallel β-sheets arranged in a squashed β-barrel. The carboxyl terminal helix caps the edge of the β5 strand. A. The PLCδ PH domain shown bound to Ins (1,4,5)P_3 (Ferguson, Lemmon et al. 1995). The binding of Ins (1,4,5)P_3 is accomplished through charged interactions with residues located in the loop regions between the β1-β2 and β5-β6 strands. These residues are labeled and colored in blue-grey. The inset shows the PH domain in an orthogonal view from the large figure. B. The NMR structure of the GRK2 PH domain (Fushman, Najmabadi-Haske et al. 1998). Phospholipid binding occurs in the same β1-β2 loop region as in the BTK and phospholipase Cδ. Residues implicated in phospholipid binding are colored in yellow (Carman, Barak et al. 2000). Inset shows the ensemble of all 20 of the NMR models in a similar orientation as in the PLCδ inset. PDB accession code for the PLCδ PH domain and GRK2 PH domain are 1MAI and 1BAK respectively.

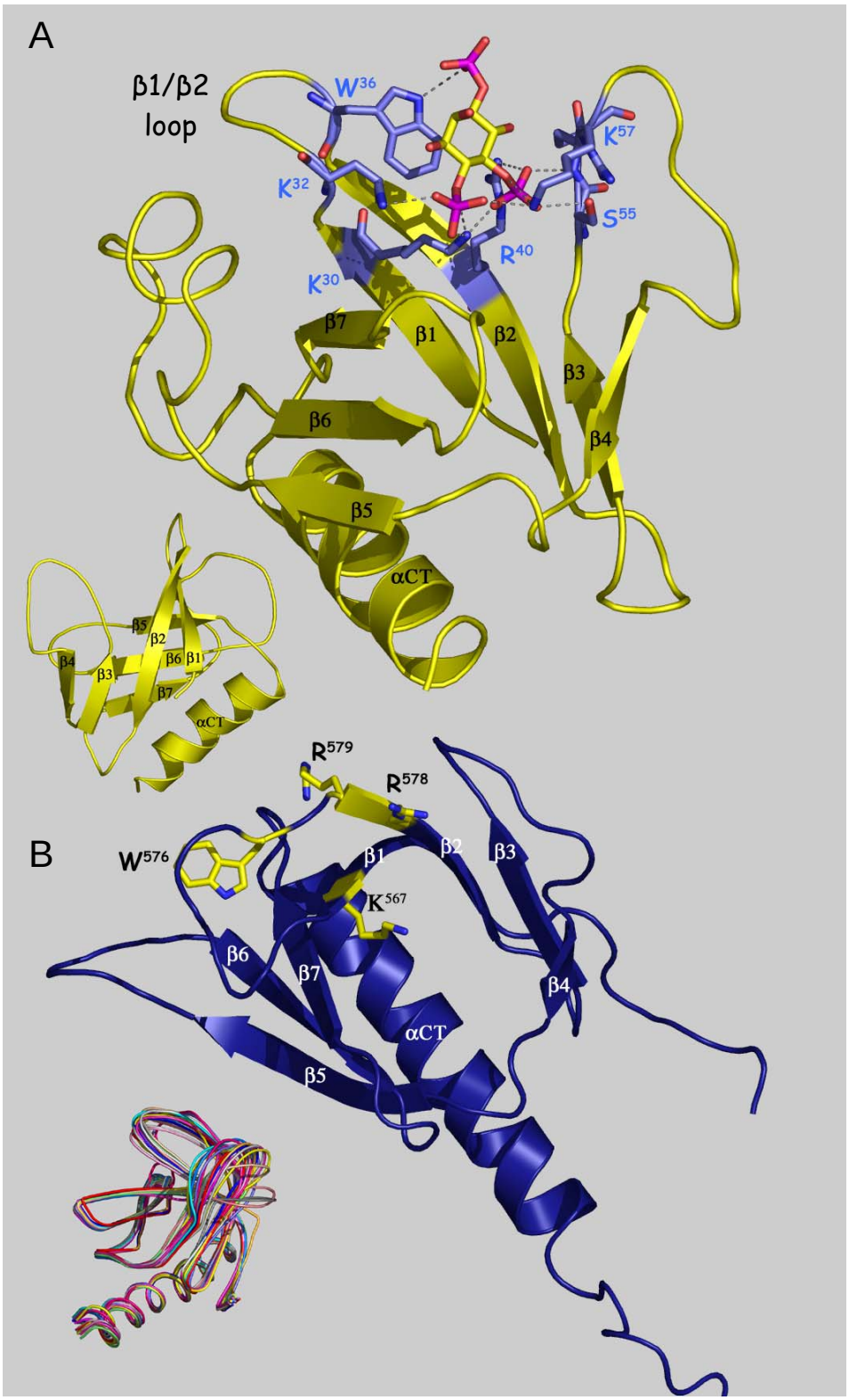
A
β1/β2
loop
W36
K57
K32
S55
R40
K30
β7
β1
β2
β3
β6
β4
β5
αCT
β5
β2
β4
β3
β6
β1
β7
αCT
R579
R578
B
W576
β1
β2
β3
K567
β6
β7
β4
αCT
β5

Protein Kinase Domains

The kinase domain of GRKs is a relatively distant member of the member of the AGC family of kinases which are named after three prototypical members, cAMP-dependent protein kinase (PKA), protein kinase G and protein kinase C (PKC). The kinase domain of GRKs shares approximately 30% sequence identity with the other AGC kinases with known structures including PKA, phosphoinositide-3 dependent kinase 1 (PDK1) and protein kinase B (PKB/Akt). One of the characteristic features of AGC kinases is an "activation loop." In many AGC kinases, it is the phosphorylation of this activation loop which fully activates the kinase toward substrate (Cenni, Doppler et al. 2002; Newton 2003). In the case of PKC, PDK1 phosphorylates a threonine within its activation loop stabilizing the active state of the kinase. Post phosphorylation of this activation loop, the contribution of a phenylalanine to the active site of the kinase assists in an increase in kinase activity. Interestingly, the kinase activity of PDK1 is partially controlled through the interactions of its PH domain with phospholipids and the kinase activity of GRK2 is also partially controlled through the interactions of anionic phospholipids with its PH domain (Pitcher, Touhara et al. 1995; Le Good, Ziegler et al. 1998). GRK2 is somewhat divergent in the mechanism of activation as it has no phosphorylatable residues or even acidic residues that could substitute for phosphorylated serines or threonines in its activation loop.

The structure of PKA has been well characterized with the crystal structures in both its "closed" (active), and "open" (inactive) and transition states (These structures reveal the structural basis for substrate specificity, nucleotide binding and catalysis of kinase activity. The kinase domain has two lobes, termed large and small joined at a

hinge. The kinase active site is located at this hinge and both lobes must close in order to phosphorylate substrate.

The substrate specificity of PKA can be attributed to the binding of specific amino acid residues within the substrate to interaction sites within its active site cleft. In most AGC kinases, highly conserved acidic side chains within the cleft (E127, E170, E203 and E230 in mouse PKA) coordinate arginine residues preferred at the P-2, P-3 and P-6 positions (Kemp, Bylund et al. 1975; Zetterqvist, Ragnarsson et al. 1976). Further substrate specificity is conferred by the "P+1 loop" of the kinase domain which binds the side chain of the residue immediately C-terminal to the phosphorylated residue of the substrate. In the substrates of many AGC kinases, hydrophobic residues such as isoleucine or phenylalanine are preferred at this position (Kemp, Bylund et al. 1975; Obata, Yaffe et al. 2000).

Interestingly, although the sites phosphorylated by GRK2 within the β_2-AR, α1-AR and δ-opioid receptors also have been characterized and determined, no clear consensus exists for the phosphorylation of residues by GRK2. The sites at which these GPCRs are phosphorylated vary widely and phosphorylation by specific GRKs may depend on both substrate specificity and relative amount of each GRK expressed within the cell (Pitcher, Freedman et al. 1998). By contrast, the preferred peptide substrates for GRK2 that have been experimentally determined contain glutamic or aspartic acids on the carboxyl terminal side of the active site and hydrophilic residues at the P+1 position (Onorato, Palczewski et al. 1991).

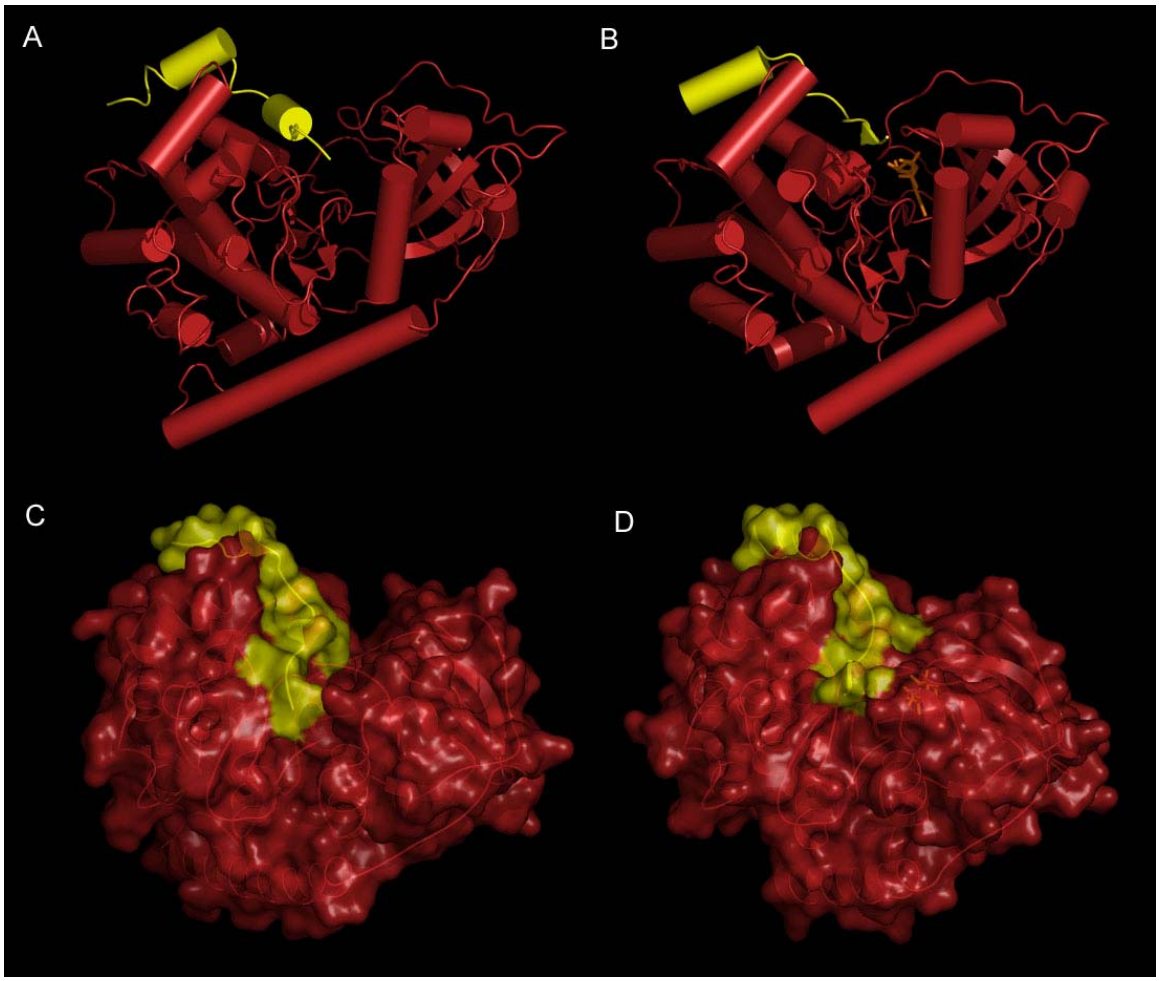

Figure 6. The open and closed conformations of protein kinase A. PKA molecule is shown in deep red and a PKA inhibitor peptide is shown in yellow. A. The "open" (inactive) conformation (PDB ID: 1CMK). The large and small lobes of the kinase domain are relatively far open and poised to bind nucleotide. B. The closed (active) conformation with ATP (orange) bound (PDB ID: 1RDQ). Both nucleotide and peptide are bound and the kinase domain has clamped down to properly order the active site. C. Molecular surface representation showing the peptide binding cleft and degree of openness of the open conformation. D. Molecular surface representation of the closed conformation; the cleft between the large and small lobes has closed upon the nucleotide and ATP molecule. Molecules in surface representation are rotated slightly with respect to A and B to emphasize the difference between the open and closed conformations.

GRK2 Regulation

Regulation of the kinase activity of GRK2 is modulated by many cellular processes. GRK2 is recruited to the cell membrane by the binding of its PH domain to Gβγ. This positions GRK2 at the plasma membrane where the PH domain is able to bind the headgroups of anionic phospholipids. The kinase activity of GRK2 is further regulated by the phosphorylation of serine residues within the amino and carboxyl termini. The binding of activated GPCR or to peptides derived from GPCRs to GRK2 has also been shown to influence the phosphorylation of substrate (Benovic, Onorato et al. 1990). Finally, the levels of GRK2 expression are up or down regulated at the protein level in response to heightened GPCR signaling.

After a GPCR is activated by the binding of a hormone and the Gα and Gβγ dissociate (Fig. 2), GRK2 is recruited to the plasma membrane by nature of its interaction with Gβγ which is tethered to the membrane through the geranylgeranyl moiety in the Gγ subunit. Overexpression of the PH domain of GRK2 has been shown to be capable of prohibiting the recruitment of GRK2 to the plasma membrane in *in vivo* assays confirming that the interactions with the PH domain are responsible for the recruitment to the plasma membrane (Touhara, Inglese et al. 1994). Furthermore, the expression of the PH domain of GRK2 with Trp^{643} mutated to alanine is unable to interfere with agonist dependant phosphorylation of βAR while the wild type PH domain almost completely abolishes this activity. This suggests that this tryptophan is in fact necessary for the recruitment of GRK2 to the membrane (Pitcher, Touhara et al. 1995). Trp^{643} has been shown to be critical for the binding of Gβγ to GRK2, and site directed mutants of this residue are deficient in binding Gβγ (Pitcher, Inglese et al. 1992). This reveals that the

mode for the recruitment of GRK2 to the plasma membrane is via the interactions of its PH domain with Gβγ.

Once GRK2 is recruited to the plasma membrane by the interactions of its PH domain with Gβγ, the β1/β2 loop and portions of the β3 strand within the PH domain bind the headgroups of anionic phospholipids. This binding event synergistically intensifies the kinase activity of GRK2 toward substrate over Gβγ or phospholipid alone. The activation of GRK2 by phospholipid is somewhat dependant on the phospholipid head group to which its PH domain binds. The greatest level of activation seen is from phosphatidylinositol 4,5-bisphosphate (PIP_2) and to a lesser extent from phosphatidylinositol 4-phosphate (PIP) and phosphatidylserine (PS) (Pitcher, Touhara et al. 1995). Furthermore, it is necessary for GRK2 to bind to both phospholipid and Gβγ in order to achieve full kinase activity in lipid micelles. It has been shown that the activated m_2 muscarinic acetylcholine receptor (m2mAChR) is not a substrate for GRK2 unless PIP2 or PIP are present, so at least in an *in vitro* assay the presence of anionic phospholipids are absolutely required for GRK2 to function (DebBurman, Ptasienski et al. 1996). This same result is observed in the β-adrenergic receptor (βAR); when GRK2 is incubated with phospholipid vesicles containing βAR it is necessary that both PIP_2 and Gβγ be present for phosphorylation of the βAR to occur (Pitcher, Touhara et al. 1995; DebBurman, Ptasienski et al. 1996; Pitcher, Fredericks et al. 1996). Therefore, the binding of anionic phospholipids is an important and necessary step in the activation of GRK2. It is possible that anionic phospholipids also interact with the activated GPCR and this plays a role in the phosphorylation of the GPCR by GRKs.

The kinase activity of GRK2 is further modulated through the phosphorylation of serine residues 29, 670, and 685 as well as an uncharacterized tyrosine phosphorylation within the RH domain. Protein kinase C (PKC) has been shown to phosphorylate GRK2

at serine 29. This increases the kinase activity of GRK2 toward activated receptors by decreasing the affinity of GRK2 for Ca^{2+}/calmodulin, which normally acts to inhibit the phosphorylation of GPCRs by GRK2 (Krasel, Dammeier et al. 2001). This represents feedback inhibition of GRK2; as a GPCR becomes activated, it activates Gα subunits which in turn activate phospholipase C (PLC). PLC produces diacylglycerol (DAG) which in turn activates PKC which in turn phosphorylates GRK2 reducing its affinity for Ca^{2+}/calmodulin, increasing its kinase activity towards activated GPCRs (Krasel, Dammeier et al. 2001).

The phosphorylation of serine 670 by extracellular-signal regulated kinase (ERK1) also modulates the activities of GRK2 towards GPCRs. Upon phosphorylation at serine 670, GRK2 is eight times less active towards activated receptor. This also represents a form of feedback inhibition as higher levels of activated GPCR lead to increased MEK activity which would in turn act upon ERK to inhibit its phosphorylation of GRK2 and increase its kinase activity, so that the more active GPCR signaling is, the less influence ERK plays in the regulation of GRK2 (Pitcher, Tesmer et al. 1999). Phosphorylation by ERK1 has also recently been shown to increase the degradation of GRK2 through the proteasome pathway, thus providing another facet to the regulation of GRK2 activity. GRK2 phosphorylated at serine 670 by ERK was shown to be preferentially degraded at a rate greater than the unphosphorylated GRK2 (Elorza, Penela et al. 2003). The reduction of the rate at which GRK2 is degraded would increase GRK activity and shorten the duration of GPCR mediated signals or conversely, degradation of the cytosolic pool of GRK2 could potentiate the GPCR mediated signal.

Protein kinase A (PKA) can also play a role in the regulation of GRK2. An adaptor protein, AKAP-79 (A kinase anchor protein) is necessary for the phosphorylation of GRK2 by PKA, this AKAP also facilitates the recruitment of PKA to the GPCR

(Cong, Perry et al. 2001; Freeman, Gonzalo et al. 2002). In the case of the β_2AR, PKA both phosphorylates the receptor and GRK2 on serine 685. This phosphorylation of GRK2 increases its affinity for Gβγ by approximately 75 percent. This in turn increases the recruitment of GRK2 to the plasma membrane and activated GPCRs, leading to an increase in GPCR desensitization (Cong, Perry et al. 2001; Freeman, Gonzalo et al. 2002).

Another possible route of regulation that is common to all GRKs is that of caveolin. The binding of caveolin to the RH domain of GRK2 at residues 63-71 which map to the α-3 helix within the RH domain inhibits GRK kinase activity (Carman, Lisanti et al. 1999). The binding of a caveolin derived peptide was sufficient to inhibit the kinase activity of GRK2 100-fold and kinetic analysis revealed the inhibition to be non-competitive (allosteric) in nature (Carman, Lisanti et al. 1999). GRK2 has also been shown to be regulated through interactions with the actin binding protein α-actinin(Freeman, Pitcher et al. 2000). The activity of all GRK family members toward substrate is potently inhibited upon binding α-actinin. Furthermore, upon interaction of α-actinin bound GRK5 with calmodulin and IP_3, the inhibition of GRK5 toward soluble substrate is regained while inhibition of GPCR phosphorylation is unaffected, revealing that α-actinin acts to inhibit recruitment to the plasma membrane(Freeman, Pitcher et al. 2000).

Phosphorylation of GRK2 by c-src kinase results in an immediate increase in GRK2 activation (Sarnago, Elorza et al. 1999). This is followed by a decrease in GRK2 activity as the phosphorylation of GRK2 by Src triggers the proteolysis of GRK2 via the proteosomal pathway (Penela, Elorza et al. 2001; Penela, Ribas et al. 2003). The phosphorylation of GR2 by Src kinase has been shown to be dependant on the ability of β-arrestin to recruit Src to GRK2. This could also represent a method for the regulation

of GPCR signaling by GRKs; the reduction GRK2 levels via proteosomal pathways would assist in the potentiation of GPCR mediated signaling.

The highest level of regulation of the kinase activity comes from interactions with activated GPCRs. Activated GPCRs have been shown to increase the phosphorylation of both peptide substrates and GPCRs by 10,000 fold (Chen, Dion et al. 1993). Furthermore, peptides derived from the cytoplasmic loops at sites distant to the GRK phosphorylation sites inhibit the phosphorylation of activated GPCRs suggesting that binding to sites distant from the phosphorylation site is a necessary event in the activation of GRK2 (Benovic, Onorato et al. 1990; Brown, Fowles et al. 1992). Light activated rhodopsin was shown to activate rhodopsin kinase and GRK2 toward peptide substrates, suggesting that activated GPCRs interact with GRKs both at the active site and at a relatively distant allosteric activation site (Onorato, Palczewski et al. 1991; Brown, Fowles et al. 1992). The existence of this distal GPCR binding/activation site is further supported by the ability of peptide derived from the first and second intracellular loops of GPCRs to reduce kinase activity toward full length GPCRs while having no effect on kinase activity toward soluble peptide substrates (Benovic, Onorato et al. 1990).

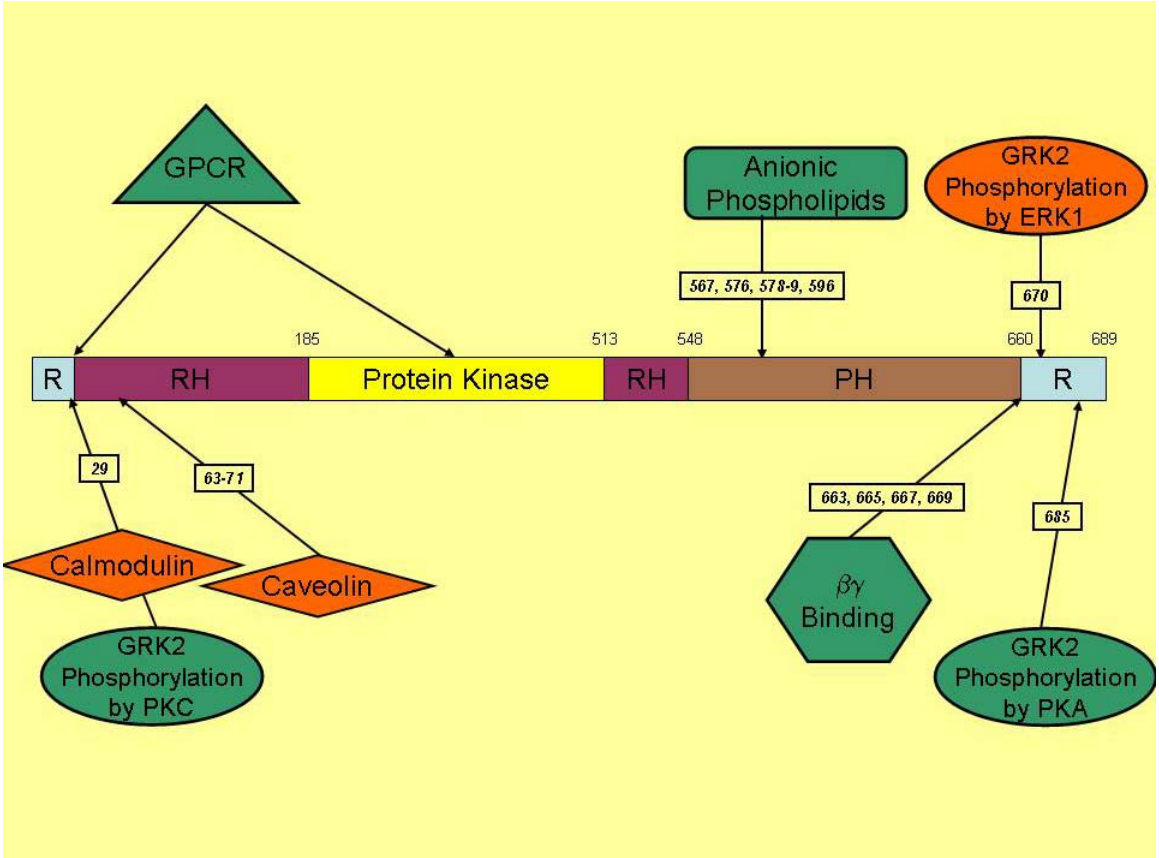

Figure 7. Regulation of GRK2. Effectors that increase the activity of GRK2 toward GPCRs are shown in green and those that decrease activity are shown in orange. The binding of activated GPCR provides the greatest boost in GRK2 activity, up to 10,000 times the basal rate. The binding of anionic phospholipids and Gβγ subunits alone increase GPCR phosphorylation to a slight extent while the binding of both results in a synergistic activation of GRK2. GRK2 phosphorylation by PKA also increases its affinity for Gβγ, thus increasing the recruitment of GRK2 to activated GPCRs. Phosphorylation of GRK2 by PKC results in a loss of the inhibition of GRK2 due to Ca^{2+}/calmodulin. The phosphorylation of GRK2 by ERK1 decreases the activity of GRK2 by a factor of eight toward activated GPCR. The interplay between these and other mechanisms allows for the exquisite regulation of GRK2.

GRK2 Physiology and Disease

GRK2 has been shown to be necessary for the proper development of the heart as well as being implicated in several disease states. Mice heterozygous for the knockout of GRK2 have markedly higher cardiac output in response to isoprotenerol treatment (Rockman, Choi et al. 1998) while the homozygous knockouts are embryonic lethal due to malformed cardiac tissues (Jaber, Koch et al. 1996; Rockman, Koch et al. 1996). When GRK2 is overexpressed in the cardiac tissue of transgenic mice they exhibit a marked decrease in adenylyl cyclase activity as well as reduced signaling through β-adrenergic receptors revealing the crucial role that GRK2 plays in the regulation of β-adrenergic signaling (Koch, Rockman et al. 1995).

GRK2 has also been implicated in a form of congenital familial primary hypertension in which the β_2-adrenergic receptors (β_2-AR) are refractory to external regulation by epinephrine. This is due to extremely high cellular concentrations of GRK2 (Gros, Benovic et al. 1997; Gros, Tan et al. 1999; Gros, Chorazyczewski et al. 2000). These high levels of GRK2 prohibit β-adrenergic receptor signaling, which leads to the inability of blood vessels to vasodialate upon stimulation by epinephrine, causing high blood pressure. In transgenic mice that had GRK2 overexpressed in their vascular tissue, hypertension due to challenge with isoprotenerol (a β-adrenergic agonist) was 2-3 times that of wild type mice, indicating that proper levels of GRK2 were necessary for proper vascular function (Eckhart, Ozaki et al. 2002). Furthermore, the overexpression of the PH domain of GRK2, which abolishes the kinase activity of GRK2 toward activated GPCRs by blocking the interactions of Gβγ with full length GRK2, enhances β-adrenergic signaling, suggesting that the level of GRK2 activity is directly coupled to the degree of β-adrenergic receptor signaling (Rockman, Choi et al. 1998).

In chronic heart failure (CHF) and after a heart attack episode, patients have lowered response to epinephrine and thus lowered heart contractility due to greatly increased levels of GRK2. When GRK2 activity was inhibited in transgenic mice expressing a peptide inhibitor of GRK2, survival after induced heart failure was increased (Rockman, Chien et al. 1998; Harding, Jones et al. 2001). This suggests that small molecule inhibitors of GRK2 would serve as excellent therapeutic agents to treat persons suffering from heart attack or CHF (Iaccarino, Lefkowitz et al. 1999).

Experimental rationale and methodology

The atomic structure of GRK2 or any other GRK was not known prior to this work. The structures of homologues to the individual RH and protein kinase domains or in the case of the PH domain, an NMR structure had been determined, but the arrangement of these modular domains in the context of the full length protein was unknown. In order to determine the crystal structure of GRK2, it would be necessary to design a methodology for the purification of crystallographic quantities of pure GRK2, determine conditions under which the protein or protein complex crystallized, to collect X-ray diffraction data and solve the atomic structure of GRK2.

The determination of the crystal structure of GRK2 would elucidate the roles that each domain plays in the regulation and activity of GRK2 as well as possible routes of interdomain communication. Furthermore, as the mechanism of recognition of activated from inactive GPCRs by GRKs is unknown, determination of the atomic structure of GRK2 would help to elucidate the molecular processes involved in the regulation and desentization of GPCRs. The determination of the GRK2 structure would be the first structure of a PH domain in the context of a full length modular protein, and the

determination of the complex structure would reveal the mechanism of Gβγ binding to PH domains. Lastly, the structure of GRK2 would serve as a structural model for the other GRK family members. The interdomain contacts of GRK2 would provide further insight into the regulation of GRK function as well as the role GRKs play in the desensitization of GPCRs.

The structure of the GRK2·Gβγ complex would also elucidate how Gβγ recruits GRK2 to the membrane as well as provide a structural paradigm to describe how PH domains bind to Gβγ subunits. Further information that would be determined from the complex structure could be the role of Gβγ in the desensitization of activated GPCRs. By crystallizing and solving the structure of both the GRK2·Gβγ complex and GRK2 alone, changes in structure upon Gβγ binding and membrane would hopefully be made apparent.

The determination of the crystal structure of GRK2 and the GRK2·Gβγ complex was undertaken as a way to elucidate the roles that GRK2 and Gβγ play in the homologous desensitization of activated GPCRs. In addition to the determination of the crystal structure, a series of limited protease digestions were undertaken to identify flexible regions within GRK2 and structural changes upon binding Gβγ. Finally, gel filtration and sedimentation equilibrium studies would be utilized to determine the role of membrane and detergent in the formation and crystallization of the GRK2·Gβγ complex and their ramifications for the regulation of GRK2 activity.

METHODS

Expression of Recombinant Bovine GRK2 and $G\beta_1\gamma_2$ in Sf9 Insect Cells

Sf9 cells that had been co-infected with the baculoviruses encoding the genes for GRK2-S670A, $G\beta_1$ and $G\gamma_2$-His were generously donated by the Laboratory of Robert Lefkowitz. The GRK2-S670A baculovirus vector contains a serine to alanine mutation at position 670 to remove an ERK1 kinase phosphorylation site(Pitcher, Tesmer et al. 1999). The $G\gamma_2$-His virus also contains an amino terminal hexahistidine tag for purification purposes (Kozasa 1999). The co-expression of these proteins was carried out as follows: 8 liters (16 x 500ml) of IPL-41 media supplemented with 5% fetal bovine serum (FBS) containing Sf9 cells in log phase was co-infected with baculovirus encoding GRK2-S670A, wild type $G\beta_1$ and $G\gamma_2$-His. The multiplicity of infection was between 5 and 10 for all three viruses. The infected cells were allowed to grow for 48 hours, then harvested by centrifugation (2,500*g* for 15 min) and resuspended in a final volume of 100 ml of ice-cold 25 m*M* Tris HCl pH 7.5, 100 m*M* NaCl, 5 m*M* EDTA, 5 m*M* EGTA, 2 m*M* DTT and protease inhibitors (1 mM PMSF, 1 mM benzamidine, 1 μ*M* leupeptin and 1 μ*M* pepstatin A). The resuspended cells were then transferred into two 50 ml conical tubes and immediately flash frozen in liquid nitrogen. The frozen cell pellets were then stored at 193 K.

Lysis of Sf9 cells and separation of GRK2 from $G\beta_1$ and $G\gamma_2$

Cells from one 8 liter co-expression of GRK2-S670A, wild type $G\beta_1$ and $G\gamma_2$-His were thawed in a 37° C water bath and diluted in 100 ml of ice cold 20 m*M* HEPES pH 8.0, 50 m*M* NaCl, 2 m*M* DTT, and protease inhibitors (4 μ*M* leupeptin, 4 m*M* lima bean

trypsin inhibitor, 4 m*M* PMSF and 4 m*M* TPCK). The diluted cells are briefly stirred on ice and are lysed with 10 passes of the loose pestle followed by 10 passes of the tight pestle in a 40 ml dounce homogenizer (Wheaton). This solution is then subjected to 30 one second pulses of a sonicator to ensure complete lysis. These lysed cells are transferred to ice cold 34 ml Oakridge tubes and transferred to a Beckman JA-17 rotor and centrifuged at 38,000*g* for 15 minutes (17,000 RPM). After centrifugation, the supernatant is stored on ice. The cell pellets from the centrifugation are resuspended in 100 ml of ice cold 20 m*M* HEPES pH 8.0, 50 m*M* NaCl, 2 m*M* DTT using a Virtris Vertishear tissue homogenizer on the lowest speed setting. These resuspended cells are again dounced and sonicated as this is necessary for the complete lysis of the Sf9 cells. The supernatant from the first centrifugation and the cell lysate from the second round of douncing are combined and subjected to ultracentrifugation in a Beckman type Ti-45 rotor at 186,000*g* for 45 minutes (40,000 RPM). The supernatant fraction contains all of the soluble protein including all of the GRK2 that was expressed and the pellets contain all of the membrane bound proteins including the recombinant $G\beta_1$ and $G\gamma_2$-His. The pellets are resuspended in 250 ml of 20 m*M* HEPES pH 8.0, 50 m*M* NaCl, 5 m*M* β-mercaptoethanol using the Vertishear tissue homogenizer and very slowly poured into 4 liters of liquid nitrogen. The liquid nitrogen is poured off and the popcorn-like residue is transferred to a 1 liter Nalgene bottle with holes pierced in the lid and is stored at 193K.

Purification of GRK2 from Sf9 lysate

After ultracentrifugation, the supernatant is transferred to a 500 ml beaker and diluted to a final volume of 400 ml in 20 m*M* HEPES pH 8.0, 50 m*M* NaCl, 2 m*M* DTT (buffer A) containing fresh protease inhibitors (1 μ*M* leupeptin, 1 m*M* lima bean trypsin

inhibitor, 1 m*M* PMSF and 1 m*M* TPCK). This supernatant is then applied to a 25 ml Macro-DEAE (BioRad) and a 25 ml Macro-S (BioRad) column connected in tandem at a flow rate of 3 ml/minute using a peristaltic pump. The tandem columns are then washed with 50 ml of buffer A, and the Macro S column transferred to a BioRad Duoflow HPLC. GRK2 is eluted with a 12 column volume (300 ml) gradient of 50-400 m*M* NaCl with Buffer B (20 m*M* HEPES pH 8.0, 1000 m*M* NaCl, 2 m*M* DTT) at a flow rate of 2 ml/minute and 3 ml fractions collected. The GRK2 containing fractions elute from the column at approximately 100 to 150 m*M* NaCl which corresponds to approximately 90 ml into the gradient (Fig. 8A). A further method of determining the approximate starting fractions containing GRK2 are the red tinted fractions which elute from the Macro S column just prior to GRK2.

GRK2 containing fractions are identified by SDS-PAGE and the resultant GRK2 containing fractions pooled together and diluted in 5 times their volume of 20 m*M* HEPES pH 8.0 and 2 m*M* DTT to reduce the residual NaCl from the previous step to a concentration compatible with binding to a cation exchange/heparin column. The diluted supernatant was then loaded at a flow rate of 2 ml/minute onto a 35 ml Heparin Sepharose FF column (Pharmacia), washed with 30 ml buffer A and eluted with a ~5 column volume (180 ml) 50-400 m*M* NaCl gradient in buffer B at a flow rate of 1.5 ml/minute and 1.5 ml fractions are collected (Fig. 8B). Fractions containing GRK2 elute at NaCl concentrations of between 150 mM and 220 mM (180 to 230 ml) and are identified with SDS-PAGE, pooled and diluted in 5 times their volume of 20 m*M* HEPES pH 8.0 and 2 m*M* DTT. Diluted fractions are then applied to an 8ml Source 15S column (Pharmacia), washed with 8 ml buffer A and eluted with a 12 column volume (100 ml) gradient of 50-400 m*M* NaCl in buffer B and 1 ml fractions collected. GRK2 elutes from the Source S column beginning at ~70 mM NaCl (Fig. 8C).

GRK2 containing fractions are again identified by SDS-PAGE, pooled, and concentrated to a final volume of less than 5ml in a 50 kDa molecular weight cut-off Centriprep (Millipore) (Fig. 8C). This concentrated GRK2 is then purified by gel filtration chromatography in a 16/60 Superdex 200 preparative gel filtration column at a flow rate of 0.75 ml per minute. Fractions of 1 ml volume are collected and the resulting fractions assayed by SDS-PAGE, the typical gel filtration chromatogram finds the GRK2 in (6-8) fractions with an elution volume that indicates an apparent molecular weight of (88 kDa). The fractions containing pure GRK2 are then concentrated to at least 12 mg/ml in a 50 kDa MWCO Centriprep (Millipore), and the GRK2 is then frozen down by dropping 50 μl drops of protein with a pipettor into liquid nitrogen to form frozen protein pellets. These pellets are transferred to cryovials with pierced lids and are then stored under liquid nitrogen until needed. Typical yield of GRK2 from an 8 liter prep varies widely due to quality of baculovirus and induction and generally results in 25 to 300 mg of 99% pure GRK2 (by Coomassie blue staining) (Fig. 8d). Percent yield from each step of the purification average above 85% with the exception of the Source 15S column which averages only 60%.

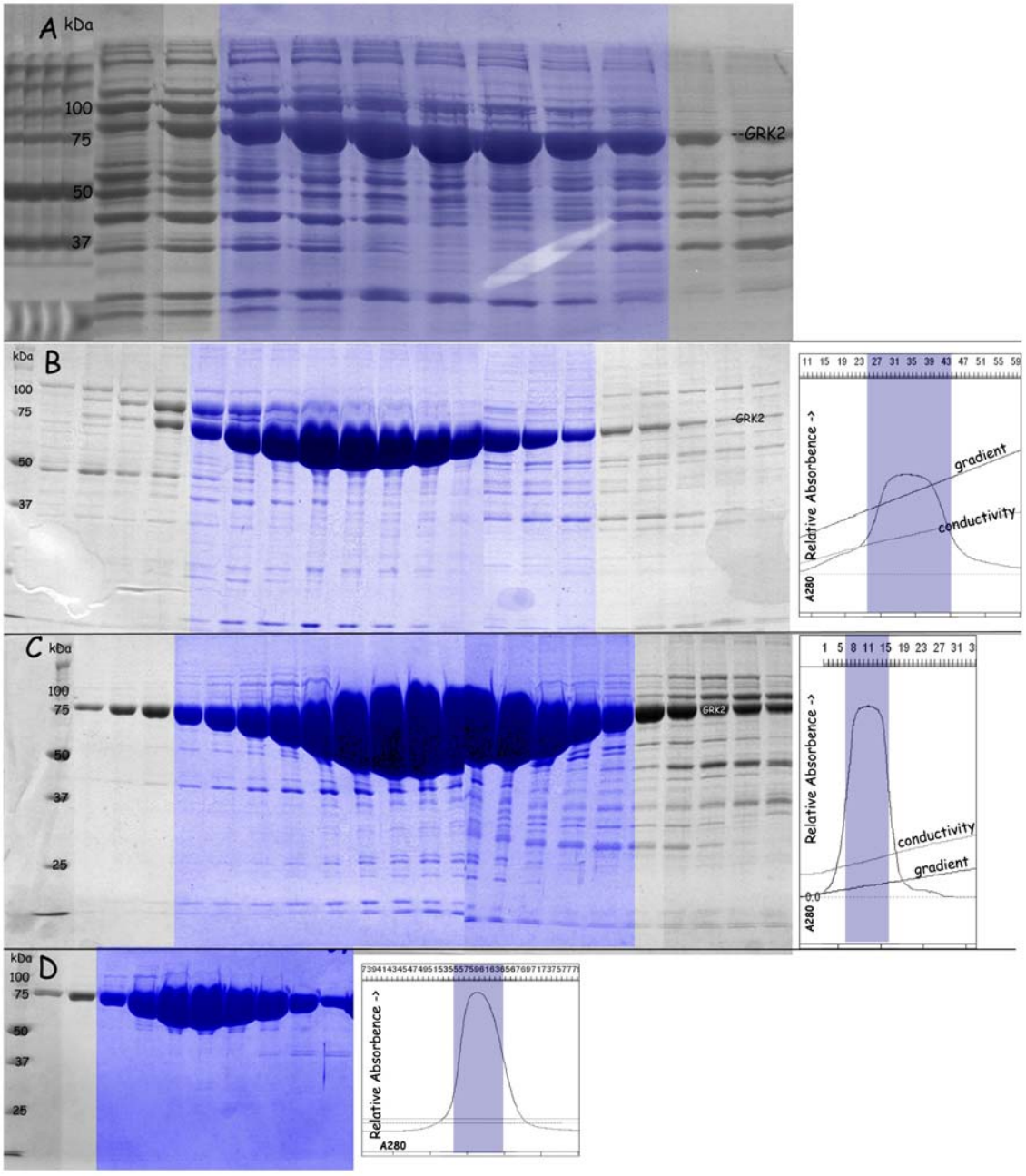

Figure 8. SDS-PAGE gels and chromatograms from a typical GRK2 purification. A. SDS-PAGE gel fractions from the Macro S column elution. Gel is of every other 3 ml fraction. All fractions containing appreciable levels of GRK2 are retained. No chromatogram is shown as the GRK2 peak is obscured by other Sf9 proteins eluting from the column. Fractions pooled and used in the next round of purification are shown in blue. B. Chromatogram and merged image of two SDS-PAGE gels of every other 1.5 ml fraction from the heparin column elution. Fractions retained for all of the following steps are chosen on the basis of purity. C. SDS-PAGE gel of elution from the Source 15S

column elution. GRK2 begins to elute from this column as soon as the NaCl gradient begins. D. SDS-PAGE gel of the final Superdex 200 preparative column. This column is used to both exchange buffer and to remove and low molecular weight contaminants. The fractions retained at this step are pooled and concentrated to >10 mg/ml, and frozen as pellets in liquid nitrogen.

Purification of $G\beta_1$ and $G\gamma_2$-His from Sf9 Membranes

$G\beta_1$ and $G\gamma_2$ are purified from the membrane "popcorn" produced when the resuspended pellets from the lysis of the recombinant Sf9 cells were poured into liquid nitrogen. The purification scheme is very similar to that described by Kozasa (Kozasa 1999). The membranes are thawed and the resultant liquid is adjusted to a final concentration of 1% cholate (w/v) with 20% (w/v) sodium cholate (Sigma). This solution is slowly stirred on ice for one hour to allow the cholate to extract the membrane bound proteins from the membrane phospholipids. After extraction, the solution is transferred to a Beckman type Ti-45 ultracentrifuge rotor and is centrifuged at 186,000*g* (40,000 rpm) for 45 minutes to remove insoluble cellular debris and intact cells.

The supernatant from the ultracentrifugation is then diluted in twice its volume of loading buffer (20 m*M* HEPES pH 8.0, 100 m*M* NaCl, 1 m*M* $MgCl_2$, 10 mM β-mercaptoethanol and 0.05% (w/v) Thesit detergent). This diluted supernatant is then applied to a 5 ml Ni-NTA Superflow resin column (Qiagen) at 4° that has been pre-equilibrated in loading buffer. The resin is then washed with 100 ml of a high salt wash (loading buffer containing 300 m*M* NaCl and 20 mM imidazole pH 8.0) to remove proteins bound to the Ni-NTA matrix by ionic interactions. The resin is then washed with 12 ml of 4° cholate wash buffer (loading buffer containing 100 m*M* NaCl, 20 mM imidazole pH 8.0, and 1% cholate) to help remove residual phospholipids. The column is then wrapped in saran wrap and placed in a 37° C incubator for 15 minutes. The column is washed with 18 ml of 37° C cholate wash buffer to bring the temperature of the resin to 37° C. The heating of the column to 37° C is necessary to allow the endogenous Sf9 Gα subunits to exchange nucleotide such that the transition state analog $GDP \cdot AlF_3$ may bind and release the Gβγ subunits in the next step.

Endogenous Gα subunits are then eluted with 30 ml of 37° Gα elution buffer (20 m*M* HEPES pH 8.0, 100 m*M* NaCl, 1 m*M* $MgCl_2$, 20 mM imidazole pH 8.0, 10 mM β-mercaptoethanol, 10 μ*M* GDP, 10 m*M* NaF, 10 μ*M* $AlCl_3$ and 1% (w/v) sodium cholate). The elution is accomplished by the loss of affinity for Gβγ by Gα upon binding of the GTP transition state analog GDP · AlF_3. The Gβγ subunits bound to the Ni-NTA column are then eluted with ice cold Gβγ elution buffer (20 m*M* HEPES pH 8.0, 100 m*M* NaCl, 1 m*M* $MgCl_2$, 150 m*M* imidazole pH 8.0, 10 m*M* β-Mercaptoethanol and 10 m*M* CHAPS detergent) and 1 ml fractions collected. Fractions are assayed by micro-Bradford assay and the protein containing fractions are pooled and diluted in thrice their volume of Mono Q low salt buffer (20 m*M* HEPES pH 8.0, 1 m*M* $MgCl_2$, 10 m*M* DTT and 10 m*M* CHAPS detergent).

Diluted protein is loaded onto a 1 ml Mono Q column (Pharmacia), is washed with 3 ml Mono Q low salt buffer and eluted with a 0-40 % gradient of Mono Q low salt buffer containing 1M NaCl. Gβγ typically elutes at a NaCl concentration of 220 mM. Fractions of 0.5 ml volume are collected and those containing Gβγ are identified by SDS-PAGE and are pooled and concentrated to at least 5 mg/ml in a 50 kDa Centricon (Amicon). Concentrated Gβγ is then aliquotted into 0.5 ml eppendorf tubes, snap frozen in liquid nitrogen, and stored at 193 K until needed. Typical yield of Gβγ from an 8 liter induction varies from 2 to 16 mg of 99% pure Gβγ by coomassie stain.

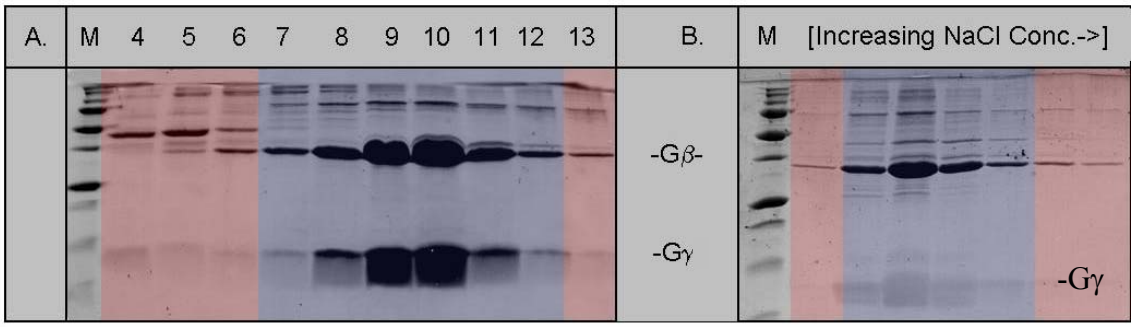

Figure 9. Purification of Gβγ. A. Ni-NTA affinity column purification. Gγ subunits have been engineered to have an amino terminal hexahistidine tag by which the Gβγ dimer is purified. Fractions are normally assayed via micro-Bradford assay and are not characterized by SDS-PAGE. Fractions retained for subsequent use or purification are tinted blue while fractions discarded are tinted red. All fractions containing enough protein such that 2 µl of fraction placed in 100 µl of Bradford reagent causes a visible blue color change are pooled and purified by anion exchange chromatography with a 1 ml Mono Q column (Pharmacia). B. Mono Q purification. Protein is diluted in a low salt buffer and bound to a Mono Q column. Protein is eluted with an increasing gradient of NaCl. Fractions are analyzed via SDS-PAGE and the cleanest fractions are pooled. Depending on purity, Gβγ is either purified further by gel filtration chromatography on tandem Superdex 200 columns or is frozen down in small aliquots. This particular preparation of Gβγ was further purified when it was used to make a GRK2·Gβγ complex. Gγ is only faintly visible on the second gel because it does not retain stain when the gel is completely destained.

Reconstitution and Purification of the GRK2 · Gβγ Complex

To reconstitute the GRK2·Gβγ complex, GRK2 was mixed with excess Gβγ in order to facilitate separation of the complex from uncomplexed protein by gel-filtration chromatography. GRK2 and Gβγ concentrations were determined by the Bradford assay and the proteins were then mixed together in a mass ratio of 0.85 (which equates to approximately a 2:3 molar ratio of GRK2:Gβγ) in a buffer containing 20 m*M* HEPES pH 8.0, 50 m*M* NaCl, 10 m*M* CHAPS, 5 m*M* ATP, 10 m*M* $MgCl_2$ and 1 m*M* DTT. After incubation on ice for at least 30 minutes, the GRK2-Gβγ complex was injected onto two 10/30 Superdex 200 columns connected in tandem that had been pre-equilibrated with 20 m*M* HEPES pH 8.0, 50 m*M* NaCl, 10 m*M* CHAPS, 1 m*M* ATP, 1 m*M* $MgCl_2$ and 2 m*M* DTT. When compared with gel-filtration standards (BioRad), the GRK2/Gβγ/detergent micelle mixture elutes in two peaks with effective molecular weights of 180-150 and 70-65 kDa respectively. The 180 kDa peak was consistent with a 1:1 complex between GRK2 and Gβγ bound to a CHAPS detergent micelle and the 70 kDa peak to a Gβγ-CHAPS detergent micelle complex. SDS-PAGE and sedimentation equilibrium studies corroborate this assignment. GRK2 eluted from the same gel-filtration columns in the same buffer with an effective molecular weight of 110 kDa. Omission of ATP from the running buffer delays the elution time of the GRK2-Gβγ complex, indicating that the GRK2 loses some of its affinity for Gβγ in the absence of ATP. Crystals grown from protein thus purified were also much smaller in size and ill-formed compared with those grown in the presence of ATP. Peak fractions of the complex were pooled, concentrated to 12 mg/ml and frozen as 50 µl pellets in liquid nitrogen. Excess Gβγ was saved from multiple runs, concentrated and recycled for use in future reconstitutions.

Frustratingly, the formation of crystals was found to be dependant on the preparation of the complex. Approximately one half of all complex purifications were unable to crystallize. Upon analysis of all preparations of GRK2-Gβγ complex, it appears that the higher the apparent molecular weight of the complex coming off of the gel filtration columns, the more likely that the GRK2-Gβγ complex would crystallize. The apparent molecular weight of the GRK2-Gβγ complex is dependant on the loading concentration of the gel filtration columns. The more complex that was loaded, the higher the apparent molecular weight of the complex and the more likely the GRK2-Gβγ complex would crystallize. As long as the apparent molecular weight was higher than ~165 KDa and the amount of protein originally loaded onto the gel filtration column was more than 2.1 mg of total protein GRK2·Gβγ crystals formed. When less than 2 mg of total protein was loaded onto the gel filtration column, the apparent molecular weight of the complex was smaller (<155 kDa) and usually failed to crystallize. Surprisingly, the SDS-PAGE gels for complexes that crystallize and those that do not both appear to have a 1:1 ratio of GRK2 to Gβγ although they vary in where they come out of the gel filtration column. It is likely that the dilution of GRK2·Gβγ complex during the gel filtration process brings the concentration of GRK2 and Gβγ down to a point the concentration favors monomer species rather than complex.

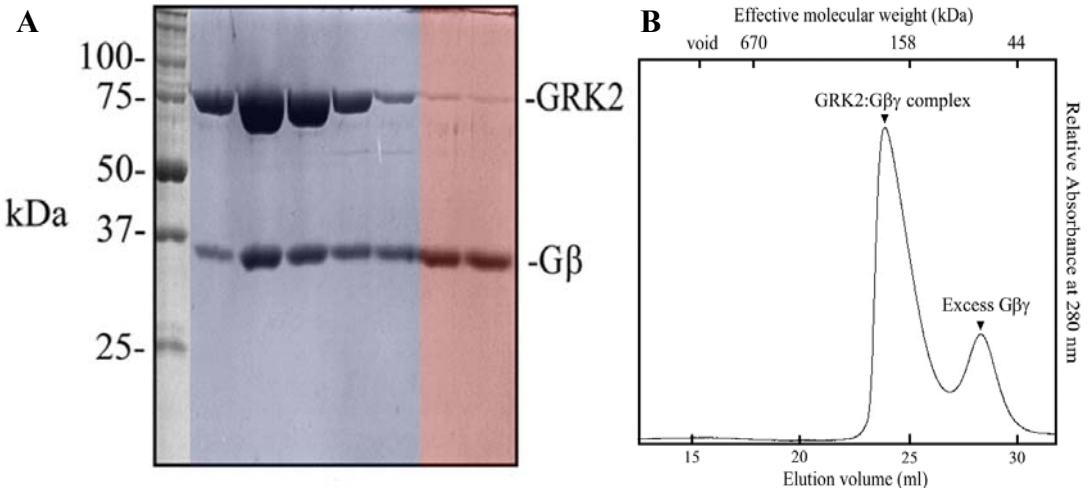

Figure 10. Typical Purification of the GRK2·Gβγ complex. A. SDS-PAGE analysis of fractions eluted from the gel-filtration column. The leftmost lane contains BioRad Precision protein standards. Fractions pooled and utilized in crystallization trials are shown in blue while those pooled for use in later complex purifications are shown in red. B. Separation of the GRK2-Gβγ complex from excess Gβγ using two tandem Superdex 200 gel filtration columns. The molecular weights listed at the top of the chromatogram correspond to the molecular weights of gel-filtration standards (BioRad) eluted under the same conditions.

Crystallization of GRK2 and Cryoprotection

In order to identify possible crystallization conditions, purified GRK2 at a concentration of 10 mg/ml was set up at room temperature in a series of hanging drop screens. These included sparse matrix screens (Jancarik and Kim 1991) as well as a series of rational screens which consisted of pH being varied along the X direction and various molecular weights of polyethylene glycol (PEG) concentration in the Y dimension with either 100 mM or 1 M NaCl being present in all wells. After approximately 100 of these initial screens it became obvious that GRK2 would not crystallize at room temperature. Interestingly, at conditions similar to the final crystallization conditions, small spherolites and objects resembling coral did form. Upon setting up similar screens at 4 ºC, poorly formed initial crystals were observed in conditions that consisted of 100 mM ACES pH 7.0, 1 M NaCl and 12% PEG 8000. Upon further optimization, the highest quality crystals were found to grow in the following conditions 100 mM HEPES pH 7.5 – 8.0, 1 M NaCl, 1 M urea, 2.5%-5% (v/v) glycerol and 9.5%-11.5% Peg 8000. A possible explanation for the increase in crystal quality with the addition of 1M urea would be the suppression of secondary interactions between monomers that are not conducive to crystallization. Crystals can be grown from well solutions containing urea concentrations of up to 2.5M. Crystals of similar diffraction quality were grown from the above conditions with the substitution of 1 M KBr for the NaCl and 5% ethylene glycol for the glycerol.

Crystals were freed from a sticky gel-like skin by diluting the hanging drop with a similar volume of cryo solution and carefully excising them from the skin with an eye scalpel (Beaver) or Cryoloop (Hampton Research). The GRK2 crystals were then transferred to a cryoprotectant solution containing 75% well solution and 25% of a

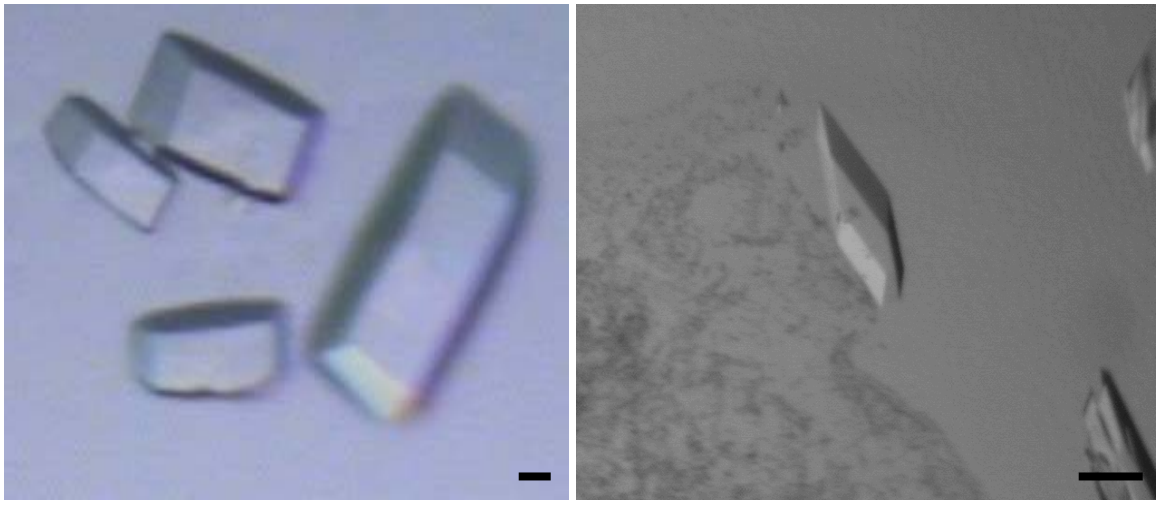

Figure 11. Crystals of GRK2 and GRK2·Gβγ. A. Crystals of GRK2. Crystals nucleate at 277 K over the course of one to two weeks and reach maximum size after one month. Crystals belong to space group P2 and resemble large blocks. Crystals have typical dimensions 1000 x 250 x 250 μm. B. Crystal of the GRK2-Gβγ complex. Crystals of the GRK2-Gβγ complex nucleate over the course of 10-20 days at 277 K and reach maximum dimensions (typically 350 × 150 × 50 μm) after one month. Crystals are shaped like thin diamonds, with the 350 μm and 150 μm lengths corresponding to the long and short axes of the diamond, respectively. The scale bar corresponds to 100 μm.

solution containing 20 mM HEPES pH 8.0 in ethylene glycol and allowed to equilibrate for 5 minutes. Crystals were then removed from the cryoprotectant solution with a crystal loop (Hampton Research) and immediately flash frozen in liquid nitrogen.

Crystallization and Cryoprotection of GRK2-Gβγ

Small plate-like crystals of GRK2-Gβγ complex were initially observed in a two-dimensional hanging-drop screen using PEG 3350 (5-20%) *versus* pH (5-7.5) as the variable parameters. All wells also contained 1 *M* NaCl. Upon further optimization, the best quality crystals grew from hanging drops containing 1 µl complex at ~12 mg/ml and 1 µl of a well solution containing 100 m*M* MES pH 5.25, 200 m*M* NaCl, 1 m*M* inositol-3,4,5-triphosphate (IP_3), 1 m*M* $MgCl_2$, 1 mg/ml mastoparan and 6.9-7.8% PEG 3350 suspended over 1 ml of the well solution. IP_3 was included as a soluble analog of the head group of PIP_2, a regulator of GRK2 (Pitcher, Fredericks et al. 1996). Mastoparan, a peptide derived from wasp venom, was included as a soluble mimic of activated GPCR(Tanaka, Kohno et al. 1998). Diffraction quality crystals also grew in the absence of IP_3, mastoparan and phosphatidylserine. It is interesting to note that there is no electron density observed for IP_3 or ATP in the crystals grown under these conditions.

Crystals were equilibrated in a cryoprotectant solution containing 25% ethylene glycol, 8% PEG 3350, 20 m*M* HEPES pH 8.0, 100 m*M* MES pH 5.25, 300 m*M* NaCl, 1 m*M* DTT, 2 m*M* $MgCl_2$, 1 m*M* IP_3, 1 m*M* ATP and 10 m*M* CHAPS by gradually adding cryoprotectant to the hanging drop in 0.5 µl aliquots. Crystals were then transferred to a 100% cryoprotectant solution using an appropriately sized cryoloop (Hampton Research) and allowed to equilibrate for 5-10 minutes. The crystals were then suspended in a cryoloop and immediately flash frozen in liquid nitrogen.

Limited proteolysis assays of GRK2

In order to assess the conformational flexibility of GRK2 and changes upon ligand binding, we set out to perform a series of limited proteolytic digests. As a starting point, GRK2 alone was titrated with serial dilutions of several proteases including endoprotease Asp-N (Endo-Asp-N), clostripain, trypsin and thrombin. Amounts of protease were chosen such that only after 24 hours was the full length GRK2 completely digested into 2-3 fragments. It was decided to utilize clostripain and Endo-Asp-N as the results achieved with trypsin and thrombin either left all of the protein uncut or completely digested it over the course of 1 hour. Furthermore, the cut sites for both clostripain and Endo-Asp-N cut GRK2 in only a few sites that eventually turned out to be in flexible regions protected by ligand binding or proximity to CHAPS detergent molecules.

A time course for the proteolysis of GRK2 with increasing amounts of Endo-Asp-N found that the optimal ratio of protease and GRK2 for limited proteolysis was 185 units of Endo-Asp-N per μg of GRK2. This ratio was used for subsequent digests. Proteolysis of GRK2 by increasing amounts of clostripain revealed that the optimal amount of clostripain per μg of GRK2 was 2.5×10^{-5} units. One unit is defined as the amount of enzyme that will hydrolyze 1.0 mmol of N-tosyl-arginine methyl ester per minute at 25°C at pH 8.0. Proteolytic digests were analyzed by matrix assisted laser desorption ionization (MALDI) mass spectroscopy and their identities assigned by comparing molecular weights to possible protease fragments. Analysis of the Endo-Asp-N digests revealed a single major cut site at position 480, but the assignment of clostripain cut sites with MALDI data was unsuccessful. To correctly assign sites within clostripain digests it was necessary to identify the proteolytic fragments using both

amino-terminal sequencing and MALDI spectroscopy. This tandem approach identified two major clostripain cut sites, at Arg^{404} and at Arg^{660}.

The activity of Endo-Asp-N in the presence and absence of CHAPS detergent was measured due to the apparent partial protection of GRK2 conferred by CHAPS. These activity assays utilized azocoll substrate (EMD Biosciences) a chemically modified collagen which when subjected to proteolysis liberates a red azo dye (Moore 1969; Braganza and Simmons 1991; Poilane, Karjalainen et al. 1998). The amount of dye liberated is directly proportional to the activity of a protease and can be quantified by measuring the absorbance at 510nm in a spectrophotometer. The protease activity assays were performed as follows: 50 mg of azocoll substrate was dissolved in 5ml of standard proteolysis buffer (20 mM HEPES, 200 mM NaCl and 2 mM DTT) in the presence and absence of 10mM CHAPS detergent. At all times the solutions were protected from light. One ml of each solution was aliquotted into four 2 ml tubes and 5 units of freshly reconstituted Endo-Asp-N was added to three of the tubes (the last tube was reserved for use as a blank). Theses tubes were transferred to a 30° heat block and were mixed every five minutes by inverting twice over the course of 1.5 hours. After this incubation, tubes were transferred to a 4° centrifuge and the insoluble dye was removed by centrifugation at 14,000 x g for 5 minutes. Absorbencies at 510 nm were read in a Beckman DU530 spectrophotometer utilizing a 1 ml portion of the buffer dye mixture that had been incubated at 30° along with the samples containing dye as a blank. Absorbencies of the digests containing CHAPS revealed that Endo-Asp-N is 18.5% more active in the presence of CHAPS detergent. In terms of units, 1 μg of Endo-Asp-N is equal to 48.5 units in the absence of CHAPS detergent whereas in the presence of CHAPS it has an activity of 66.25 units.

X-RAY STRUCTURE DETERMINATION

Initial Data Collection and Processing of GRK2-Gβγ

A complete data set of the GRK2-Gβγ complex crystals (346 frames with 30 min 0.5° oscillations totaling 173°) was collected with a Rigaku RU-200H Cu *K*α X-ray source using Osmic confocal mirrors and a MAR345 imaging-plate system. A cold stream from an Oxford Instruments Cryojet maintained the temperature of the crystal at 90 K. The GRK2·Gβγ complex crystals belong to space group *C*2, with unit-cell parameters a = 187.0, b = 72.1, c = 122.0 Å, β= 115.2° (See Table 1). The crystals have a Matthews coefficient (V_M) of 2.5 $Å^3$ / Da (Matthews 1968) suggesting that only one complex is found in each asymmetric unit. Exposures of one hour yielded higher resolution diffraction, indicating that a synchrotron source would allow the collection of superior data. The data were reduced and scaled together using the *HKL* package (Otwinowski and Minor 1997). Analysis using the crystallographic program *TRUNCATE* (CCP4 1994) indicated that the diffraction intensities are severely anisotropic, with the highest resolution data extending in a direction nearly bisecting the a^* and c^* axes (~3.2Å) and the weakest extending along the b^* axis (~4.1Å). This anisotropy obscures the presence of well measured reflections in some directions in the highest resolution shells.

Initial phases were generated by molecular replacement as implemented by the program *MOLREP* (CCP4 1994) using the structure of $G\beta_1\gamma_2$ (PDB entry 1GG2, 100% identity) (Wall, Coleman et al. 1995) as a search model. Subsequent rounds of molecular replacement using either a homology model of the kinase domain based on the structure of PKA (PDB entry 1ATP, 32% identity) (Smith, Radzio-Andzelm et al. 1999), a

homology model of the RH domain based on the structure of axin (PDB entry 1DK8, 25% identity), or the NMR structure of the GRK2 PH domain (PDB entry 1BAK, 100% identity) failed to yield convincing solutions. Solvent flattened maps phased by the $G\beta_1\gamma_2$ molecular replacement solution were then compared to the candidate molecular replacement solutions for the PKA homology model. This comparison allowed the placement of the large lobe of the kinase domain. Another round of molecular replacement utilizing just the small lobe of the kinase domain successfully placed the small lobe. Solvent flattened maps phased with the molecular replacement solutions of $G\beta\gamma$ and the kinase domains revealed the position of the carboxyl-terminal helix in the PH domain. This allowed the placement of the energy minimized model from the NMR GRK2 PH domain structure that had the loop regions excised close enough to the correct position that rigid body refinement in *CNS* was able locate it correctly in the electron density map. A final round of molecular replacement utilizing a homology model based on the RH domain of axin failed to find a solution. Solvent flattened maps phased by the model consisting of $G\beta\gamma$ and GRK2 minus the RH domain allowed the RH domain to be built by hand.

Model building was performed using the program O (Jones, Zou et al. 1991), alternating with simulated annealing, individual B-factor refinement and gradient minimization in CNS(Brunger, Adams et al. 1998). During each round of refinement and model building, the structure was analyzed with *PROCHECK* (CCP4 1994) and care was taken to minimize all stereochemical outliers. In the later rounds of refinement, CNS's composite omit maps were useful to reveal parts of the structure that that had been misbuilt or had previously could not be built. After eleven iterations of model building, model analysis and refinement, no improvements were seen in the stereochemistry of the model or in the R factors (R_{work} 27.3, and R_{free} 37.8) and no additional information was

apparent in the electron density maps. The final model of the low resolution complex structure consists of residues 30-430, 437-474, 501-549 and 553-666 (of 689 total residues) in GRK2, residues 10-126 and 132-340 (of 340 total residues) in $G\beta_1$ and residues 9-68 (of 68 total) in $G\gamma_2$ (Table 1).

High Resolution GRK2·Gβγ Data Collection and Initial Data Processing

Diffraction maxima were collected at the Advanced Light Source, Beamline 8.2.1. The intense highly collimated x-ray beam allowed the collection of diffraction data at a much higher resolution than had been previously achieved using a *Cu Kα* x-ray source. The maximum resolution for the GRK2 crystals improved from ~ 6.2 to approximately 3.98 Å and the resolution for the GRK2·Gβγ complex improved from a maximum resolution of ~ 3.4 Å to ~ 2.4 Å (Table 1).

Analysis of the data sets using *TRUNCATE* once again indicated severe anisotropy in the GRK2-Gβγ complex crystals. This was probably due to the fact that the crystals were quite thin in one dimension and indeed, the direction in which the anisotropy exists corresponds to this direction. To address the anisotropy within the high resolution complex data set, mock precession photos were generated using the program *HKLVIEW* (CCP4 1994) and were used to define the axes along which the anisotropy existed. These axes were used to define a three-dimensional ellipsoid that contained all well measured reflections with a generous border. Those reflections falling outside of the ellipsoid were subjected to a -2 sigma cutoff. This process was necessary to remove the poorly measured reflections due to the anisotropy and was able to improve the initial maps that were generated from the data. Data were then scaled using the adsorption correction features in *HKL2000* (Otwinowski 1997).

Table 1. Structure determination and refinement statistics

Data Set	Low Resolution GRK2·Gβγ	ALS Beamline 8.2.1 GRK2·Gβγ	ALS Beamline 8.2.1 GRK2 Soluble
Wavelength (Å)	1.5418	1.000	1.000
D_{min} (Å, direction 1, b*, direction 3)[a]	3.2	2.4, 2.8, 3.0	3.98
Spacegroup	C2	C2	P2
Molecules in A.S.U	1	1	4
Cell constants (Å, °)	a= 187.0 b= 72.1 c= 122.0 β= 115.2	a= 188.2 b= 72.4 c= 122.7 β= 115.2	a= 115.2 b=82.2 c=218.8 β=95.6
Mosaicity (°)	1.2	0.83	0.4
Unique reflections	23,608	38,258	34,766
Average redundancy	3.4	2.4	3.73
R_{sym} (%)[b]	9.6 (50.3)	5.3 (25.3)	3.8 (99.9)
Completeness (%)[c,d]	98.2 (97.3)	73.6 (12.7)	99.9 (99.9)
<I>/<σI>	12.5 (2.6)	15.3 (2.7)	15.8(0.7)
Refine Resolution (Å)	25 to 3.0	20 to 2.5	20 to 4.0
Total Reflections	81,000	36,307	127,754
Protein atoms	8682	8133	20034
Water molecules	0	26	0
RMSD bond lengths (Å)		0.024	0.021
RMSD bond angles (°)		2.035	1.759
RMSD bonded *B* factors (Å^2)		1.9	0.183
R_{work}[e]	27.2	20.2	26.6
R_{free}[f]	37.8	25.2	33.7
Average *B* factor (Å^2)	83	27.9	50.6

[a]Because of anisotropy, data beyond these limits were excluded during scaling and refinement. Direction 1 is 37.9° inclined from *a** in the *a**-*c** plane, and direction 3 corresponds to direction 1 x *b**.

[b] $R_{sym} = \Sigma_h\Sigma_i|I(h) - I(h)_i|/\Sigma_h\Sigma_i I(h)_i$, where $I(h)$ is the mean intensity after rejections.

[c]Numbers in parentheses correspond to the highest resolution shell of data, which was 3.3 to 3.2 Å for the Cu *Kα* data set and 2.59 to 2.5 Å for the ALS data set and 3.9 -4.08 for the GRK2 soluble data set.

[d]Before ellipsoidal truncation of the data, completeness was 97.4% (90.8% in the highest shell).

[e] $R_{work} = \Sigma_h||F_{obs}(h)| - |F_{calc}(h)||/\Sigma_h|F_{obs}(h)|$; no I/σ cutoff was used during refinement.

[f]5.1% of the truncated data set was excluded from refinement to calculate R_{free}. During the last three rounds of model building, all data were included in refinement.

Molecular Replacement and Refinement using CNS

An initial molecular replacement solution for the high resolution GRK2·Gβγ data set was found using the program *MOLREP* (CCP4 1994) utilizing the low resolution GRK2·Gβγ complex structure as a search model and the anisothermal correction option. Initially the model was refined using the simulated annealing, gradient minimization and individual B-factor refinement features of the CNS program suite(Brunger, Adams et al. 1998). While the stereochemical statistics of the model that was refined with CNS were acceptable, the R factors were high for a structure of this resolution (R_{work} = 30% R_{free} = 35%) and the average B factor for the complex was unacceptably high ~80 $Å^2$.

Modeling Atomic Displacement and Model Building

Various methods for modeling atomic displacement parameters (ADPs) exist including isotropic and individual anisotropic B-factor refinement and torsional librational screw (TLS) refinement. Isotropic atomic displacement is the most common choice for the refinement of structures at low to medium resolution but its limitation is that it assumes that any atom is displaced from its mean position uniformly in all directions. Anisotropic temperature factors model the atomic displacement of each atom individually as an ellipsoid defined by six parameters. Without high resolution x-ray data, anisotropic temperature factors increase the ratio of parameters to observations to an unacceptable level because each atom acquires six parameters to represent its thermal motion. Conversely, TLS refinement does not effect a large change in the ratio of observations to parameters when large groups of atoms are used because in TLS refinement only twenty parameters are fit per group of atoms. Furthermore, TLS

refinement can help to model ADPs due to anisotropy within the data, thus improving maps derived from anisotropic data.

To remedy the high R-factors and B factors within the CNS refined model it was decided that the isotropic B factors refined by CNS were insufficient to model the atomic displacements within the structure. The program *REFMAC* (Winn, Isupov et al. 2001) with it implementation of TLS refinement for the modeling of ADPs was utilized for 17 additional rounds of refinement.

The TLS convention of modeling atomic displacement parameters represents the shared translational and librational motions of pseudo-rigid groups of atoms within the asymmetric unit of the crystal (Winn, Isupov et al. 2001). The structure is divided up into groups based on their expected shared molecular motions and three matrices defining tensors along which these motions occur are refined prior to isotropic temperature factor refinement. The T matrix defines three tensors on which shared translational movements within a defined group of atoms occur while the L matrix describes another three tensors describing the librational movements within the same group. The S matrix defines the relationship between the movements along the T and L tensors (Cruickshank 1956; Schomaker and Trueblood 1998).

TLS groups utilized for the modeling of ADPs of protein structures generally consist of domains or subdomains and include all ligands associated with the domain or subdomain, but in the case of high resolution data, they can correspond to secondary structural elements or even individual amino acid sidechains (Winn, Isupov et al. 2001). These groups are should consist of groups of atoms that are thought to share ADPs. It is important that all of the atoms within the structure are included in a TLS group because the temperature factors for atoms excluded from TLS groups become artificially inflated. The best choice of number and members of groups is determined empirically through the

examination of the model for regions that might have shared ADPs, electron density maps and R-factors after TLS refinement.

For the GRK2·Gβγ complex many combinations of TLS groups were attempted, but the best improvements in R-factors and in the quality of the electron density maps occurred when we chose the following TLS groups: the RH domain (residues 29-187 and 512-550 of GRK2), the large lobe of the kinase domain (residues 275-475 and 496-511 of GRK2), the small lobe of the kinase domain (residues 188-274 of GRK2), the PH domain (residues 551-569 and 576-668 in GRK2) and all of Gβγ. Refinement using these groups in REFMAC resulted in improvements in the model including an improvement in R_{work} from 24.1 to 20.2 percent and in R_{free} from 31.0 to 24.9 percent. Furthermore, the average temperature factor decreased from 80.0Å^2 to 28.9Å^2 and the quality of the electron density maps increased such that additional residues were able to be built in regions previously seen to be completely disordered.

All model building was performed in *O*, and during model building the structure was analyzed using *PROCHECK*. Again, care was taken to minimize stereochemical outliers during model building. The final refined GRK2·Gβγ model spans residues 29 to 475, 496 to 569, and 576 to 668 of GRK2 (out of 689 total), residues 2 to 340 of $G\beta_1$ (out of 340), and residues 8 to 68 of $G\gamma_2$ (out of 68). The final model has 99.4% of its residues within the allowed or additionally allowed regions in the Ramachandran plot and no disallowed residues. (Table 1, Fig. 12)

Molecular Replacement and Refinement of GRK2 Soluble Data

The GRK2 crystal structure was solved using the molecular replacement program, *MOLREP* with the GRK2 portion of the GRK2·Gβγ complex structure as the search

model. This rotation function gave peak heights of ~7.5 sigma and found four molecules per asymmetric unit using resolution limits of 30 to 4 Å. The correlation coefficient rose from 0.375 for one molecule to 0.545 for all four. The structure contains the four GRK2 molecules arranged as two sets of dimers whose dimer axes are inclined ~83° with respect to one another. This was an improvement on the molecular replacement results achieved with a 6.2Å home source dataset where it was only possible to place three of the four monomers in the asymmetric unit and it was not apparent where the fourth monomer could be placed. The GRK2 crystals belong to spacegroup P2 with unit cell parameters of a= 115.2 Å b=82.2 Å c=218.8 Å and β=95.6° (Table 1). This solution yields a Matthews coefficient (V_m) of 3.2 (62% solvent) possibly accounting for the poor diffraction resolution and high levels of diffuse scatter observed from the GRK2 crystals.

For the refinement of the structure, it was again necessary to utilize the TLS refinement features of *REFMAC*. Initially, the refinement was attempted using CNS, but the models arising from simulated annealing and gradient minimization options gave extremely high R-factors in the neighborhood of 50% which only increased during subsequent rounds of refinement and therefore were abandoned. Refinements utilizing *REFMAC* were determined to be more stable and resulted in lower R factors as well as allowing the modeling of shared domain motions within the structure. In order for *REFMAC* refinements to proceed, it was necessary to turn off the default bulk solvent correction and instead choose a simple bulk solvent model with resolution cutoff of 8 Å to 6Å. This also was a requirement for the TLS portion of the refinement to remain stable.

As there are four monomers in the asymmetric unit it was possible to refine the structure using the non-crystallographic symmetry present in the structure. By examining the TLS groups from the GRK2·Gβγ structure and adapting them to the range of residues

present within the GRK2 soluble structure new TLS groups for refinement were defined. These TLS groups formed a basis for the definitions of the NCS groups. The NCS groups chosen comprise 4 groups; the terminal subdomain of the RH domain (29-77, 159-185 and 513-547), the bundle subdomain of the RH domain (78-158), the kinase domain (186-512), and PH domain (548-655). The use of NCS restraints should not obscure changes in the orientations of the individual domains to one another, because the movement of NCS groups compared to one another is not restrained. Nine rounds of *REFMAC* refinement utilizing TLS refinement and loose NCS restraints followed by model building in *O* while analyzing stereochemistry with *PROCHECK* were performed. During each round of refinement all residues were made to conform to the allowed or additionally allowed regions of the Ramachandran plot. The final model consists of residues 29-474, 494-569 and 575-656 in monomer A, residues 29-475, 493-570, and 575-656 in monomer B, residues 29-474, 494-569 and 575-656 in monomer C, and residues 29-474, 494-569 and 575-656 in monomer D (Table 1, Fig. 13). This structure revealed the positions of several residues that were unseen in the complex structure (residues 493-495 in all four monomers) but lacked residues 657-670 which were apparent in the GRK2·Gβγ complex structure. The final model has 99.7 % of its residues in the allowed or additionally allowed regions of the Ramachandran plot and no disallowed residues (Fig. 13).

Figure 12

Ramachandran Plot

GRK2·Gβ$_1$γ$_2$ Complex

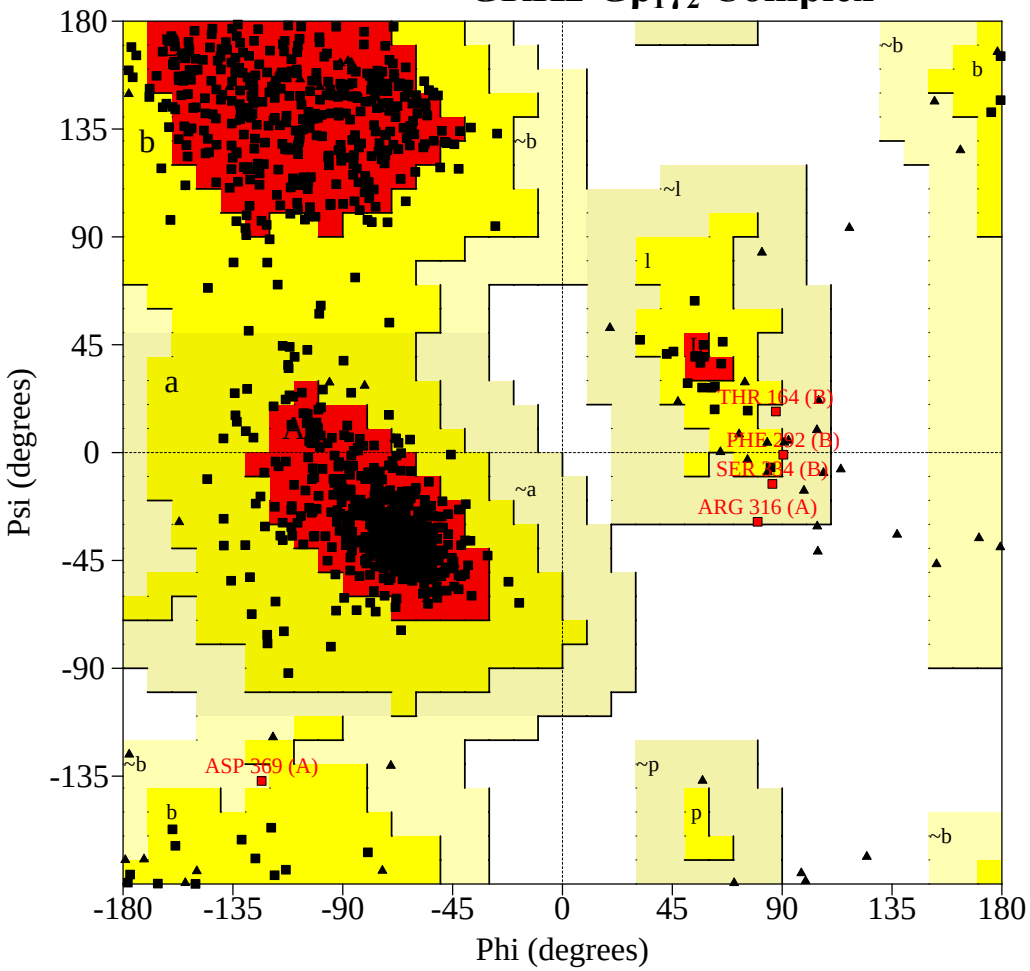

Plot statistics

Residues in most favoured regions [A,B,L]	780	85.9%
Residues in additional allowed regions [a,b,l,p]	123	13.5%
Residues in generously allowed regions [~a,~b,~l,~p]	5	0.6%
Residues in disallowed regions	0	0.0%
Number of non-glycine and non-proline residues	908	100.0%
Number of end-residues (excl. Gly and Pro)	7	
Number of glycine residues (shown as triangles)	63	
Number of proline residues	36	
Total number of residues	1014	

Based on an analysis of 118 structures of resolution of at least 2.0 Angstroms and R-factor no greater than 20%, a good quality model would be expected to have over 90% in the most favoured regions.

Figure 13

Ramachandran Plot

GRK2 Soluble Structure

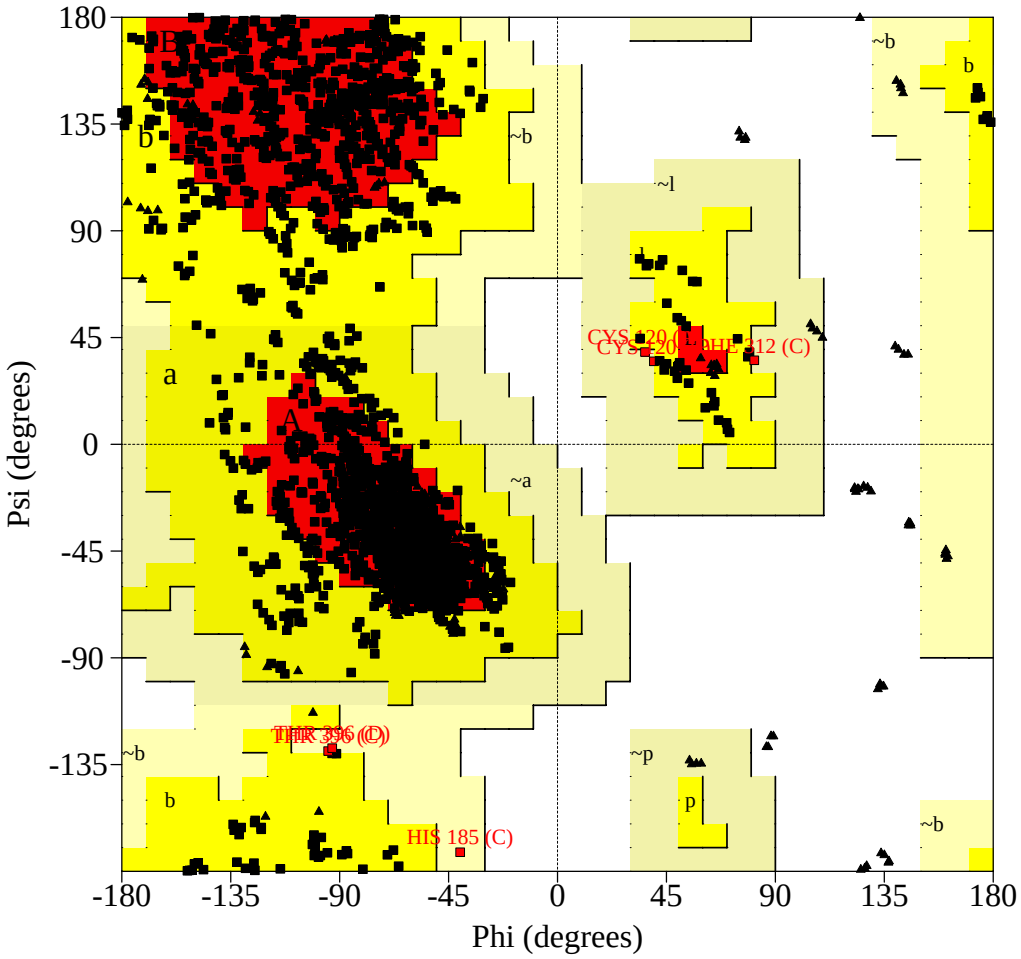

Plot statistics

Residues in most favoured regions [A,B,L]	1705	80.1%
Residues in additional allowed regions [a,b,l,p]	417	19.6%
Residues in generously allowed regions [~a,~b,~l,~p]	6	0.3%
Residues in disallowed regions	0	0.0%
	----	------
Number of non-glycine and non-proline residues	2128	100.0%
Number of end-residues (excl. Gly and Pro)	23	
Number of glycine residues (shown as triangles)	141	
Number of proline residues	100	

Total number of residues	2392	

Based on an analysis of 118 structures of resolution of at least 2.0 Angstroms and R-factor no greater than 20%, a good quality model would be expected to have over 90% in the most favoured regions.

Modeling of the GRK2:Gβγ:GPCR:$G\alpha_q$ Complex

The kinase domain of GRK2 was first modeled in a closed conformation similar to those observed for PKA (Madhusudan, Akamine et al. 2002) and PKB(Yang, Cron et al. 2002; Yang, Cron et al. 2002). This conformational change brings the large lobe of the kinase domain up towards the membrane as defined in Fig. 15 (compare Fig. 15B with Fig. 23B). The crystal structure of inactive rhodopsin (Okada, Fujiyoshi et al. 2002), used as a rough model of an activated GPCR, was positioned such that the exposed hydrophobic residues of its transmembrane helices were within the plane of the membrane defined by the GRK2:Gβγ complex. The receptor was then rotated and translated within the plane of the membrane until its C-terminal tail was in an appropriate orientation to enter the polypeptide binding cleft of GRK2, and residues within the cytosolic loops of rhodopsin known to be involved in binding GRKs were juxtaposed with the kinase domain. The homology model of $G\alpha_q$ (dark blue) was built based on the structure of $G\alpha_i$ in complex with RGS4 (Tesmer, Sunahara et al. 1997) omitting the flexible amino-terminal helix. $G\alpha_q$ was positioned with respect to the modeled membrane (Fig. 23b) by docking it against the Gβγ subunits of the GRK2:Gβγ complex in a similar orientation as $G\alpha_i$ in the $G\alpha i1G\beta_1\gamma_2$ structure (Wall, Coleman et al. 1995). $G\alpha_q$ was then translated and rotated within the plane of Fig. 23a until its switch regions (red) packed snuggly against the $G\alpha_q$-binding residues identified in the RH bundle subdomain of GRK2 (Sterne-Marr, Tesmer et al. 2003).

THE GRK2·Gβγ COMPLEX STRUCTURE

G protein coupled Receptor kinase 2 (GRK2) consists of three modular domains: a predominantly amino-terminal RGS (regulator of G protein signaling) homology (RH) domain (Siderovski, Hessel et al. 1996), a central protein kinase domain (Benovic, DeBlasi et al. 1989) that belongs to the AGC superfamily of kinases, and a C-terminal pleckstrin homology (PH) domain (Fushman, Najmabadi-Haske et al. 1998; Lodowski, Pitcher et al. 2003). The RH and kinase domains are common to all GRKs, whereas the PH domain is unique to GRK2 and GRK3 (Fig. 14). Gβγ binds to the PH domain of GRK2 (Koch, Inglese et al. 1993) and greatly enhances the phosphorylation of activated GPCRs, at least in part by recruiting the enzyme from the cytoplasm to the plasma membrane (Pitcher, Inglese et al. 1992). To a lesser extent, activation of GRK2 is also dependent on the binding of anionic phospholipids to the PH domain (Pitcher, Touhara et al. 1995; DebBurman, Ptasienski et al. 1996).

We have determined the x-ray crystal structure of the complex between bovine GRK2 and Gβ1γ2 in detergent micelles. The atomic structure of GRK2 reveals how its RH, kinase, and PH domains integrate their activities to bring the enzyme to the membrane in an orientation that facilitates receptor phosphorylation. This orientation allows for the simultaneous desensitization of GPCRs while binding up free both free GTP-Gα and Gβγ subunits. Furthermore, the GRK2-Gβγ complex serves as a model for the interaction between Gβγ and the PH domains of other important effector enzymes, including phospholipase Cβ (PLCβ) (Razzini, Brancaccio et al. 2000).

Figure 14. Primary and Secondary Structure of GRK2

A) Structural alignment of RH domains from GRKs, RGS4 and RhoGEFs. In all panels, the elements of secondary structure are labeled according to the established convention for each domain. Coils correspond to α-helices, arrows to β-strands. The left column contains the acronym of the protein from which the sequence is derived. Sequence numbering and secondary structure along the top of the alignment corresponds to that of bovine GRK2. Within the alignment, gray amino acids are not observed or included in an atomic structure (if known). Within this specific panel, gray columns indicate conserved contributions to the hydrophobic core of the RH domain. Residues from GRK2 highlighted in orange or yellow are those that form the interface with the PH or kinase domain, respectively, and those highlighted in violet have been identified to be important for binding $G\alpha_{q/11}$ (Sterne-Marr, Tesmer et al. 2003). Residues from RGS4 highlighted in green contact $G\alpha_i$ (Tesmer, Berman et al. 1997). Amino acids drawn in red are known PKC phosphorylation sites (Pronin, Satpaev et al. 1997; Krasel, Dammeier et al. 2001). Only the portions of the α10 helices of P115-RhoGEF (P115) and PDZ-RhoGEF (PDZ) that are structurally homologous to GRK2 are shown; RGS4 does not have an equivalent helix. Accession codes for the sequences used in the alignment are as follows; GRK2:P216, GRK3:P35626, GRK4:P32298, GRK5:P34947, GRK6:P43250, GRK7:Q8WTQ7, GRK1:Q15835, RGS4:P49799. All sequences are human except for GRK2 (bovine) and RGS4 (rat). **B)** Structural alignment of kinase domains from GRK2, GRK5 and other AGC kinases. Residues highlighted in violet are those that interact with the RH domain of GRK2, and green columns correspond to positions within the polypeptide binding cleft of the kinase domain that coordinate consensus arginine residues of peptide substrates in PKA (Knighton, Zheng et al. 1991). Residues highlighted in blue are established phosphorylation sites required for full activation of their respective kinase domains (Newton 2002). Accession codes for the sequences used in the alignment are as follows; GRK2:P216, GRK5:P34947, PKB: P31749, PKCβ: P05771, PKA: P05132. All sequences are human except GRK2 (bovine) and PKA (mouse). **C)** Alignment of the PH domain of GRK2 with those of PLCβ isozymes and other PH domains of known structure. Green asterisks indicate individual residues in GRK2 whose mutation leads to loss of Gβγ responsiveness (Touhara 1997; Carman, Barak et al. 2000). Red asterisks indicate residues in GRK2 involved in phospholipid binding (Fushman, Najmabadi-Haske et al. 1998; Carman, Barak et al. 2000). Gray columns indicate conserved positions within these PH domains. In the GRK2 PH domain, residues highlighted in blue are those that interact with Gβγ. In other PH domains, blue highlights indicate residues that seem compatible with the same Gβγ interface. Residues highlighted in violet contact the RH domain of GRK2, and residues drawn in red are known PKA (Cong, Perry et al. 2001)and MAP kinase (Pitcher, Tesmer et al. 1999; Elorza, Sarnago et al. 2000) phosphorylation sites. Columns highlighted in tan correspond to superimposable regions among the known atomic structures of PH domains. Residues within these regions were used for structural comparisons in Table 2. Accession codes for the sequences used in the alignment are as follows; GRK2:P216, GRK3:P26818, PLCβ1:Q9NQ66,PLCβ2:Q00722, PLCβ3:Q01970, IRS1:P35568, PLCδ:P10688, BTK:Q06187,DAPP1:AAD49697, Dynamin:Q05193,TAPPI:AAH01136, GRP1:O08967,PLKN:P08567, DBS:Q64096, ITN1:Q15811 hSOS:Q07889.

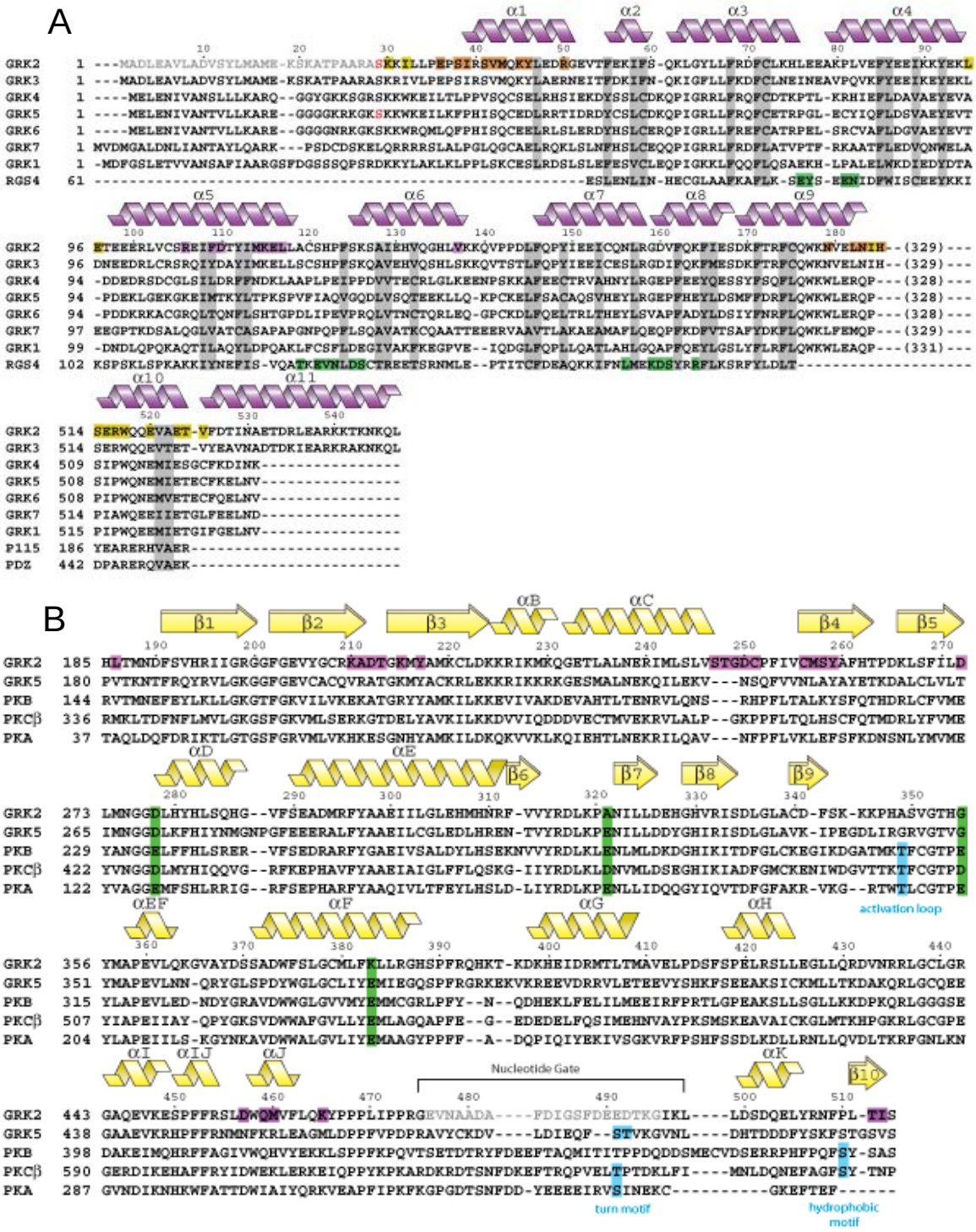
A
α1
α2
α3
α4
α5
α6
α7
α8
α9
α10
α11
GRK2
GRK3
GRK4
GRK5
GRK6
GRK7
GRK1
RGS4
P115
PDZ
B
β1
β2
β3
αB
αC
β4
β5
αD
αE
β6
β7
β8
β9
αEF
αF
αG
αH
activation loop
αI
αIJ
αJ
Nucleotide Gate
αK
β10
turn motif
hydrophobic motif
GRK2
GRK5
PKB
PKCβ
PKA

C

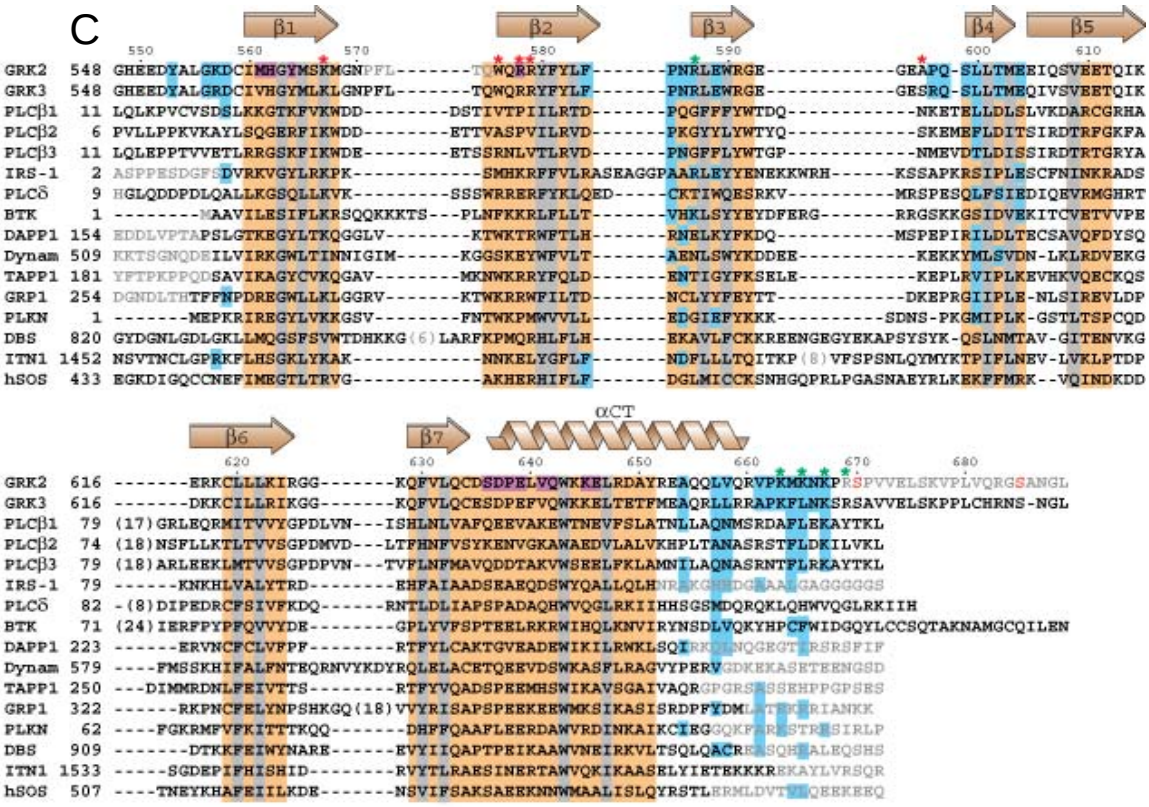
β1
β2
β3
β4
β5
β6
β7
αCT
550
560
570
580
590
600
610
620
630
640
650
660
670
680
GRK2 548 GHEEDYALGKDCIMHGYMSKMGNPFL-------TQWQRRYFYLF-------PNRLEWRGE------------GEAPQ-SLLTMEEIQSVEETQIK
GRK3 548 GHEEDYALGRDCIVHGYMLKLGNPFL-------TQWQRRYFYLF-------PNRLEWRGE------------GESRQ-SLLTMEQIVSVEETQIK
PLCβ1 11 LQLKPVCVSDSLKKGTKFVKWDD--------DSTIVTPIILRTD-------PQGFFFYWTDQ-----------NKETELLDLSLVKDARCGRHA
PLCβ2 6 PVLLPPKVKAYLSQGERFIKWDD--------ETTVASPVILRVD-------PKGYYLYWTYQ-----------SKEMEFLDITSIRDTRFGKFA
PLCβ3 11 LQLEPPTVVETLRRGSKFIKWDE--------ETSSRNLVTLRVD-------PNGFFLYWTGP-----------NMEVDTLDISSIRDTRTGRYA
IRS-1 2 ASPPESDGFSDVRKVGYLRKPK----------SMHKRFFVLRASEAGGPAARLEYYENEKKWRH------KSSAPKRSIPLESCFNINKRADS
PLCδ 9 HGLQDDPDLQALLKGSQLLKVK---------SSSWRRERFYKLQED-----CKTIWQESRKV----------MRSPESQLFSIEDIQEVRMGHRT
BTK 1 --------MAAVILESIFLKRSQQKKKTS---PLNFKKRLFLLT-------VHKLSYYEYDFERG-------RRGSKKGSIDVEKITCVETVVPE
DAPP1 154 EDDLVPTAPSLGTKEGYLTKQGGLV--------KTWKTRWFTLH-------RNELKYFKDQ-----------MSPEPIRILDLTECSAVQFDYSQ
Dynam 509 KKTSGNQDEILVIRKGWLTINNIGIM------KGGSKEYWFVLT-------AENLSWYKDDEE----------KEKKYMLSVDN-LKLRDVEKG
TAPP1 181 YFTPKPPQDSAVIKAGYCVKQGAV--------MKNWKRRYFQLD-------ENTIGYFKSELE----------KEPLRVIPLKEVHKVQECKQS
GRP1 254 DGNDLTHTFFNPDREGWLLKLGGRV-------KTWKRRWFILTD-------NCLYYFEYTT-----------DKEPRGIIPLE-NLSIREVLDP
PLKN 1 -------MEPKRIREGYLVKKGSV--------FNTWKPMWVVLL-------EDGIEFYKKK----------SDNS-PKGMIPLK-GSTLTSPCQD
DBS 820 GYDGNLGDLGKLLMQGSFSVWTDHKKG(6)LARFKPMQRHLFLH-------EKAVLFCKKREENGEGYEKAPSYSYK-QSLNMTAV-GITENVKG
ITN1 1452 NSVTNCLGPRKFLHSGKLYKAK-----------NNKELYGFLF-------NDFLLLTQITKP(8)VFSPSNLQYMYKTPIFLNEV-LVKLPTDP
hSOS 433 EGKDIGQCCNEFIMEGTLTRVG-----------AKHERHIFLF-------DGLMICCKSNHGQPRLPGASNAEYRLKEKFFMRK--VQINDKDD
GRK2 616 -------ERKCLLLKIRGG-------KQFVLQCDSDPELVQWKKELRDAYREAQQLVQRVPKMKNKPRSPVVELSKVPLVQRGSANGL
GRK3 616 -------DKKCILLRIKGG-------KQFVLQCESDPEFVQWKKELTETFMEAQRLLRRAPKFLNKSRSAVVELSKPPLCHRNS-NGL
PLCβ1 79 (17)GRLEQRMITVVYGPDLVN---ISHLNLVAFQEEVAKEWTNEVFSLATNLLAQNMSRDAFLEKAYTKL
PLCβ2 74 (18)NSFLLKTLTVVSGPDMVD---LTFHNFVSYKENVGKAWAEDVLALVKHPLTANASRSTFLDKILVKL
PLCβ3 79 (18)ARLEEKLMTVVSGPDPVN---TVFLNFMAVQDDTAKVWSEELFKLAMNILAQNASRNTFLRKAYTKL
IRS-1 79 ------KNKHLVALYTRD--------EHFAIAADSEAEQDSWYQALLQLHNRSKGHHDGAAAGAGGGGGS
PLCδ 82 -(8)DIPEDRCFSIVFKDQ------RNTLDLIAPSPADAQHWVQGLRKIIHHSGSMDQRQKLQHWVQGLRKIIH
BTK 71 (24)IERFPYPFQVVYDE--------GPLYVFSPTEELRKRWIHQLKNVIRYNSDLVQKYHPCFWIDGQYLCCSQTAKNAMGCQILEN
DAPP1 223 ------ERVNCFCLVFPF--------RTFYLCAKTGVEADEWIKILRWKLSQIRKQLNQGEGTERSRSFIF
Dynam 579 ----FMSSKHIFALFNTEQRNVYKDYRQLELACETQEEVDSWKASFLRAGVYPERVGDKEKASETEENGSD
TAPP1 250 ---DIMMRDNLFEIVTTS--------RTFYVQADSPEEMHSWIKAVSGAIVAQRGPGRSNSSEHPPGPSES
GRP1 322 ------RKPNCFELYNPSHKGQ(18)VVYRISAPSPEEKEEWMKSIKASISRDPFYDMLATFCERIAMKK
PLKN 62 ----FGKRMFVFKITTTKQQ-------DHFFQAAFLEERDAWVRDINKAIKCIEGGQKFARESTRESIRLP
DBS 909 -------DTKKFEIWYNARE------EVYIIQAPTPEIKAAWVNEIRKVLTSQLQACRASQHEALEQSHS
ITN1 1533 -----SGDEPIFHISHID--------RVYTLRAESINERTAWVQKIKAASELYIETEKKKREKAYLVRSQR
hSOS 507 ----TNEYKHAFEIILKDE-------NSVIFSAKSAEEKNNWMAALISLQYRSTLERMLDVTYLQEEKEEQ

Quaternary structure of the GRK2-Gβγ complex

When viewed as in Fig. 15A, the RH, kinase, and PH domains of GRK2 fill the vertices of an equilateral triangle roughly 80 Å on a side. The RH domain contacts both the kinase and PH domains, burying 1700 and 1400 $Å^2$ of surface area, respectively. Gβγ binds exclusively to the PH domain and buries 2200 $Å^2$ of surface area, similar to the area buried between Gα and Gβγ in the $G\alpha_s\beta_1\gamma_2$ heterotrimer (Wall, Coleman et al. 1995; Lambright, Sondek et al. 1996).

Several lines of evidence suggest that the side of the GRK2-Gβγ complex shown in Fig. 15A packs against negatively charged membranes in the cell. This membrane-proximal surface is both positively charged and flat (Fig. 15, B to D) and thereby defines a plane that would coincide with the predicted phospholipid-binding site of the PH domain, the geranylgeranylation site of Gγ, and the surface of Gβγ previously predicted to interact with the plasma membrane (Lambright, Sondek et al. 1996). As expected, superposition of the $G\alpha_s\beta_1\gamma_2$ heterotrimer (Wall, Coleman et al. 1995) with $G\beta_1\gamma_2$ in the GRK2-Gβγ complex places the myristoylated N terminus of $G\alpha_i$ within this same plane. Finally, three regions in GRK2 known to be important for receptor and/or membrane targeting (Pao and Benovic 2002) reside on the membrane-proximal side of the complex (residues 1 to 28, 476 to 495, and 571 to 575). These regions although disordered in the crystal structure are positioned in such a way that they could interact with activated GPCR or with phospholipid headgroups in the plasma membrane.

Fig. 15. Quaternary structure of the GRK2-Gβ1γ2 complex. (**A**) Membrane-proximal view of the GRK2-Gβγ complex. The RH (RGS homology) domain of GRK2 is colored violet. The kinase domain is depicted in yellow. The PH domain is tan, $G\beta_1$ blue green, and $G\gamma_2$ green. The long axis of the RH domain is declined from the center of the enzyme into the page by about 45°. The first and last observed residues of GRK2 are labeled "N" (residue 29) and "C" (residue 668), respectively. The C-terminal residue of Gγ (Cys^{68}) is labeled "geranylgeranyl" to indicate the site of geranylgeranylation. Connections of disordered loops in GRK2 are annotated as follows: I and I' correspond to residues 475 and 496, respectively, of the kinase domain; II and II' to residues 569 and 576, respectively, of the PH domain. (**B**) Side view of the GRK2-Gßγ complex, rotated 90° around a horizontal axis from the view in (A). The flat, membrane-proximal surface spans the top of the complex. (**C**) Electrostatic surface potential of the membrane-proximal surface of the complex. The orientation is the same as in (A). Basic regions are colored blue, acidic regions red and neutral regions white. (**D**) Electrostatic surface potential of the GRK2-Gβγ complex in the same orientation as in (B).

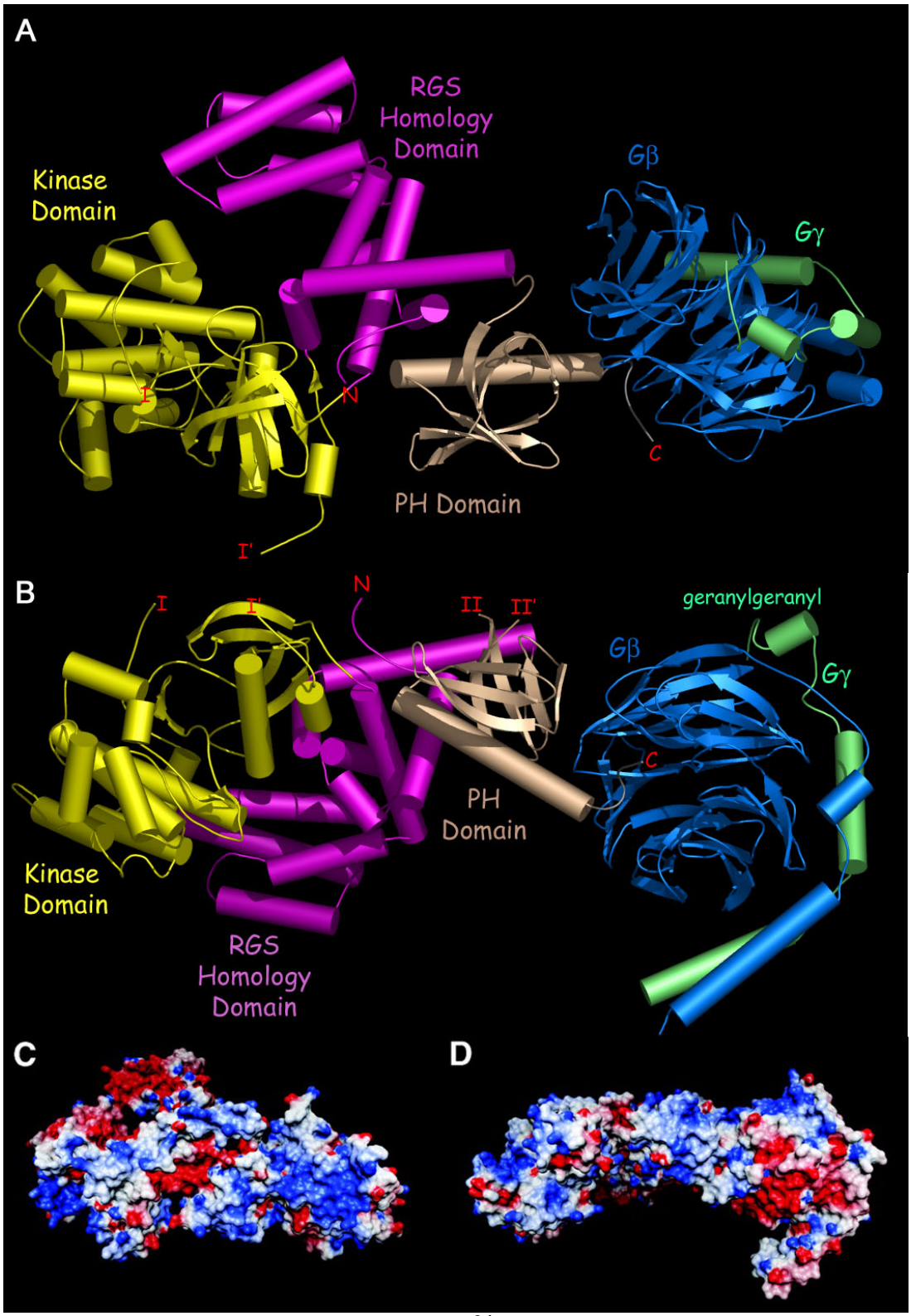
A
RGS
Homology
Domain
Kinase
Domain
Gβ
Gγ
I
N
C
PH Domain
I′
B
I
I′
N
II
II′
geranylgeranyl
Gβ
Gγ
C
PH
Domain
Kinase
Domain
RGS
Homology
Domain
C
D

The GRK2 RH domain

The RH domain of all GRKs was assumed to have the nine prototypical helices seen in all RH domains before we solved this structure. With the structure of the GRK2·Gβγ complex it became obvious that the RH domain actually consists of two discontinuous segments within the primary sequence of GRK2 (Fig. 14A and 16). The first segment (residues 30 to 185) forms the characteristic nine-helix bundle (α1 to α9) found in most RH domains (Tesmer, Berman et al. 1997). These helices cluster into two lobes referred to as the "terminal" and "bundle" subdomains (Fig. 16, A and B). The second segment (residues 513 to 547) follows the kinase domain in the primary sequence and contributes two additional helices (α10 and α11) to the terminal subdomain. This discontinuous segment of the RGS domain was unexpected prior to the structure determination, calling into question results from biochemical studies performed with constructs containing only the first nine helices of GRK RH domains. The last three turns of helix α11 (residues 538 to 547) extend away from the core of the RH domain and bear five highly conserved arginine and lysine residues (Figs. 14A and 16A) that are in close proximity to the proposed surface of the cell membrane (Fig. 15). The RH domains of p115-RhoGEF and PDZ-RhoGEF [GEF, guanine nucleotide exchange factor (Longenecker, Lewis et al. 2001; Zhong and Neubig 2001)] also have two additional helices, the first of which appears to be structurally homologous to helix α10 of GRK2 (Fig. 16C).

The best characterized RH domains are those of the RGS proteins (Tesmer, Berman et al. 1997; Ross and Wilkie 2000; Zhong and Neubig 2001), which bind to activated [i.e., guanosine triphosphate (GTP)–bound] $G\alpha_i$ or $G\alpha_{q/11}$ subunits and serve either as GTPase activating proteins (Berman, Kozasa et al. 1996; Berman, Wilkie et al.

1996) or as competitive inhibitors versus downstream effectors of Gα (Hepler, Berman et al. 1997).

The RH domains of GRK2 and GRK3 likewise bind activated $G\alpha_{q/11}$ (Carman, Parent et al. 1999; Sterne-Marr, Tesmer et al. 2003). However, the Gα-interaction surface of the GRK2 RH domain is remarkably different from those of the RGS family of proteins (Fig. 16, A and B, Fig. 15A). The $G\alpha_q$ binding surface is completely distinct from that of either axin or RGS4. While RGS4 binds $G\alpha_i$ on the loops between α3-α4 and α5-α6 as well as the α8 helix (Tesmer, Berman et al. 1997), and axin binds the APC peptide in the valley between the terminal and bundle subdomains (Spink, Polakis et al. 2000), the $G\alpha_q$ binding surface of GRK2 is distinctly different (Day, Carman et al. 2003; Sterne-Marr, Tesmer et al. 2003). This binding surface consists of both hydrophobic and charged residues arrayed along the α5 and α6 helices and is distinct from that of both axin and RGS4. The binding of RGS4 to $G\alpha_i$ increases the rate of GTP hydrolysis by $G\alpha_i$ and therefore terminates the signaling cascade. The binding of the GRK2 RH domain to $G\alpha_q$ has no effect upon GTP hydrolysis, but rather binds up activated $G\alpha_q$ sequestering it away from its cellular signaling targets and thusly reducing activation of $G\alpha_q$ downstream signaling targets.

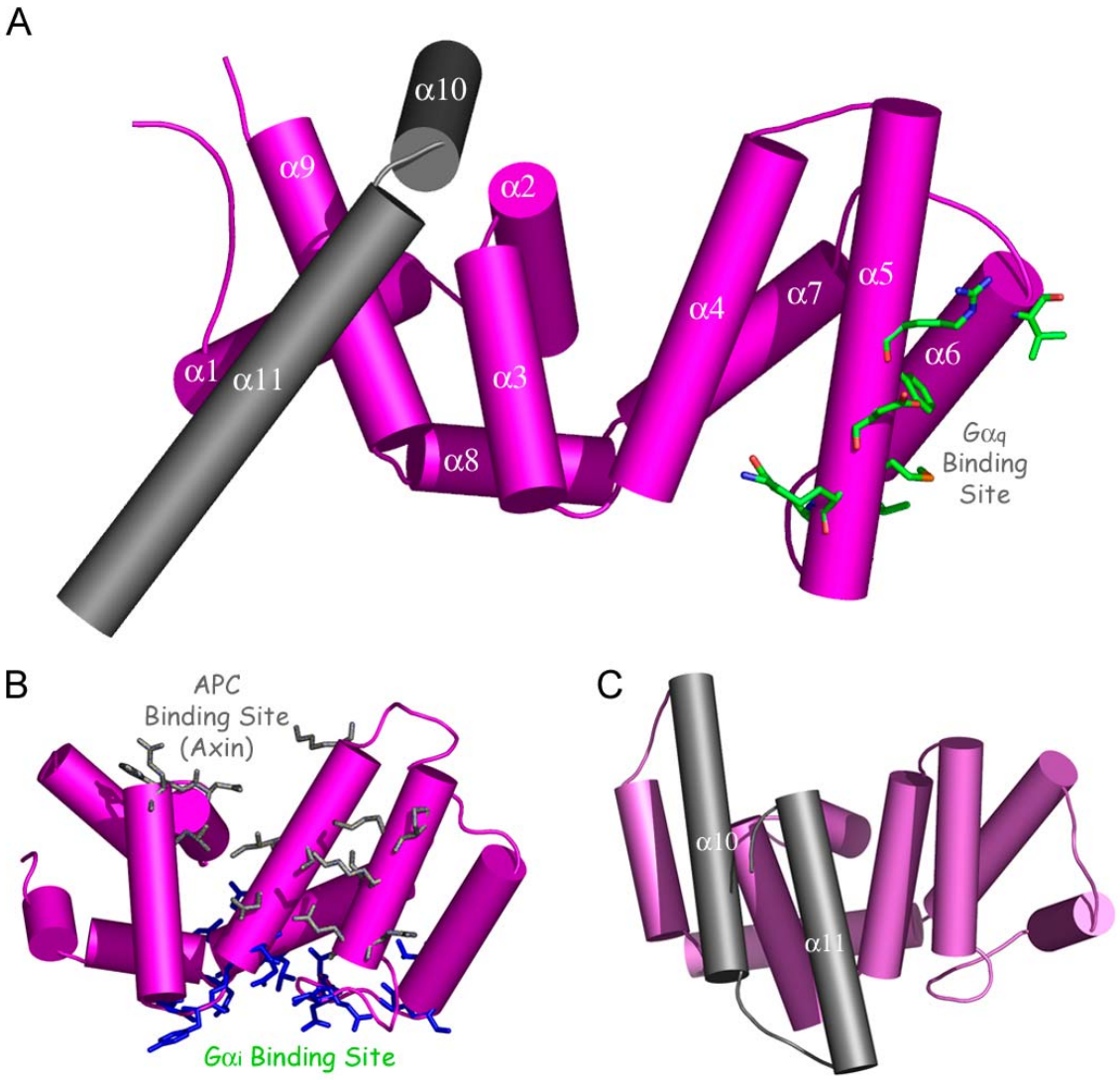

Figure 16. Comparison of RH domain of GRK2 with that of RGS4 and P115RhoGEF. (A) The GRK2 RH domain. Helices that belong to the core RH domain fold are colored violet. Helices α4 to α7 constitute the "bundle" subdomain: a classic antiparallel, four-helix bundle. The amino- and carboxyl-terminal helices (α1 to α3, α8, and α9) constitute the "terminal" subdomain. Helices α10 and α11 (residues 513 to 547), which follow the kinase domain in the primary sequence (Fig. 14a), are colored gray. Residues that bind $G\alpha_{q/11}$ are drawn with green side chains. The α1 helix is displaced by 13 Å from its position in RGS proteins. (B) The RGS4 RH domain. The terminal and bundle domains of GRK2 and RGS4 superimpose with RMSDs of 0.8 and 1.0 Å for equivalent Cα atoms, respectively. When their terminal subdomains are superimposed,

their bundle subdomains are related by 20° around an axis that runs through the long axis of the domain (horizontally in the plane of this diagram). Side chains of residues that interact with $G\alpha_i$ are in blue, and residues that interact with the adenomatous polyposis coli (APC) peptide bound in the closely related RH domain of axin are shown in grey. These sites, in addition to the $G\alpha_{q/11}$ binding site of GRK2 shown in (A), demonstrate that RH domains have evolved at least three distinct protein binding sites. (C) The p115-RhoGEF RH domain. For this view, residues from the terminal subdomain of p115-RhoGEF (including α2, α3, α8 and portions of α9 and 10) were superimposed on analogous residues from the terminal subdomain of GRK2 (RMSD of 2.1 Å for 57 equivalent C atoms). The bundle subdomains of p115-RhoGEF and GRK2 are then related by ~26° around an axis similar to that described in (B). Because the α10 helix of the RhoGEF RH domain appears homologous with that of GRK2, the GRK2 kinase domain can be thought of as an insertion within the α 9- α10 loop of an ancestral RH domain, which consisted of at least 10 α-helices.

The GRK2 kinase domain

GRK2 is roughly 32% identical in sequence to other AGC kinases of known structure (Fig. 15B), including protein kinase A (PKA)(Smith, Radzio-Andzelm et al. 1999), protein kinase B (PKB/Akt) (Yang, Cron et al. 2002; Yang, Cron et al. 2002), and 3-phosphoinositide–dependent kinase 1 (PDK1) (Biondi, Komander et al. 2002). Upon comparison with the structures of these other kinases, it is clear that the GRK2 kinase domain is in an inactive conformation (Fig. 3). The two lobes of the GRK2 kinase domain are splayed 6° farther apart than in the most open conformations observed for PKA (Zheng, Knighton et al. 1993) but to a similar extent as that described for the inactive conformation of PKB (Yang, Cron et al. 2002; Yang, Cron et al. 2002). In addition, the "nucleotide gate" (residues 476 to 495) of the GRK2 kinase domain is disordered, as it is in structures of PKA that adopt an open conformation (Narayana, Cox et al. 1997; Narayana, Cox et al. 1997). However, unlike in other inactive kinases (Yang, Cron et al. 2002; Yang, Cron et al. 2002), the αC helix of GRK2 is completely ordered and properly oriented with respect to the active site.

Although the crystals of the GRK2·Gβγ complex were grown in the presence of 1 mM ATP and 1 mM $MgCl_2$, no density for ATP is observed in the active site. It is possible to superimpose the active site for PKA with nucleotide bound on the GRK2·Gβγ structure, and there are no steric reasons why nucleotide should not be bound. Furthermore, residues to which ATP would bind appear to be correctly positioned and poised to bind nucleotide. Soaking the GRK2·Gβγ crystals in 5 and 10 mM ATP before X-ray data collection did not reveal ATP bound in an ordered manner in the active site. However, some slight vestigial density in the active site suggested the presence of ATP in a loosely-bound with low-occupancy. Attempts to model the ATP within the active site

ultimately failed because models with ATP modeled in their active sites had poorer statistics than those without ATP. A possible explanation for the low occupancy of ATP within the active site would be that the pH at which the crystals were grown (pH 5.0-5.25) is incompatible with ATP binding while the pH at which the complex is purified (pH 8.0) is much more compatible with ATP binding.

A striking difference between GRK2 and other AGC kinases is that its catalytic activity is solely regulated by the binding of substrates and ligands, not by phosphorylation of its kinase domain. Other AGC kinases achieve full activity only after phosphorylation of their activation loop and at one or two additional sites termed the "turn" and "hydrophobic" motifs (Newton 2002). GRK2 lacks serines, threonines, or even acidic side chains that could mimic phosphorylation at equivalent positions within the hydrophobic motif and activation loop (Fig. 14b). GRK2 does however have a stretch of aspartic and glutamic residues within the turn motif that could substitute for the phosphorylated serines and threonines within the motif in other kinases (Fig. 14b). Even so, the GRK hydrophobic motif could still play an important role in regulating enzymatic activity (Figs. 14b, 17).

The polypeptide-binding cleft of GRK2 is a groove on the surface of the large lobe, ending immediately adjacent to the active site (Fig. 17). In most AGC kinases, highly conserved acidic side chains within the cleft (E^{127}, E^{170}, E^{203} and E^{230} in mouse PKA) coordinate arginine residues preferred at positions either 6, 3 or 2 residues N-terminal to the phosphorylated residue (P-6, P-3 and P-2, respectively) (Fig. 15b) (Kemp, Bylund et al. 1975; Zetterqvist, Ragnarsson et al. 1976; Knighton, Zheng et al. 1991). Although these positions are well-conserved in most GRKs, they are strikingly different in GRK2 (Asp^{278}, Ala^{321}, Gly^{355} and Lys^{383}, respectively). GRK2 instead prefers acidic amino acids amino-terminal to the phosphorylated residue (Onorato, Palczewski et

al. 1991). This preference can be explained by the Lys^{383} side chain, which could form a salt bridge with a glutamic or aspartic acid at the P-3 position of a substrate, and by the strikingly basic surface potential of the polypeptide binding cleft of GRK2 (far left side of Fig. 16d). This is not too surprising as the best peptide substrates of GRK2 that have been found contain glutamic or aspartic residues at this position (Onorato, Palczewski et al. 1991). Interestingly, although the sites phosphorylated by GRK2 within the β_2-AR, α1-AR and δ-opioid receptors also have been characterized and determined, no clear consensus exists for the phosphorylation of residues by GRK2 (Pitcher, Freedman et al. 1998).

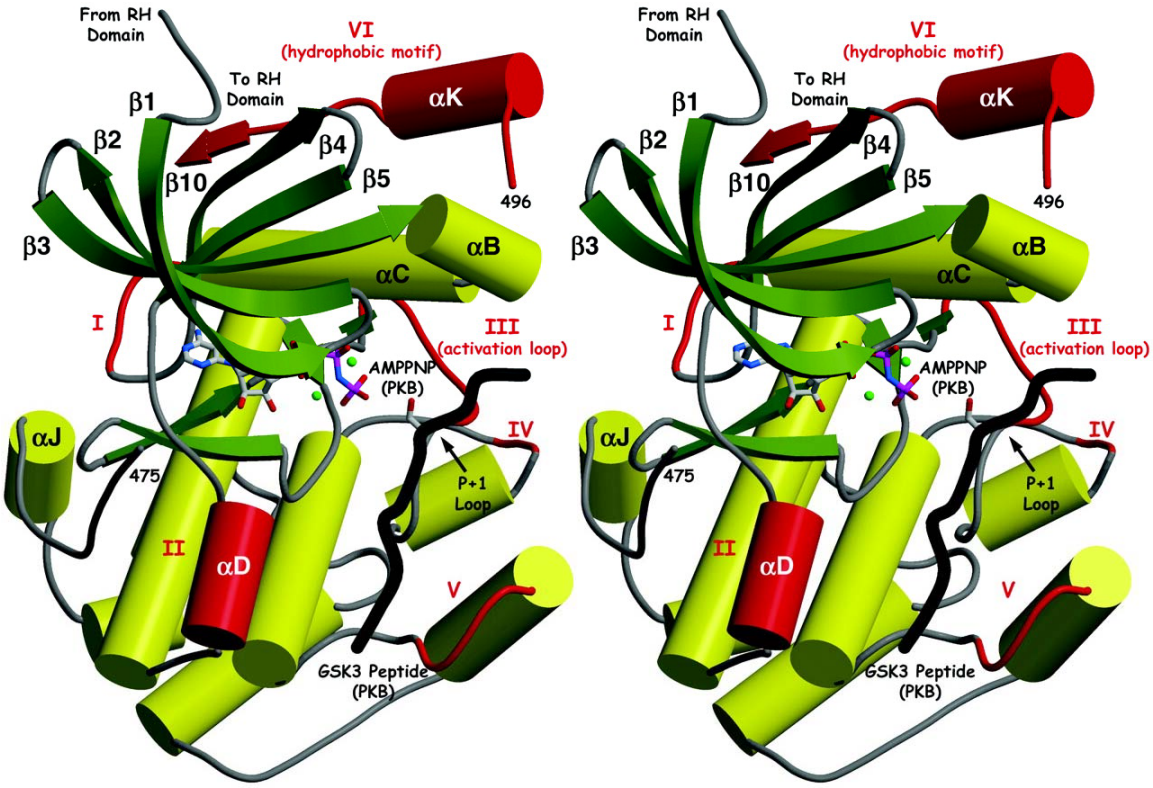

Figure 17. Stereoview of the GRK2 kinase domain. The view is roughly from the proposed plane of the plasma membrane (Fig. 15). Like other protein kinases, the GRK2 kinase domain is composed of small and large lobes. The small lobe (residues 186 to 272 and 496 to 513) consists of a six-stranded antiparallel β sheet (β1 to β5, β10) and three α helices (αB, αC, and αK). The β10 strand (residues 511 to 513) has no structural equivalent in PKA, whose primary sequence ends two residues before the strand at Phe^{350} (equivalent to Phe^{509} in GRK2). The large lobe of GRK2 (residues 273 to 475) is predominantly α-helical except for four antiparallel β-strands. Adenylyl-imidodiphosphate (AMP-PNP; ball-and-stick model) and a substrate peptide which binds to PKB (black coil with serine residue) are modeled from the structure of PKB (Yang, Cron et al. 2002) and indicate the locations of the active site and the polypeptide binding cleft, respectively. Elements of secondary structure discussed in the text are labeled. Insertions, deletions (Fig. 14b), or elements that have a different conformation in GRK2 from their counterparts in mouse PKA are drawn in red and are labeled as follows: I, residues 246 to 252 (insertion of three residues in the αC-ß4 loop, which form part of the interface with the RH domain); II, residues 279 to 287 (helix αD rolls α2.5 Å to the left in this view compared to PKA); III, residues 342 to 351 (one-residue deletion); IV, residues 364 to 366 (one-residue insertion); V, residues 392 to 399 (two-residue insertion); and VI, residues 495 to 513 (end of nucleotide gate, αK and β10). The residues on either end of the disordered nucleotide gate of GRK2 are labeled with their amino acid numbers (475 and 496).

The "P+1 loop" of the kinase domain binds the side chain of the residue immediately C-terminal to the phosphorylated residue of the substrate. In the substrates of many AGC kinases, hydrophobic residues such as isoleucine or phenylalanine are preferred at this position (Tesmer, Berman et al. 1997; Ross and Wilkie 2000). The analogous loop of GRK2 has the same backbone structure as that of PKA, but Ser^{350} and His^{354} in GRK2 replace $Leu1^{98}$ and Pro^{202} in PKA, respectively. Therefore, the P+1 loop in GRK2 is expected to favor the binding of hydrophilic, rather than hydrophobic, residues at P+1. Interestingly, the best peptide substrates for GRK2 have alanine at this position suggesting that the interactions of the peptide sidechains at this position with the P+1 loop are not necessary for either peptide binding or phosphorylation.

The RH and kinase domain core

The RH and kinase domains represent the conserved functional core found in all GRKs, and they are intimately associated with each other in the GRK2·Gβγ structure (Fig. 18, 19). The most highly conserved portion of their interface (1500 $Å^2$ of buried surface area) is formed between the α10 helix of the RH terminal subdomain and the β2-β3 and αC-β4 loops of the kinase small lobe (Fig. 18A). The second section of the interface (~250 $Å^2$ of buried surface area) is formed between the α4-α5 loop of the RH bundle subdomain and the αJ helix of the kinase large lobe (Fig. 18B). This interface consists of one salt bridge between Asp^{96} in the RH domain and Lys^{465} in the kinase domain as well as several hydrophobic contacts.

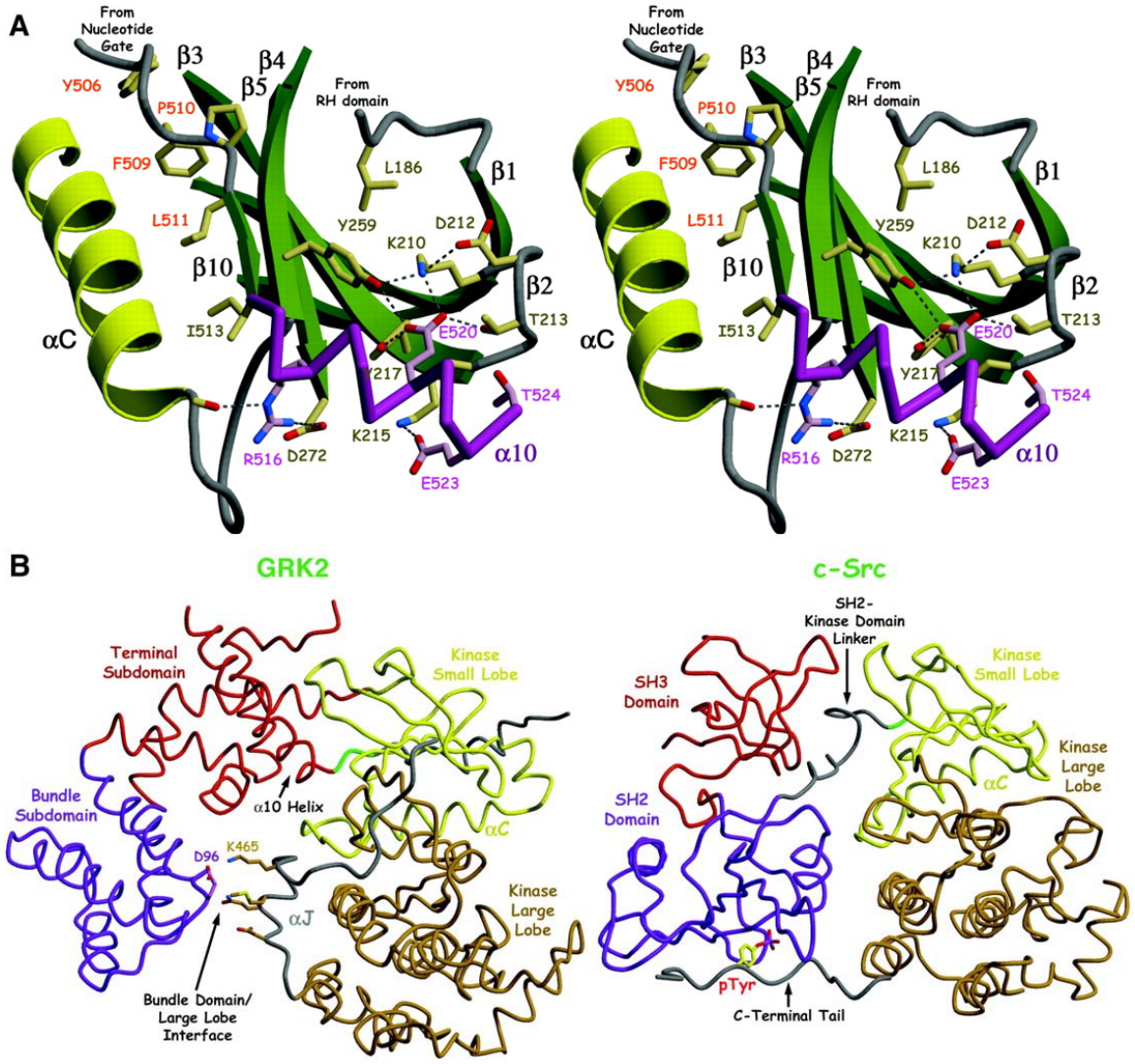

Figure 18. The RH domain–kinase domain interface of GRK2. (**A**) The hydrophobic motif of GRK2 and the interface between the α10 helix and the kinase domain. The kinase domain is colored as described in Fig. 1, and residues from each domain have side-chain carbon atoms colored the same as their respective domains. Amino acids with orange labels belong to the hydrophobic motif of GRK2, which consists of a serine, threonine, or acidic residue preceded by two aromatic residues (Tyr^{506} and Phe^{509} in GRK2) and immediately followed by a hydrophobic residue (Leu^{511}, the first residue of the ß10 strand). In other AGC kinases, but not GRKs, phosphorylation of the residue equivalent to Pro^{510} is required for full activation (Newton 2002). The most striking feature of the interface between the α10 helix of the RH domain (violet Cα trace) and the kinase domain is a buried interdomain salt bridge between Glu^{520} and Lys^{210}. The side chain of each residue is fully coordinated with hydrogen bonds. The N-terminal loop of

the RH domain (residues 29 to 35) and the two linkers that join the RH and kinase domains also contribute several hydrophobic residues to the RH domain–kinase domain interface (Fig. 14a, b). Arg^{516} forms a salt bridge with Asp^{272} in the kinase domain, whose backbone carbonyl will accept a hydrogen bond from the purine ring of adenosine triphosphate. Arg^{516} also forms extensive contacts with the αC-β4 loop. Just before this loop within αC are several essential active-site residues. Conformational changes at this domain interface could therefore influence the catalytic activity of the kinase domain through the hydrophobic motif and/or Arg^{516}. (**B**) Comparison of two modular kinases, GRK2 and c-Src. Both kinases are shown as Cα traces. The phosphotyrosine residue (pTyr) in the C-terminal tail of c-Src is shown as a ball-and-stick model. Domains that are expected to play analogous functional roles in each kinase are colored similarly. Gray coils correspond to regions outside the conventional boundaries of each signaling domain. The short green segment in each kinase corresponds to residues 511-513 in GRK2 and residues 260 and 261 in c-Src. Both segments form short, superimposable β strands in the small lobe (although their orientations are antiparallel and parallel, respectively), and both are expected to play regulatory roles within their respective small lobes. The interaction of the GRK2 α10 helix with the kinase small lobe is analogous to that of the SH2–catalytic domain linker (Sicheri and Kuriyan 1997; Xu, Doshi et al. 1999). Side chains of residues that form the interface between the bundle subdomain and the large lobe of the kinase domain are drawn as ball-and-stick models.

The domain arrangement of the RH and kinase domain core of GRK2 has intriguing similarities with the inactive structure of Src (Sicheri and Kuriyan 1997; Xu, Harrison et al. 1997). When the small lobes of the GRK2 and Src kinase domains are superimposed, the RH terminal and bundle subdomains of GRK2 roughly align with the SH3 and SH2 domains of Src, respectively, and make analogous contacts with the small and large lobes of their kinase domains (Fig. 18B). Like the SH3 and SH2 domains, the terminal and bundle subdomains of GRK2 interact with other proteins and/or domains that could modulate their interactions with the kinase domain. Interestingly, the α10 helix of GRK2 appears structurally analogous to the SH2–kinase domain linker, which is thought to play an important role in Src activation (Gonfloni, Williams et al. 1997; LaFevre-Bernt, Sicheri et al. 1998). As both elements are sandwiched between the same surface of the kinase small lobe and a regulatory domain, (terminal subdomain in GRK2; SH3 domain in Src) the α10 helix is therefore in prime position to similarly regulate the activity of GRK2. Although much less extensive, the interface between the RH bundle subdomain and the kinase large lobe could modulate GRK2 activity by influencing the relative orientation of the kinase small and large lobes, as does the analogous contact in Src (Huse and Kuriyan 2002).

The binding of Ca^{2+}/Calmodulin has been shown to inhibit the kinase activity of GRK2 (Krasel, Dammeier et al. 2001). The Ca^{2+}/Calmodulin binding site within GRK2 includes the RH domain of GRK2. Constructs containing the first nine α-helices of the RH domain of both GRK5 and GRK2 were able to abolish the inhibition seen by the respective kinase (Pronin, Satpaev et al. 1997; Levay, Satpaev et al. 1998). The ability of Ca^{2+}/Calmodulin to regulate the activity of GRK2 suggests that when Ca^{2+}/Calmodulin is bound to the RH domain of GRK2 it is able to influence the activity of the kinase domain either directly or through its contacts with the kinase domain of GRK2. A possible route

for this inhibition to take would be the utilization of the RH domain-kinase domain interactions to influence the relative activity of the kinase domain in much the same manner as C-terminal Src Kinase (CSK) (Ogawa, Takayama et al. 2002). In CSK, the binding of proteins such as PAG to the SH2 domain are transmitted to the kinase domain through a SH3-SH2 linker helix. In the structure of GRK2, the α10 helix could play a similar role; upon the binding of a protein to the terminal subdomain of the RH domain, this event could regulate structural changes within the kinase domain resulting in a different level of phosphorylation activity. For instance, the binding site of caveolin which also inhibits the kinase activity of GRK2 has been localized to the residues 63-71 which map to the α3 helix within the RH domain (Carman, Lisanti et al. 1999). As this is located within the terminal subdomain of the RH domain of GRK2, the binding of caveolin would be poised to influence the relative orientation of the α10 helix and this change in orientation could influence relative orientations of the large small lobe of the kinase domain in a manner that would be less conducive for phosphorylation.

Finally, the binding of GTP bound $G\alpha_{q/11}$ subunits to the α5 helix of the RH domain puts the $G\alpha_{q/11}$ subunits in a position to regulate the orientation and conformation of the bundle subdomain. Although $G\alpha_{q/11}$ subunits have not been shown to regulate the kinase activity of GRK2, the binding of GRK RH domain has been shown to participate in a phosphorylation independent form of desensitization of the metabotropic glutamate receptor (Dhami, Dale et al. 2004). Residues necessary for the binding of $G\alpha_{q/11}$ subunits were necessary for this activity and were also necessary for the recruitment of GRK2 to activated receptor (Dhami, Dale et al. 2004). Furthermore, it would make sense that the binding of $G\alpha_{q/11}$ subunits potentiate the recruitment of GRK2 to the plasma membrane or even increase the kinase activity itself as this feedback inhibition would be appropriate for assisting in the rapid desensitization of activated GPCRs.

The GRK2 PH domain

The PH domain of GRK2 (residues 553 to 661) is a flattened, seven-stranded antiparallel β barrel that is capped on one end with a C-terminal helix (αCT) (Fig. 19a). The β1-β2, β3-β4, and β5-β6 loops circumscribe the open end of the barrel. As in other PH domains(Lemmon and Ferguson 2001), residues from GRK2 known to be involved in phospholipid binding (Fushman, Najmabadi-Haske et al. 1998; Carman, Barak et al. 2000) map primarily to the inner face of the β1-β2 loop (Fig. 21A). Accordingly, the β1-β2 loop in the GRK2-Gβγ structure is juxtaposed with the proposed plane of the plasma membrane. Furthermore, the loop is poorly ordered and the temperature factors for the β1-β2 loop are higher than that of the surrounding residues.

The conformation of the PH domain in the GRK2·Gβγ complex is distinct from that of its nuclear magnetic resonance solution structure (Fushman, Najmabadi-Haske et al. 1998). In fact, structural alignments of the structural core of the GRK2 PH domain with PH domains of known structure that have been shown to bind Gβγ subunits with high affinity reveal that the PH domain of GRK2 in the crystal structure is more similar to other PH domains than that of the GRK2 PH domain NMR structure (Fushman, Najmabadi-Haske et al. 1998) (Table 2). The PH domain of GRK2 in the context of the full length protein is quite different from that of the NMR structure. The Conditions under which the NMR data were collected were quite extreme (pH 8.0, 10 mM DTT and 10 mM EDTA) and it is likely that the NMR structure is either incorrect when compared to that in the full length structure or that the NMR restraints while consistent with their structure would also be consistent with the structure seen in the GRK2·Gβγ structure.

R.m.s. Deviation of Equivalent Cα Positions (Å)															
Domain	GRK2 *	1BAK *	IRS1 *	BTK *	DAPP ‡	TAPP ‡	GRP1 ‡	DYN *	DBS ‡	ITN1 ‡	HSOS †,‖	TIAM †,‖	PLKN *	PLCδ *	SPEC †
GRK2	-	1.5	1.3	1.2	1.1	1.2	1.0	1.4	1.6	1.3	1.2	1.7	1.5	1.7	2.3
1BAK		-	2.0	1.7	1.5	1.7	1.7	1.9	1.8	1.6	1.8	1.9	1.8	1.7	2.5
IRS1			-	1.0	0.9	0.9	1.1	1.1	1.4	1.3	1.2	1.4	1.4	1.7	2.5
BTK				-	1.0	0.7	1.1	1.3	1.1	1.1	1.1	1.2	1.4	1.6	2.3
DAPP					-	0.8	0.9	1.1	1.2	1.1	0.9	1.3	1.4	1.3	2.3
TAPP						-	1.0	1.2	1.2	1.0	1.2	1.0	1.2	1.5	2.4
GRP1							-	1.2	1.5	1.4	1.2	1.7	1.4	1.7	2.4
DYN								-	1.6	1.6	1.3	1.6	1.6	1.9	2.5
DBS									-	1.1	1.2	1.1	1.6	1.5	2.3
ITN1										-	1.3	1.1	1.3	1.4	2.5
HSOS											-	1.3	1.4	1.6	2.3
TIAM												-	1.5	1.6	2.6
PLKN													-	1.8	2.5
PLCδ														-	2.7
SPEC															-

* PH domain binds to Gβγ with apparent K_d <1 μM.
‡ The ability of this PH domain to interact with Gβγ has not been reported.
† PH domain binds to Gβγ with apparent K_d > 100 μM. The β-spectrin PH domain, which binds Gβγ poorly(Zhang, Talluri et al. 1995), has a significantly different conformation from high affinity Gβγ-binding PH domains.
‖ The Gβγ-binding surface of the PH domain, as defined by the GRK2:Gβγ complex, are occluded by other structural elements. For example, the PH domain of hSOS has a subdomain that folds against the β1-β4 sheet, thereby blocking its potential interaction with Gβγ(Soisson, Nimnual et al. 1998).

Table 2. Structural Comparison of PH Domains. Each element in the table represents the pair-wise r.m.s.d. of common secondary structural elements of PH domains currently in the PDB (65 equivalent Cα atoms, as defined by the tan boxes in Fig. 14c). Structural alignments were performed with Swiss-PDB Viewer (Kaplan and Littlejohn 2001). 1BAK is the solution structure of the GRK PH domain fragment (1BAK). IRS1 is the PH domain of insulin receptor substrate 1 (1QGG). BTK: Bruton's tyrosine kinase (1B55). DAPP: dual adaptor of phosphotyrosine and 3-phosphoinositides (1FAO). TAPP: tandem PH domain containing protein 1 (1EAZ). GRP1: ARF1 guanine nucleotide exchange factor (1FGY). DYN: dynamin (1DYN). DBS: DBL's big sister (1LB1). ITN1: intersectin (1KI1). HSOS: human son of sevenless protein 1 (1DBH). TIAM: T-lymphoma invasion and metastasis inducing protein 1 (1FOE). PLKN: pleckstrin N terminal domain (1PLS). PLCδ: phospholipase Cδ (1MAI). SPEC: β-spectrin (1DRO).

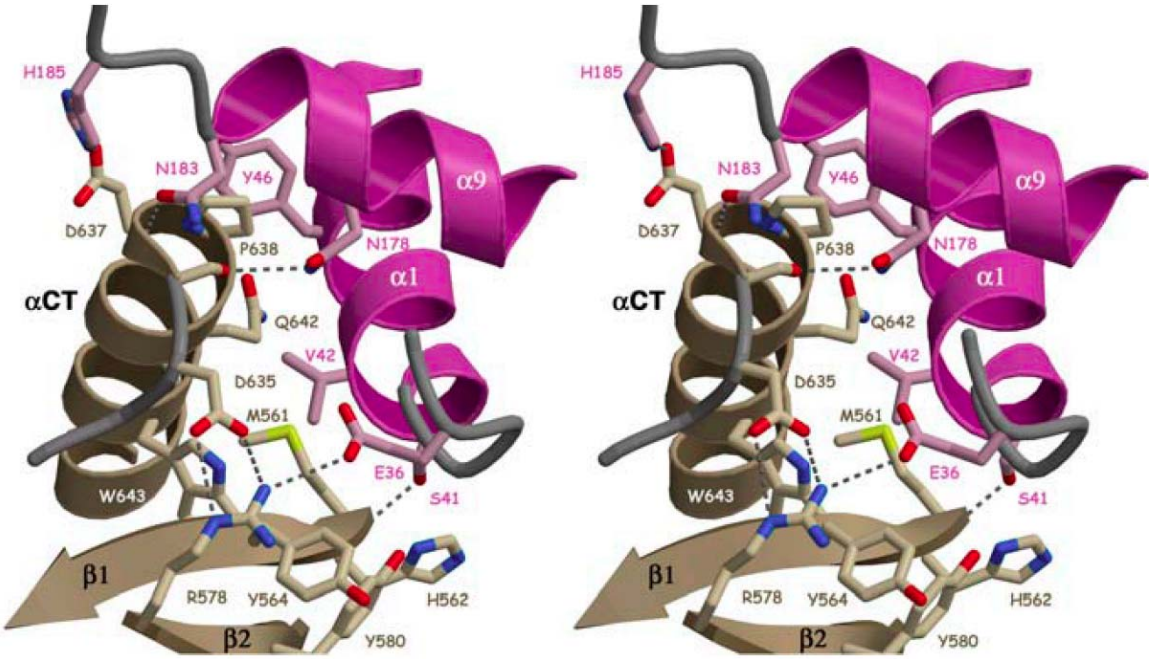

Figure 19. Stereo view of the RH:PH domain Interface. Val[42] of the RH domain docks into a pocket on the PH domain formed by Met[561], Glu[639] (not shown), Gln[642] and Trp[643]. Pro[638], at the N-terminus of αCT, docks into a pocket formed by Met[43], Tyr[46], Leu[182] and the backbone of α1 on the RH domain. Met[43] and Leu[182] are between the α1 and α9 helices in this view, and were omitted for clarity. Site-directed mutagenesis of Arg[578] to glutamic acid leads to a loss of phospholipid-mediated activation (Carman, Barak et al. 2000). Because Arg[578] appears to play a structural role within the PH domain, the R578E mutation could destabilize the β1-β2 loop and thereby decrease its affinity for phospholipids. However, Arg[578] also contacts the RH domain, and so the observed loss of phospholipid-mediated activation could also result from perturbation of the PH:RH domain interface.

In some other PH domains (Ferguson, Kavran et al. 2000) and possibly in GRK2 (Fushman, Najmabadi-Haske et al. 1998), the β3 and β4 strands contribute residues to the phospholipid binding site. Therefore, conformational changes induced by Gβγ could explain the cooperative binding of Gβγ and phospholipids to GRK2 (Touhara 1997).

The RH-PH domain interface

Adjacent to the phospholipid binding site is the RH domain–PH domain interface, formed primarily between a groove between the β1 strand and αCT helix of the PH domain and the α1 and α9 helices of the RH terminal subdomain (Figs. 18 and 19). The interface has a substantial hydrophobic core in addition to a salt bridge and two ion pairs. Site-directed mutagenesis of one of these ion pairs leads to a deficiency in the phospholipid mediated activation of GRK2 (Carman, Barak et al. 2000), suggesting a possible route for allosteric communication between the PH and RH domains. Residues within the α1 helix of the RH domain and preceding loop (residues 19 to 29) are not conserved in GRKs that lack PH domains (Fig. 14a). However, given the close structural proximity of the amino and carboxyl termini of the conserved RH and kinase domain core, it seems likely that in each GRK analogous interactions will occur between the α1 region and the C-terminal membrane-targeting domain.

The structure of $G\beta_1\gamma_2$ in complex with GRK2

In prior studies, structures of Gβγ have been determined alone (Sondek, Bohm et al. 1996) and in complex with Gα subunits (Wall, Coleman et al. 1995; Lambright, Sondek et al. 1996) or phosducin (Gaudet, Bohm et al. 1996; Loew, Ho et al. 1998).

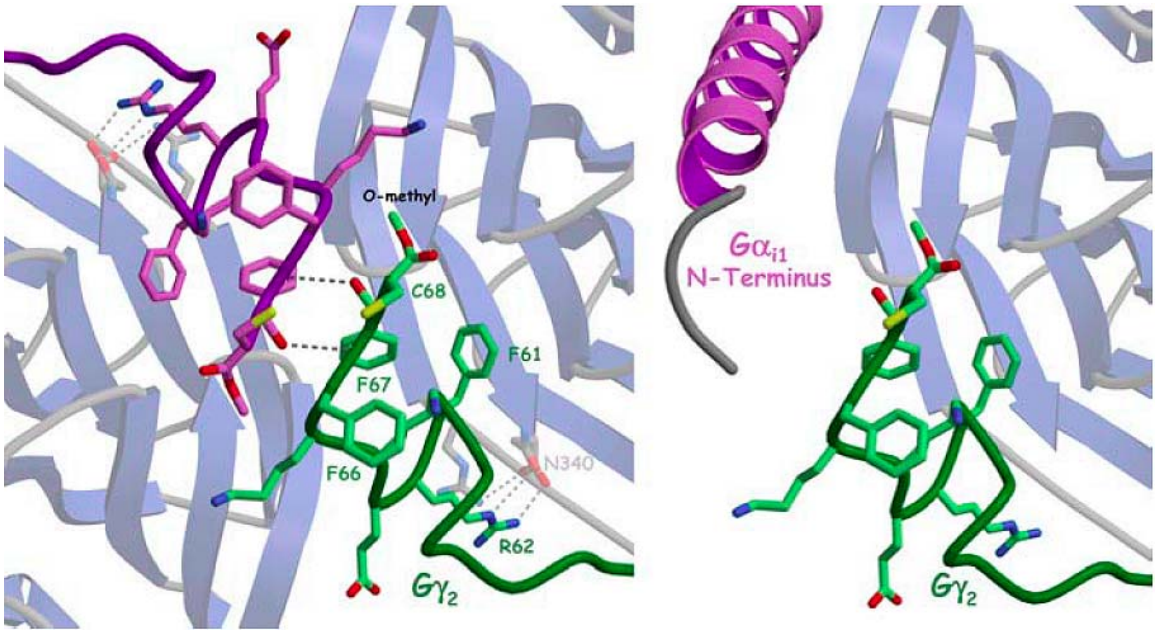

Figure 20. The C-terminal Region of Gγ2

A) The crystallographic Gβγ dimer interface. The C-terminus of $G\gamma_2$ (green) is supported by a crystallographic two-fold related $G\gamma_2$ subunit (purple). The side chain of Cys^{68} is geranylgeranylated, but no electron density is observed for the modification. However, the two symmetry-related geranylgeranyl groups would be close enough to interact across the two-fold axis. $G\beta_1$ (blue) is shown beneath the C-termini for perspective. Arg62 of Gγ forms a salt bridge with the C-terminal carboxylate of Gβ (Asn^{340}). **B)** Comparison with $G\alpha_{i1}$ from the structure of the $G\alpha_{i1}G\beta\gamma$ heterotrimer. The Gβγ subunits of the GRK:$G\beta_1\gamma_2$ and $G\alpha_{i1}G\beta_1\gamma_2$(C68S) heterotrimeric complexes were superimposed (Wall, Coleman et al. 1995). The N-terminal helix of $G\alpha_{i1}$ (purple; first observed residue Ser^6) begins close to the C-terminus of $G\gamma_2$. Gly^2 of $G\alpha_{i1}$ is myristoylated via an amide linkage, and this covalent modification enhances the affinity of Gα subunits for Gβγ complexes(Linder, Pang et al. 1991). Due to their proximity in this model, enhanced binding could be mediated, at least in part, by hydrophobic contacts between the myristoyl and geranylgeranyl groups.

The structure of $G\beta_1$ in the GRK2-$G\beta\gamma$ complex agrees well with these structures [root mean square deviation (RMSD) of 0.85 Å for equivalent Cα atoms] except for those of thephosducin complexes which involve the remodeling of one of the blades of the Gβ subunit (RMSD ~1.2 Å). The β5-β6 loop and the side chains of Tyr^{59} and Gln^{75} of $G\beta_1$, which make extensive contacts with the PH domain (Fig. 21), adopt distinct conformations from their positions in other Gβ complexes. Compared with the structure of the $G\alpha_i\beta_1\gamma_2$ heterotrimer (Wall, Coleman et al. 1995), seven additional residues are observed at the carboxyl terminus of $G\gamma_2$, including the terminal residue Cys^{68}, whose α-carboxylate and sulfhydryl are methylated and geranylgeranylated, respectively, both *in vivo* and in our structure (Lambright, Sondek et al. 1996) (Fig. 20). In addition, residues 52 to 61 of $G\gamma_2$ adopt a distinct conformation, perhaps as a result of the ordered carboxyl terminus.

The C Terminus of Gγ

In contrast with prior structure determinations of Gγ, wherein the last well-ordered residue of Gγ is a conserved phenylalanine (Phe64 in $G\gamma_1$, Phe61 in $G\gamma_2$), the complete carboxyl terminus of $G\gamma_2$ (residues 62-68) is observed in the GRK2·Gβγ complex (Fig. 20). The geranylgeranyl group of Cys68 is not observed, as might be expected for a moiety that partitions to the mobile detergent phase of the crystals. The carboxyl terminal region of $G\gamma_2$ in the GRK2·Gβγ complex is stabilized in part by an interface with its counterpart in a crystallographic two-fold related Gβγ subunit, which buries ~1800 Å2 of surface area. This interface is not expected to be physiological as neither dimer would be oriented properly with respect to the same membrane surface. However, when the Gβγ subunits of the $G\alpha i\beta_1\gamma_2$ heterotrimer (Wall, Coleman et al. 1995)

are superimposed with those of the GRK2:Gβγ complex, the myristoylated amino-terminal helix of $G\alpha_i$ occupies the same position as the two-fold related, geranylgeranylated Gγ subunit (Fig. 20b). By packing against the amino terminal helix of $G\alpha_{i1}$, the carboxyl terminus of $G\gamma_2$ may adopt a similar structure in a native, membrane-bound $G\alpha_{i1}G\beta_1\gamma_2$ complex. Similarly, in the $G\alpha_i\beta_1\gamma_2$ complex it is expected that the myristoylated helix will bind in a similar orientation to that of the symmetry related molecule in the GRK2·Gβγ complex.

The PH domain–Gβγ interface

Many PH domains have been shown to bind Gβγ, some with dissociation constants on the order of 20 to 50 nM (Touhara, Inglese et al. 1994; Mahadevan, Thanki et al. 1995). The complementarity, sequence conservation, and extent of the PH domain–Gβγ interface observed in our crystal structure strongly support its physiological relevance. As predicted (Ford, Skiba et al. 1998; Li, Sternweis et al. 1998), the footprint of the GRK2 PH domain on Gγ overlaps extensively with the binding sites for Gα subunits and other Gβγ effectors, including PLCβ and ion channels (Fig. 21, B and C). Therefore, GRK2 will compete with these proteins for binding to Gβγ. Four regions within the primary sequence of the PH domain contribute to the Gβγ interface (Fig. 14C). These regions form a continuous surface that includes strands ß1 to ß4 and the extended portion of the αCT helix (Fig. 21A).

Contact residues within the GRK2 PH domain are not well conserved in other PH domains known to bind Gβγ (Fig. 14c). The specific details of the interface of each PH domain with Gβγ will obviously differ, although some general features are apparent. Superposition of the core secondary structures of PH domains known to bind Gβγ with

high affinity (Table 2 and Fig. 14C) shows that the conformation of their respective β strands (β1 to β4) is highly conserved and forms a concave surface complementary to the effector-binding surface of Gβ. In addition, the top of the Gβ propeller responsible for binding PH domains and Gα subunits is extremely acidic (far right of Fig. 15d).

Four distinct regions within the primary sequence of the PH domain contact Gβγ (Fig. 14c). The first region (residues 555-558 of GRK2) forms a turn that leads into β1 of the PH domain. The turn contacts the β5-β6 crossover linking the seventh and first blades of Gβ (nomenclature as defined in by Wall, et al. (Wall, Coleman et al. 1995)). The carboxylate of Asp558 in GRK2 forms hydrogen bonds with both the side chain hydroxyl and the backbone amide of Ser98 in Gβ (Fig. 22b,d).

The second region (residues 584-589 of GRK2) includes a type I β-turn connecting the β2 and β3 strands of the PH domain and residues within the β3 strand. The backbone atoms of the i+1 and i+2 residues of the turn (Pro^{585} and Asn^{586}) pack against the indole side chain of Trp^{99} of Gβ (Fig. 21 B and D). The guanidinium group of Arg^{587}, a residue known to be important for Gβγ-mediated activation of GRK2 (Carman, Barak et al. 2000), stacks between the phenyl ring of Phe^{584} of GRK2 and the peptide bond of residues 76-77 in Gβ. Arg^{587} also forms a hydrogen bond with Ser^{98} in Gβ, and coordinates two other residues from the PH domain that participate in the interface (Fig. 5a,d).

The third region (residues 598-604 of GRK2) includes the β4 strand and β4-β5 loop of the PH domain. Nearly all of these residues form side chain or main chain contacts with the side chains of Leu^{55} or Gln^{75} in Gβ. Glu604 of GRK2 forms a salt bridge with Lys^{57} and a hydrogen bond with the side chain of Gln^{75} of Gβ. The fourth region (residues 654-668 of GRK2) includes the portion of αCT helix that extends from the PH domain and the following C-terminal tail. Ala^{654}, Leu^{657}, Val^{658}, Val^{661}, Pro^{662} and

Met^{664} form a hydrophobic cluster of residues that interacts with a complementary surface on Gβ formed by Tyr^{59}, Trp^{99}, Met^{101}, Leu^{117}, Tyr^{145} and Met^{188} (Fig. 21c, 21d, 22). The side chain of Lys663 in GRK2 plunges down the central channel of the β-propeller, and the basic C-terminal tail of GRK2 (residues 663-668, Fig. 14c) extends along the acidic surface of the Gβ propeller (Fig. 22). Because residues carboxyl-terminal to 668 in GRK2 do not appear to make stable contacts with Gβγ, the loss of activity that occurs when GRK2 is phosphorylated at Ser670 by MAP kinases (Kozasa 1999; Elorza, Sarnago et al. 2000) may reflect electrostatic repulsion between a negatively-charged phosphate and this same surface of Gβ. Mutations of Lys^{663}, Lys^{665}, Lys^{667} and Arg^{669} in GRK2 inhibit Gβγ-mediated receptor phosphorylation, with Lys^{663} and Lys^{665} being the most critical (Touhara 1995; Touhara, Hawes et al. 1995; Touhara, Koch et al. 1995; Carman, Barak et al. 2000). In the GRK2:Gβγ structure, the side chains of Lys^{663} and Lys^{667} directly interact with Gβ, and the side chain of Lys^{665} caps the C-terminus of αCT (Fig. 22). Accordingly**,** regions analogous to the carboxyl terminal tail of the GRK2 PH domain in other Gβγ-binding PH domains tend to harbor basic residues (Figs. 14C, 22).

Figure 21. The GRK2 PH domain and its interface with Gßγ. (A) The GRK2 PH domain. Residues implicated in the binding of anionic phospholipids (Touhara 1997; Fushman, Najmabadi-Haske et al. 1998) are drawn with blue side chains. For perspective, IP3 is modeled from the structure of PLCδ (Ferguson, Lemmon et al. 1995). Two residues from GRK2, Lys567 and Arg579, are in position to coordinate the phosphates of the anionic head group, as do equivalent residues in other PH domains (45). The four regions within the primary sequence of the GRK2 PH domain that contact Gβγ are each drawn with a different color for reference [see (B) and (D)]. These regions form a continuous surface that includes the β1-β4 sheet of the PH domain, the extended portion of the αCT helix, and the C-terminal tail. The conformation of the β1-β4 sheet is highly conserved among PH domains of known structure (Table 2). Therefore, many PH domains have a surface that is complementary in shape to the effector-binding surface of Gßγ. (B) Specific interactions between the PH domain and Gβ. The location of each interacting residue within the tertiary structure of the PH domain is indicated alongside each amino acid. In addition to the interactions shown, Arg689 of GRK2, which was not modeled because of weak electron density, is also expected to contact the surface of Gßγ. (C) Comparison of the surfaces of Gβγ that bind Gα subunits and GRK2. The molecular surface of Gβγ was colored according to its contacts with Gα (blue), GRK2 (red), or neither (white). Common binding surfaces are colored purple. The footprint of Gα on the surface of Gβγ overlaps extensively with that of the GRK2 PH domain, and thus their binding is mutually exclusive. Positions of various residues from Gβ that contact the PH domain of GRK2 are labeled for reference. (D) Stereoview of the PH domain–Gß1 interface. Residues from Gβ are drawn with gray carbons, residues from the PH domain with tan carbons. Hydrogen bonds or salt bridges between residues are indicated with dashed lines. The side chain of Met664 from the RH domain binds within a hydrophobic pocket, one wall of which is formed by Leu117 of Gβ (omitted for clarity). Trp99 of Gß docks into a hydrophobic groove at the interface such that its indole nitrogen is oriented toward solvent. Although electron density for the side chain of Lys663 is not observed beyond Cß, it could extend far enough into the central channel of Gβ to allow interaction of its Nζ atom with a ring of seven carbonyl oxygens donated by the innermost strand from each blade of Gβ.

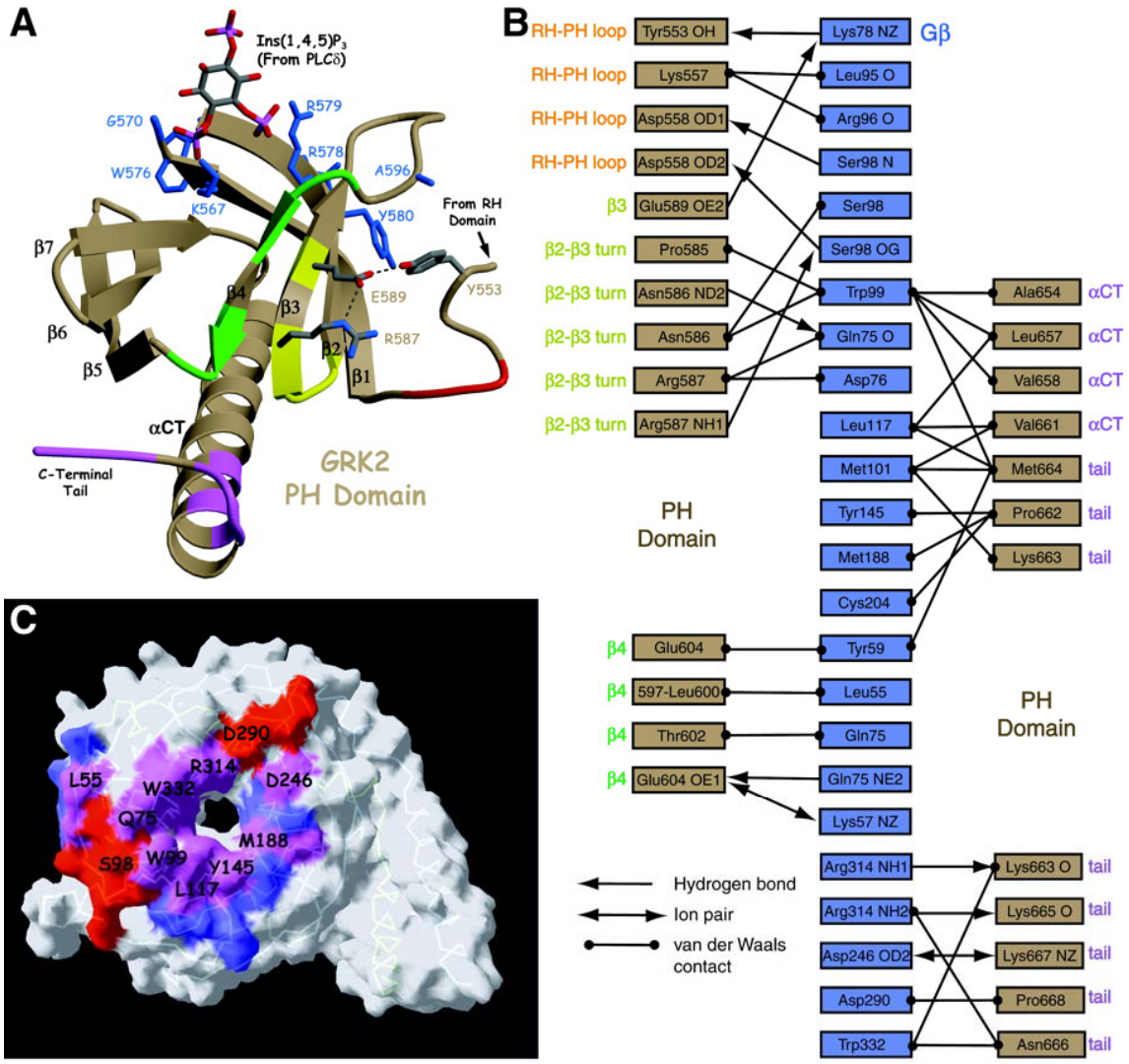
A
Ins(1,4,5)P3
(From PLCδ)
G570
R579
R578
W576
A596
K567
Y580
From RH
Domain
β7
β4
β3
E589
Y553
β6
β2
R587
β5
β1
αCT
C-Terminal
Tail
GRK2
PH Domain
B
RH-PH loop
Tyr553 OH
Lys78 NZ
Gβ
RH-PH loop
Lys557
Leu95 O
RH-PH loop
Asp558 OD1
Arg96 O
RH-PH loop
Asp558 OD2
Ser98 N
β3
Glu589 OE2
Ser98
β2-β3 turn
Pro585
Ser98 OG
β2-β3 turn
Asn586 ND2
Trp99
Ala654
αCT
β2-β3 turn
Asn586
Gln75 O
Leu657
αCT
β2-β3 turn
Arg587
Asp76
Val658
αCT
β2-β3 turn
Arg587 NH1
Leu117
Val661
αCT
Met101
Met664
tail
PH
Domain
Tyr145
Pro662
tail
Met188
Lys663
tail
Cys204
β4
Glu604
Tyr59
β4
597-Leu600
Leu55
PH
Domain
β4
Thr602
Gln75
β4
Glu604 OE1
Gln75 NE2
Lys57 NZ
Hydrogen bond
Ion pair
van der Waals
contact
Arg314 NH1
Lys663 O
tail
Arg314 NH2
Lys665 O
tail
Asp246 OD2
Lys667 NZ
tail
Asp290
Pro668
tail
Trp332
Asn666
tail
C
D290
R314
L55
D246
W332
Q75
M188
S98
W99
Y145
L117
D
PH
Domain
αCT
β2
β4
T602
C-Terminal
Tail
β3
A654
E604
β1
N586
Q75
W99
L600
R587
L657
L55
S98
Y59
R314
D558
M664
V661
P662
K557
M101
K663
β1
Gβ
β28
β26
Propeller
Channel
β5
β4
β3
β2
PH
Domain
αCT
β2
β4
T602
C-Terminal
Tail
β3
A654
E604
β1
N586
Q75
W99
L600
R587
L657
L55
S98
Y59
R314
D558
M664
V661
P662
K557
M101
K663
β1
Gβ
β28
β26
Propeller
Channel
β5
β4
β3
β2

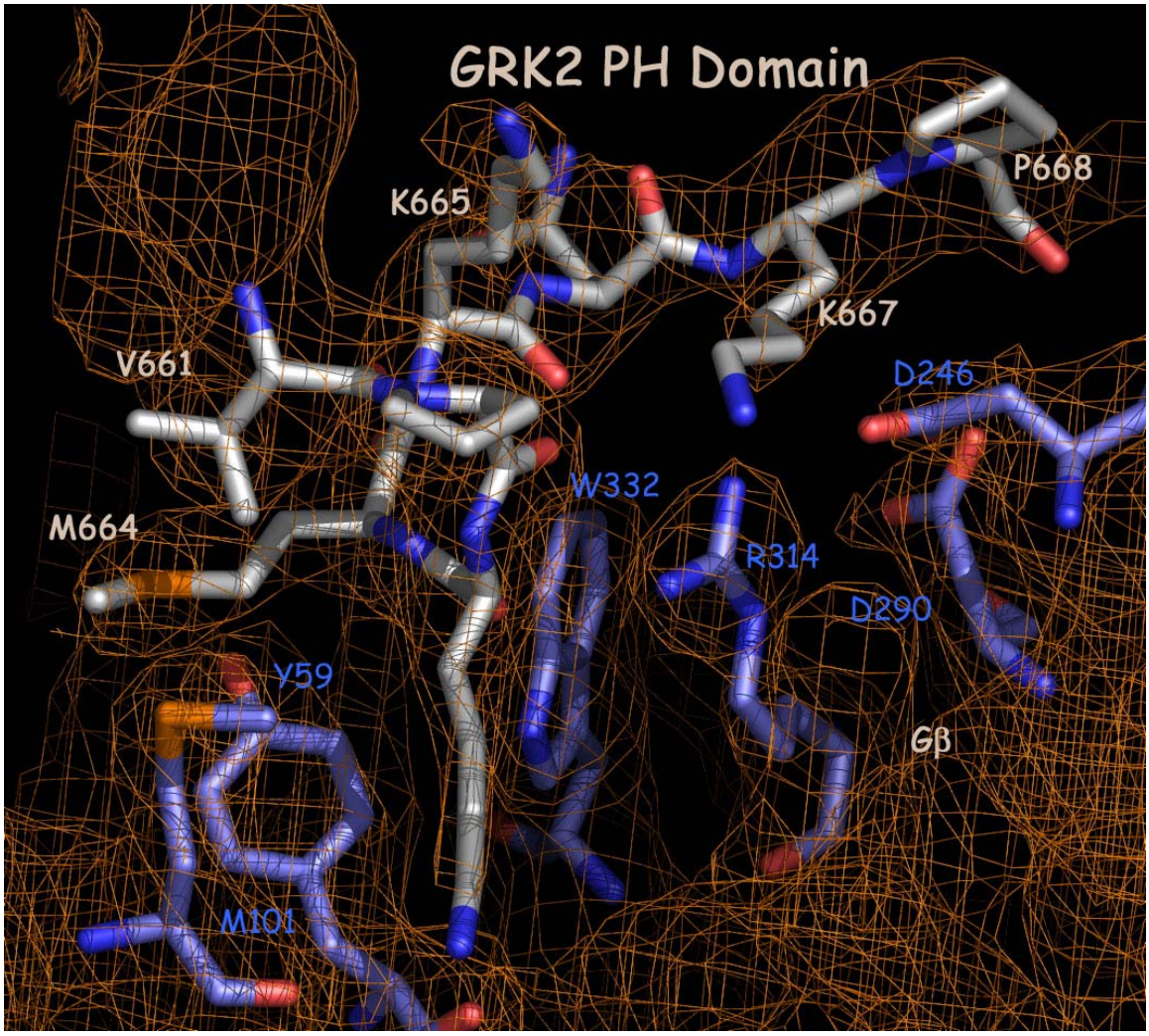

Figure 22. Interactions of the PH domain C-terminal tail with Gβ. Electron density (cages) from a 2.5 Å σA-weighted 2Fo-Fc difference map is contoured at 1.1 standard deviations above the mean(Read 1986). Residues are colored as in Fig. 21.

Implications

The GRK-Gβγ structure reveals how three common, modular signaling domains successfully coordinate their activities to perform several complex tasks. The first is to control the intrinsic activity of the kinase domain in lieu of phosphorylation. The RH terminal subdomain clearly contributes to this regulation (Fig. 23A). The subdomain is not only intimately associated with both the PH domain, which binds two synergistic activators (Gβγ and anionic phospholipids), and the bundle subdomain, which binds $G\alpha_{q/11}$·GTP; it also contacts the small lobe of the kinase domain, known by analogy with Src, PKA, and PKB to be critical for the regulation of catalytic activity (Fig. 18A). Furthermore, it makes contact with the large lobe of the kinase domain, allowing for further manipulation of the kinase domain. Therefore, a change in the conformation of the terminal subdomain, induced by the binding of Gβγ, caveolin, calmodulin, phospholipids or $G\alpha_{q/11}$·GTP, could directly lead to changes in catalytic activity via its interface with the kinase domain.

The task of recruiting GRK2 to the site of activated receptors is accomplished through multiple interactions. The binding of Gβγ to the PH domain of GRK2 positions the PH domain such that its β1-β2 loop may interact with anionic phospholipids. Because free Gβγ subunits are generated close to activated receptors, GRK2 will be targeted primarily to specific sites on the membrane where active signal transduction is taking place (Pitcher, Inglese et al. 1992).

A third task is to orient GRK2 at the membrane in a manner that facilitates interaction with and phosphorylation of activated receptors. This is achieved by the domain interfaces of GRK2, which fix each of its three domains in an optimal orientation with respect to the cell membrane (and therefore with respect to GPCRs). With the plane

of the membrane as defined in Fig. 15, there is a substantial gap between the membrane and the large lobe of the GRK2 kinase domain (Fig. 23b). The cytosolic domain of a GPCR can be docked into this gap such that receptor residues known to be important for binding GRKs (Shi, Osawa et al. 1995) are in close proximity to both lobes, the nucleotide gate, and the active site of the kinase domain. In this model, either an extended third cytoplasmic loop or the C-terminal tail of the receptor can enter the polypeptide binding cleft of GRK2 in the same orientation observed for peptides co-crystallized with PKA (Knighton, Zheng et al. 1991).

The proposed orientation of GRK2 at the membrane is also consistent with the formation of a complex between its RH domain and $G\alpha_{q/11}$·GTP (Fig. 23). The resulting interface consists of a wedge-like intrusion of the α5 and α6 helices of the RH domain into the cleft formed between the Ras-like and α-helical domains of $G\alpha_{q/11}$, making extensive contacts with the switch regions of Gα (Carman, Parent et al. 1999; Sterne-Marr, Tesmer et al. 2003).

Remarkably, the Gβγ and the proposed GPCR and $G\alpha_q$ binding sites are each on a different vertex of the "triangle" formed by the three domains of GRK2 (Fig. 23A). GRK2 could therefore bind all three proteins simultaneously. This would represent an extremely efficient way to attenuate G protein signaling. The kinase domain would bind and phosphorylate activated receptors, recruiting arrestin and thereby blocking access of G proteins and tagging the receptor for endocytosis. The RH and PH domains would bind $G\alpha_{q/11}$·GTP and Gβγ, respectively, blocking the G proteins from their downstream targets–effectively keeping them at bay until receptor signaling is terminated.

Fig. 23. Nonexclusive binding of GRK2 to Gβγ, GPCRs, and $G\alpha_q$. (**A**) Membrane-proximal view. Models of a GPCR (maroon) and $G\alpha_q$ (dark blue with tan ß strands) were docked with GRK2-Gβγ in a manner consistent with the expected orientation of each individual protein at the cell membrane. The kinase domain of GRK2 is modeled in a closed, "active" conformation, and the six C-terminal residues of the receptor have been repositioned to follow the same path as peptides bound to other AGC kinases (Knighton, Zheng et al. 1991; Yang, Cron et al. 2002). GRK2 is known to contact GPCRs at two distinct locations: within the polypeptide binding cleft of the kinase domain, and at a noncatalytic, allosteric "docking site" that discriminates between inactive and stimulated receptors (Shi, Osawa et al. 1995; Pitcher, Freedman et al. 1998). The proposed GPCR docking site is on the kinase domain, near two disordered regions of GRK2 (residues 1 to 28 and 476 to 495) that not only are believed to play important roles in receptor and/or phospholipid binding, but also contain external regulatory sites for Ca^{2+}/calmodulin, PKC, and clathrin (Ferguson, Lemmon et al. 1995; Fushman, Najmabadi-Haske et al. 1998). The switch regions of $G\alpha_q$ (red) pack against the $G\alpha_q$-binding residues identified in the RH bundle subdomain of GRK2 (Sterne-Marr, Tesmer et al. 2003), rendering their interaction dependent on the signaling state of the G protein. The amino and carboxyl termini of the GPCR and $G\alpha_q$ are indicated. GDP·AlF_4^-, bound to $G\alpha_q$, is drawn as a ball-and-stick model. (**B**) Side view of the complex, rotated 90° around a horizontal axis with respect to (A). The gray bar represents the proposed membrane bilayer, as defined by the top surface of the GRK2-Gβγ complex and the belt of hydrophobic residues presented by the transmembrane helices of the GPCR.

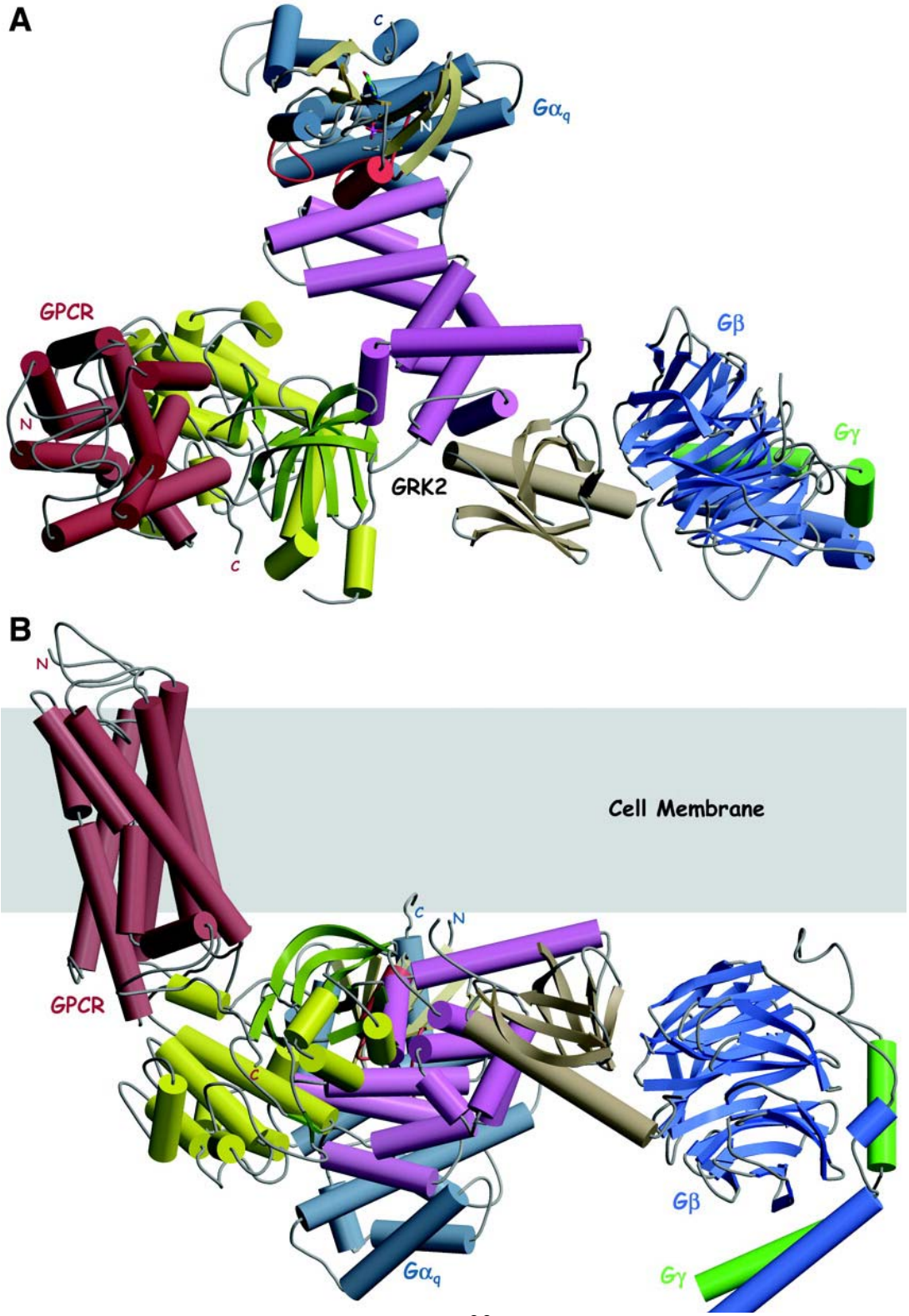
A
C
N
Gαq
GPCR
N
C
GRK2
Gβ
Gγ
B
N
Cell Membrane
C
N
GPCR
C
Gβ
Gγ
Gαq

The GRK2:Gβγ Complex: a Model for Other Gβγ-binding PH domains

Sequence conservation among PH domains at positions corresponding to residues in GRK2 that contact Gβγ are highest for proteins whose *in vivo* interactions with Gβγ are well established, particularly the PLCβ isozymes (Table 2, Fig. 14c). A conserved FLζK motif (where ζ is a hydrophilic amino acid) at the end of the PLCβ PH domain is also found in GRK3. The phenylalanine of this motif in GRK3 is expected to fulfill the same role as Met661 in GRK2 (Fig. 22d, 23), and residues within and adjacent to this motif were recently shown to be important for the interaction of PLCβ2 with Gβ (Barr, Ali et al. 2000).

Potential Routes for Allosteric Regulation by Phospholipids and Gβγ

Anionic phospholipids and Gβγ cooperatively activate GRK2 by recruiting the enzyme to the cell membrane (Pitcher, Inglese et al. 1992; DebBurman, Ptasienski et al. 1995; Pitcher, Fredericks et al. 1996; Touhara 1997; Carman, Barak et al. 2000). However, they may also contribute to allosteric activation of GRK2. The proximity of the phospholipid binding site to the PH:RH terminal subdomain interface suggests one potential route of allosteric regulation. Conformational changes at this interface could alter the relative orientation of the RH and kinase domain core with respect to the PH domain, thereby influencing how GRK2 interacts with the cell membrane and GPCRs. Alternatively, allosteric information could be transmitted from the PH domain through the long, lever-like α11 helix of the RH domain. The C-terminus of this helix not only interacts with the proposed membrane (Fig. 15a), but also is associated via a short, acidic linker to a cluster of residues in the PH domain that interact directly with Gβγ (Arg^{587}, Glu^{589} and Tyr^{553}; see Fig. 21a). The opposite end of α11 is adjacent to the kinase

domain, where it could directly influence catalytic activity in response to membrane or Gβγ binding events at its C-terminus. Finally, it seems likely that the cell membrane itself is an allosteric regulator of GRK2. The GRK2·Gβγ complex suggests that other highly conserved, basic regions of GRK2 besides the PH domain, including the extended α11 helix of the RH domain (Fig. 16a), the αB helical region of the kinase domain (Figs. 15, 17), and residues 28-31 at the N-terminus (Fig. 14a) must engage a negatively-charged membrane in order to properly orient GRK2 for receptor binding and phosphorylation.

THE GRK2 SOLUBLE STRUCTURE

The determination of the structure of the GRK2·Gβγ complex revealed the arrangement of the domains within GRK2 as well as revealing possible mechanisms by which GRK2 can bind GPCRs, Gα subunits and Gβγ subunits(Lodowski, Pitcher et al. 2003; Sterne-Marr, Tesmer et al. 2003). To further understand the role that Gβγ plays in the regulation of GRK2 and in the GRK2·Gβγ complex, we crystallized and solved the structure of GRK2 alone. By comparing the GRK2 structure to that of the complex, we can observe the structural changes upon Gβγ binding. Furthermore, we performed a series of protease protection assays and sedimentation equilibrium analysis to elucidate the effects of Gβγ and phospholipid binding upon the dynamic structure of GRK2.

The Quaternary Structure of GRK2

The GRK2 structure (from now on referred to as "soluble structure") contains four GRK2 molecules per asymmetric unit arrayed as a dimer of dimers which form a wide "V" shape (Fig. 24). The contacts within each set of dimers involve a series of hydrophobic contacts arrayed along the α5 and α6 helices of each RH domain. This interface buries ~1600 $Å^2$ of surface and includes residues implicated in $Gα_{q/11}$ binding (Figs. 25 and 27). The "dimer of dimer" contact which comprises the vertex of the "V," involves several contacts between the PH and kinase domains of the two GRK molecules and buries ~1200 $Å^2$ of surface area. (Figs. 24 and 25).

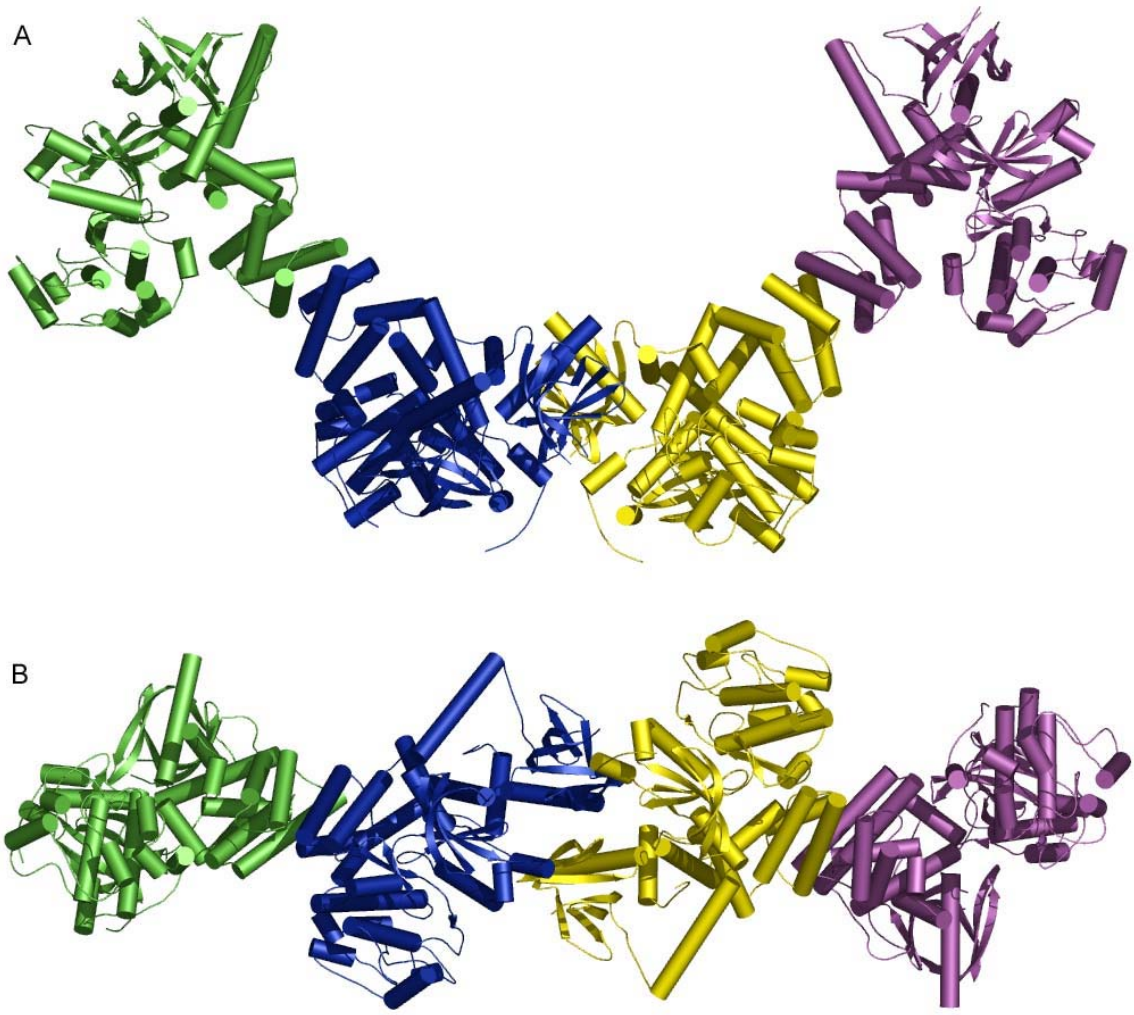

Figure 24. Orientation of individual GRK2 molecules within the asymmetric unit. A. The four GRK2 molecules within the asymmetric unit (monomers A, B, C, and D are colored yellow, blue, magenta and green respectively). The dimer axis between the blue and green (monomers B and D) and between the yellow and magenta (monomers A and C) molecules correspond to the $G\alpha_{q/11}$ binding surfaces (Sterne-Marr, Tesmer et al. 2003). The other dimer axis (between blue and yellow molecules) is not expected to be physiological as it utilizes the side of the PH domain opposite that of the $G\beta\gamma$ binding surface. B. Same as A, but rotated 90° in the plane of the page.

The domain arrangement of the RH, protein kinase and PH domains of GRK2 are arranged similarly as in the complex structure. The average RMSD for the positions of C-α atoms within the individual RH, Kinase, PH domains and GRK2 as a whole compared to the GRK2·Gβγ complex are 0.65 Å, 0.75 Å, 1.1 Å and 1.2 Å respectively. The amount of buried surface area between each domain is similar to that of the individual subunits in the complex structure.

Although the domain arrangement is generally the same between the complex structure and the soluble structure, there are some notable differences (Fig. 26D). Namely, the relative orientation of the individual domains varies. When the various domains are compared, the kinase domain has a root mean squared deviation (RMSD) of 0.6 Å while the RH and PH domains have RMSDs of 0.7 and 1.1 Å respectively. When the individual GRK2 molecules are superposed upon one another with *LSQKAB* (CCP4 1994), it is apparent that the relative orientations of the RH and PH domains with respect to the kinase domain are noticeably different. In the B and C molecules, the differences are more pronounced and it appears that the RH and PH domain have rocked or rotated as a unit (Fig. 26D). The axis of rotation for the PH and RH domain motions appears to be the junction of the kinase domain and the RH domain.

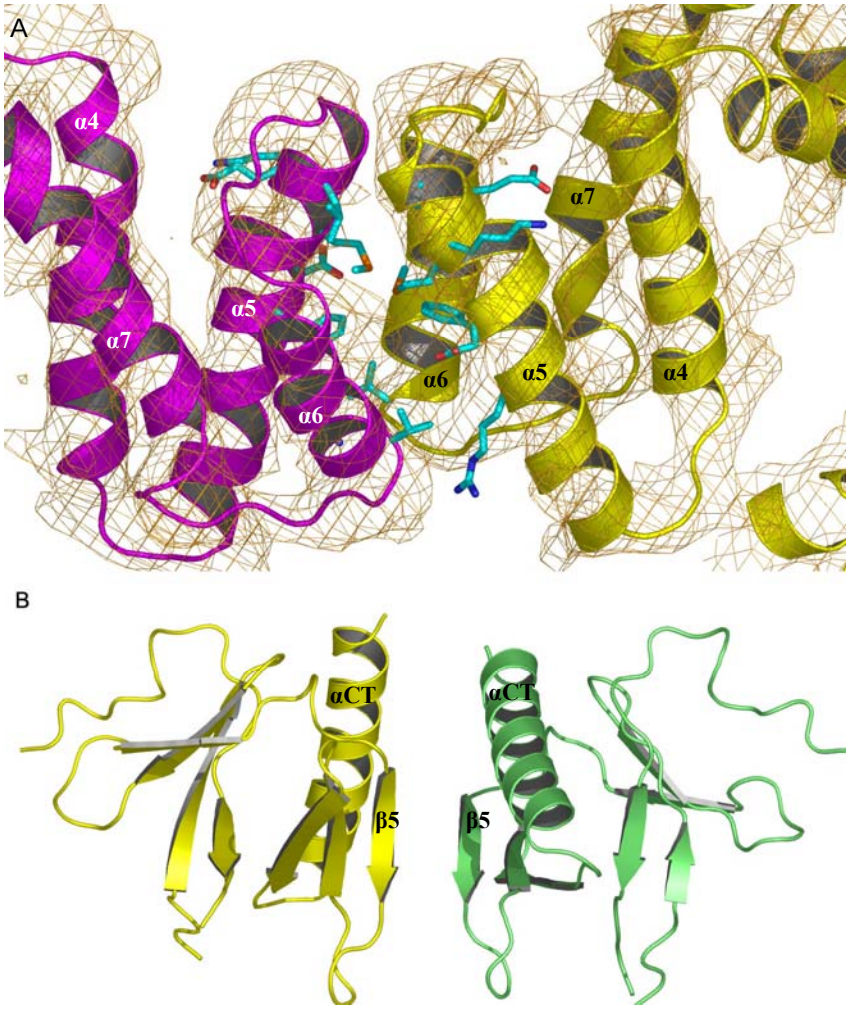

Figure 25. Dimer interfaces within the GRK2 soluble structure. A. The monomer A and monomer C dimer interface. Residues shown to be necessary for $G\alpha_q$ binding are shown in cyan. Many of these residues make up the dimer interface between the two monomers. B. The dimer interface between monomers A and B. Contacts between the two monomers utilize the αCT helix as well as the β5 strand. The interactions with the helix occur on the opposite side than where Gβγ binds.

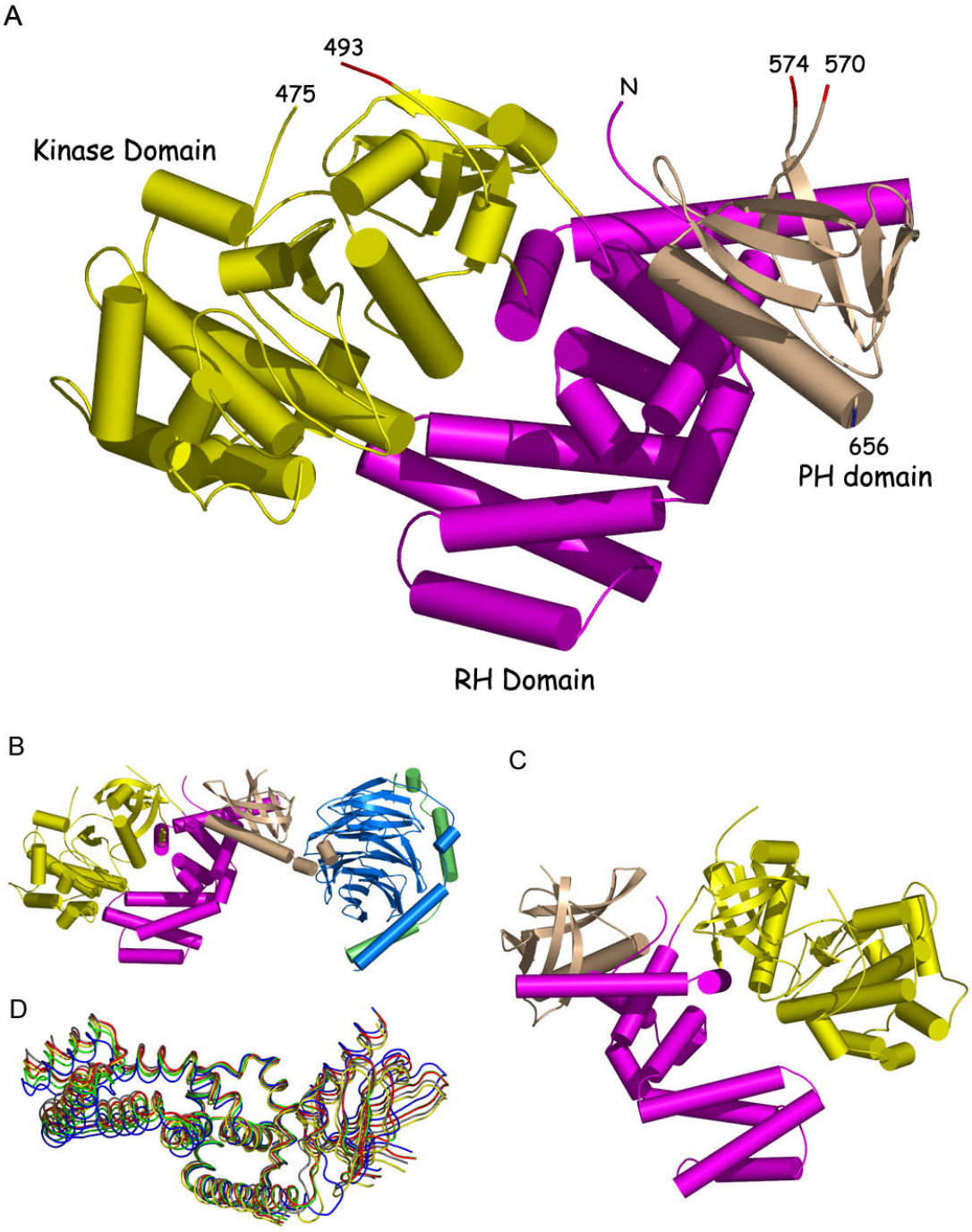

Figure 26. The soluble structure of GRK2. In panels A, B and C, the RH domains are colored in magenta, the kinase domain in yellow and the PH domain in tan. A. The domain structure of GRK2. The kinase domain is in an open conformation and is opened to a similar degree as to GRK2 in the complex structure. Regions present in the soluble

structure and absent in the complex structure are shown in red. The residues following 656 (shown in dark blue) (657-668) are present in the complex structure. B. The GRK2·Gβγ complex structure in the same orientation as A. The three domains are in a similar orientation to that of the soluble structure. The hypothetical membrane proximal surface is located on the top surface of the figure. C. Same as A, but GRK2 has been rotated 180º around the y axis so that the PH and RH domain are in front of the protein kinase domain. D. Superposition of GRK2 structures. The structures of GRK2 from the complex structure and the soluble structure were analyzed and superimposed on the small lobe of the kinase domain (average RMSD for equivalent Cα atom positions 0.55Å). Each monomer structure is colored differently; the complex structure is colored grey, and the A, B, C and D subunits of the soluble structure are colored in red, green, blue and yellow, respectively. The molecule was rotated so that RH and PH domains are above the kinase domain which has been omitted for clarity. The various structures have rotated upon an axis at the point where the kinase domain inserts into the RH domain (in the loop region preceding the kinase domain (184-188) and in the loop connecting the large lobe of the kinase domain and the amino terminus of α10 helix (511-515)).

Analysis of domain motion and domain flexibility

To better understand the structural differences between the complex structure and the four monomers from the soluble structure, it was necessary to characterize the structural differences present between the individual monomers. A series of distance difference plots comparing the individual GRK2 monomers to the structure of GRK2 in the GRK2·Gβγ complex was calculated utilizing the superpose server (Maiti, Van Domselaar et al. 2004). From these difference distance plots, it is apparent that there are significant structural differences in the relative positions of the RH and kinase domains in the B and C GRK2 molecules. A lesser movement of the PH domain with respect to the kinase domain is also evident. In the D molecule a significant difference in residues 540-554 within the transition between the RH and PH domains is also readily apparent (Figs. 26D and 27). This structural difference is manifested in a remodeling of the carboxyl-terminus of the α11 helix and in the following loop region. This helix makes a ~45° bend between residues 542-543. This bend is necessary to avoid running into a symmetry mate in a crystallographically related D subunit. If the helix were to exist in a manner similar to that within the A, B, and C monomers, it would overlap the crystallographic two-fold axis.

Because the resolution of the soluble structure is only 4.5Å, it is necessary to ensure that the structural differences seen between the complex structure and the individual monomers of the soluble structure are indeed significant. The difference distance plots shown in figure 27 fail to take into account the uncertainty in atomic positions due to resolution, B factor, redundancy of x-ray data and completeness. Cruickshank's method of determining this uncertainty allows for the calculation of a diffraction-component precision index (DPI) which allows an estimation of the

uncertainty due to resolution, R_{free} and ratio of observations to be calculated (Cruickshank 1999). The Cruickshank formula for the DPI (σ) is as follows:

$$\sigma(x, B_{average}) = (N_i/N_{obs})^{0.5}(\text{Completeness})^{-1/3}(R_{free})D_{min}$$

Where N_i = average B factor for fully occupied sites within the protein structure and N_{obs} = number of observations (Cruickshank 1999). The shortcoming of this technique is that it assumes that all atoms within the structure have the same B factor (Schneider 2000). It has been shown that the B factor is highly correlated with coordinate error, so this assumption is only a gross approximation (Chambers and Stroud 1979). To further extend this DPI and make it more useful for analysis of low resolution structures, a more exact method utilizing B factor scaling has been proposed by Schneider (Schneider 2000; Schneider 2002). Cruickshank's DPI is simply scaled by a linear factor (B_{ave}-B_{ind}/B_{ave}). Schneider's calculation involves the DPI of Cruickshank and linearly scales it to the individual B factor of each protein. This modified DPI is integrated into a structural analysis program called error-inclusive structure comparison and evaluation tool (*ESCET*). By utilizing *ESCET*, it is possible to assign a σ value to the atomic displacements seen between models of varying resolution allowing the estimation of the significance of molecular displacements.

ESCET also performs calculations upon a group of protein structures which allow the identification of conformationally invariant regions in protein molecules. Basically, a genetic algorithm is utilized to shrink and grow randomly chosen rigid bodies within the molecule based on the error correlated difference distance plots. When the GRK2·Gβγ complex structure and the structures of all four monomers are entered into *ESCET*, residues 30-79, 154-540, 554-606, 618-624 and 631-654 form structurally invariant regions. This identifies the bundle subdomain and the α11 helix of the RH domain as flexible regions within the GRK2 structures (Fig. 29).

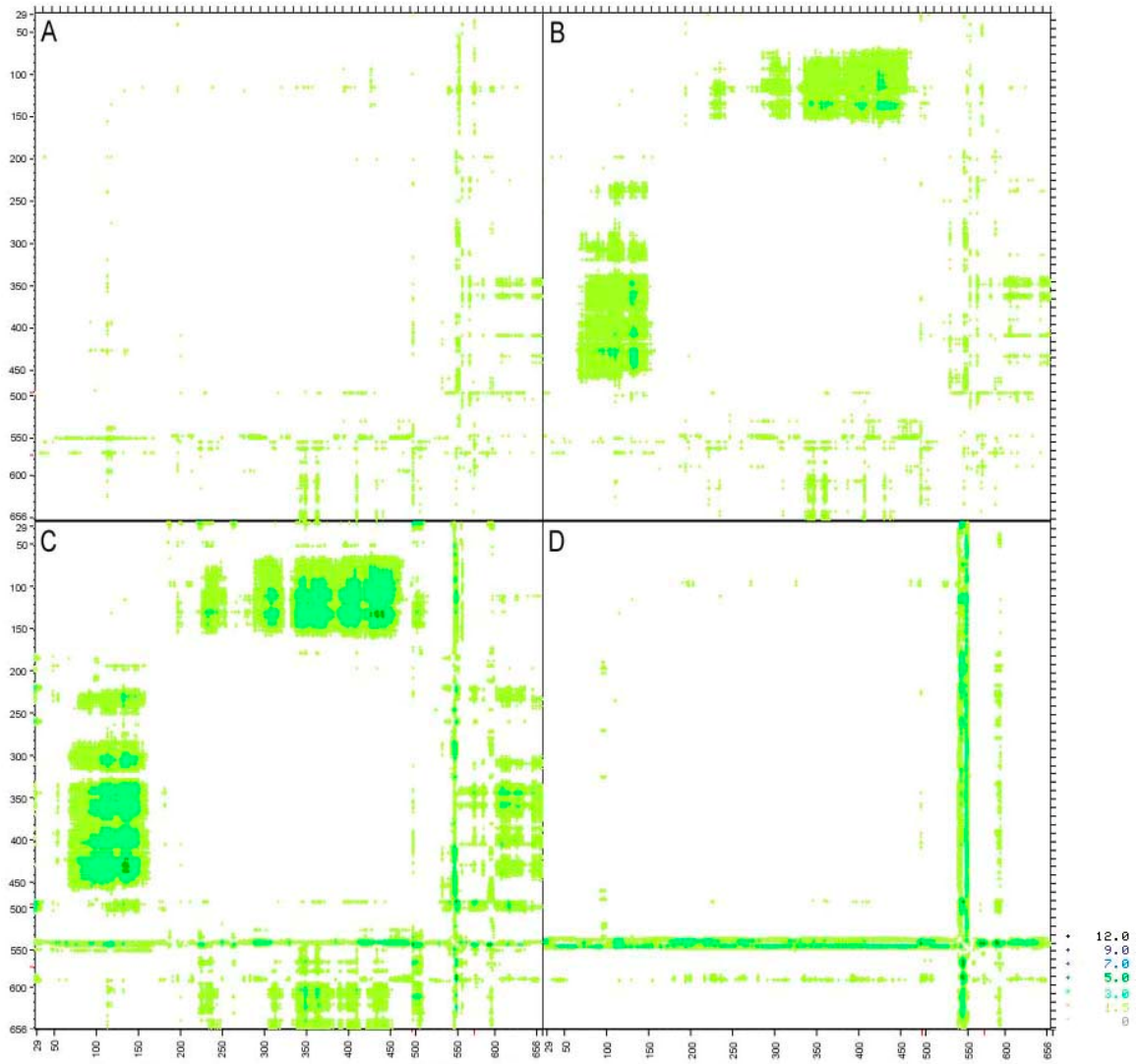

Figure 27. Difference Distance Plot GRK2(complex) vs. GRK2 monomers. Panels A, B, C and D correspond to the respective monomer in the soluble structure. From these difference distance plots, it is possible to determine the relative domain movements that have occurred in going from the complex structure to the structures of each of the monomers. A. No large domain rearrangements. B. and C. The positions of the RH, kinase and PH domains have shifted with respect to the complex structure. These distance difference plots were performed utilizing the superpose server(Maiti, Van Domselaar et al. 2004).

As this calculation is based on the significance of the spatial displacement of atoms, it fails to identify significant angular displacement when the concomitant spatial displacement is below the threshold of significance. The result is that of failing to identify angular displacement in regions close to the axis of rotation, and indeed, the flexible regions identified by *ESCET* are located in the ends of the molecule furthest from the axis of rotation (Fig. 29).

One last method undertaken to determine the relative changes in domain orientation was to "morph" from the structure of GRK2 in the complex to each of the monomers in the soluble structure. All GRK2 molecules were superimposed upon the small lobe of their kinase domains (average RMSD =0.55Å for equivalent Cα positions) and a CNS script was used to generate intermediate structures (Krebs and Gerstein 2000). This script creates a stepwise population of energy minimized structures going from one structure to another via adiabatic mapping. These structures were then animated into a movie using the program *PYMOL* and the results observed (DeLano 2002). Upon examination of this animation, two structural changes are readily apparent. The most obvious change is that of the RH and PH domains. Both domains appear to rotate approximately 5-7° with respect to the kinase domain upon which they were aligned. The region between residues 541-554 which was determined by *ESCET* to be a flexible region appears to remodel when the molecule undergoes a transition from one monomer to another. The changes in this region when transitioning from monomer A to monomer B and from monomer C to D are quite pronounced and this region appears to expand or contract as the RH and PH domains move with respect to the kinase domain. The carboxyl terminal residues of the α11 helix appear to unravel and bend up to 45° in response to the changes in each GRK2 monomer structure, but this is a crystal packing artifact. The β5, β5-6 loop and β6-7 loop regions within the PH domain are also

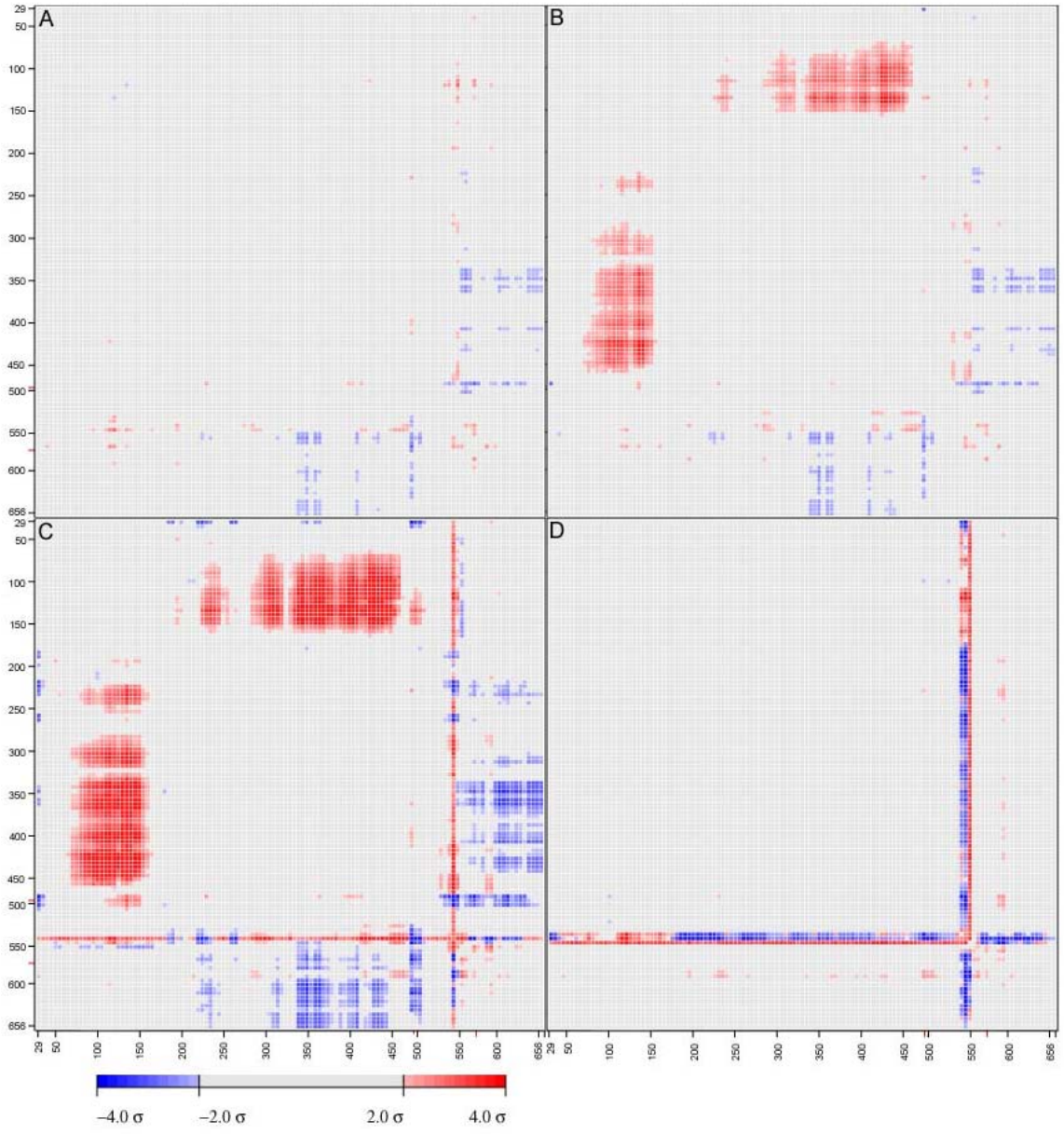

Figure 28. ***ESCET*** **analysis GRK2 monomers vs. the complex structure.** Panels A, B, C and D correspond to different chains within the soluble structure. Blue color indicates that atoms have moved closer together while red indicated expansion. In order for changes to show up within the plot, they must have a statistical significance of at least 2σ. It is evident from these plots that changes seen in the plots of figure 26 are in fact significant.

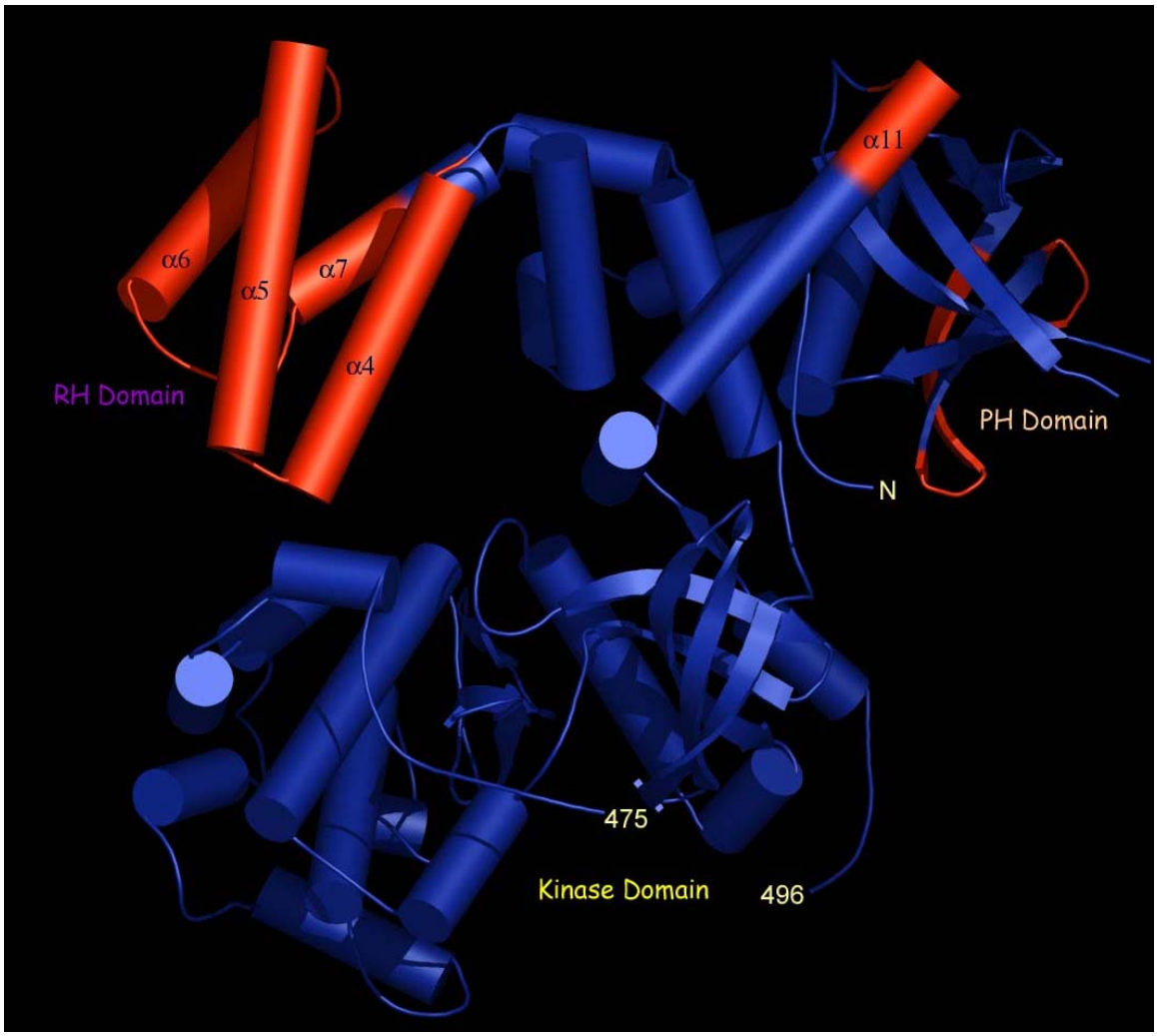

Figure 29. Conformational variance in GRK2 as determined by *ESCET*. Portions of the molecule determined to be conformationally invariant are colored in blue. The red regions are those portions of the molecule that are significantly different between all structures, indicating that they are in fact flexible regions. The bundle subdomain of the RH domain, the carboxyl-terminus of the α11 helix and portions of the PH domain are all classified as flexible. The amino and carboxyl termini as well as the nucleotide gate region and phospholipid binding loop of GRK2 are thought to be flexible as they are disordered in both crystal structures.

classified as flexible; it does not appear that the motions of these regions correlate with the activation of GRK2 because this region makes no contacts with Gβγ nor with the RH or protein kinase domains. It is possible that once GRK2 is recruited to the membrane and binds phospholipid, this region assumes a distinct conformation which participates in the activation of GRK2.

PH domain comparisons

To determine the differences between the PH domain of GRK2 in the full length structures and those of its NMR structure (Fushman, Najmabadi-Haske et al. 1998), pairwise superpositions of the five PH domains from the soluble and complex structures were performed on each of the 20 NMR ensemble models of the PH domain of GRK2. These pairwise comparisons were performed only over the core beta sheet and carboxyl-terminal α helix as determined in the NMR structure. This core secondary structure consists of residues 561–568 (β1), 578–584 (β2), 587–591 (β3), 600–602 (β4), 606–613 (β5), 618–624 (β6), 628–634 (β7) and 638–655 (carboxyl-terminal α helix) (Fushman, Najmabadi-Haske et al. 1998). R.M.S.D.s for these superpositions were 1.48 Å on average with a standard deviation of 0.06 Å. When compared to the average differences between all of the PH domains in the complex and soluble structures (0.87 Å standard deviation 0.087) it is obvious that the NMR model is significantly different than that of our full length structures. When compared to the values in table 2, it is obvious that the PH domain in the full length structure more resembles that of other protein's PH domains than it does the NMR model.

One possible explanation for the differences in PH domain structure are the extreme conditions under which the NMR spectra were collected (1–2 mM protein in 10 mM acetate buffer at pH 4.5, 0.02% sodium azide, 1 mM ^{2}H-EDTA, 5 mM ^{2}H-dithiothreitol) (Fushman, Najmabadi-Haske et al. 1998). Another possibility is that the NMR constraints that were derived from the NMR experiments are consistent with our structure and the NMR model, but this is not possible to test as the restraints were not deposited in the PDB along with the structure. The most likely explanation is that the structure of the PH domain depends on its contacts with the RH domain and without these contacts, it assumes a different conformation which is captured in the NMR model. A final possibility is that when the PH domain of GRK2 is expressed on its own, it simply does not fold up in the same manner as it does in the full length protein and instead assumes a conformation similar to that seen in the NMR structure. When the GRK2 PH domain is expressed as a maltose binding protein (MBP) fusion it only remains soluble until the PH domain is cleaved off of MPB; once the PH domain is removed from the MBP a large portion of it begins to irreversibly aggregate, indicating that it is either improperly folded or unstable in solution without its contacts within the remainder of GRK2.

Protease protection assays of GRK2

The ability of Gβγ to recruit GRK2 to activated GPCRs is well known and characterized (Pitcher, Touhara et al. 1995). The binding of Gβγ to the PH domain of GRK2 recruits GRK2 to the plasma membrane where this activation is further potentiated by the binding of anionic phospholipids to loops within the PH domain. Analysis of these binding curves suggests positive cooperativity between GRK2 and PIP_2 (Pitcher,

Touhara et al. 1995). Protease protection assays indicate that the binding of wild type Gβγ to GRK2 is sufficient to protect it from proteolysis even at sites distant to the Gβγ binding site (Figs. 30 and 31). In protease digests with the protease clostripain, which cuts on the carboxyl terminal side of arginine residues, GRK2 is proteolyzed at two main sites, residues Arg^{404} and Arg^{660} (Fig. 30A). When these same digests are carried out in the presence of wild type (geranylgeranylated) Gβγ in CHAPS detergent micelles, both cut sites are protected. Conversely, when the same digest was carried out in the presence of a soluble mutant of Gβγ, only the protease site at Arg^{660} (close to the Gβγ binding site) is protected. The protection of the site by Gβγ at Arg^{404} is remarkable as this is 80Å away from the Gβγ binding site and there is no steric reason why Gβγ should protect at the Arg^{404} site (Fig. 31). This suggests that the geranylgeranyl group of Gγ and its bound CHAPS detergent micelle are able to influence the structure of regions distant from the Gβγ binding site in the PH domain.

Similar results are seen with the protease Endoprotease-Asp-N (Endo-Asp-N) which cuts at the amino terminal side of aspartic acid residues (Fig. 30 B). When GRK2 is digested by Endo-Asp-N, a single primary cut site is seen at residue 480. This protease sensitive site is located within the nucleotide binding loop within the kinase domain, a region that is disordered in both of the GRK2 structures and implicated in the activation of other AGC kinases (Zheng, Knighton et al. 1993). Although complete protection at Asp^{480} is not seen with wild type Gβγ, it protects to a greater than the soluble mutant or detergent alone. Interestingly, while Endo-Asp-N was ~20% more active in the presence of CHAPS, the mere presence of detergent micelles caused conformational changes within GRK2 enough to partially protect the nucleotide binding loop. Protease digests performed in the presence of phospholipid vesicles containing PIP_2 also were able to partially protect protease sensitive sites within GRK2. Asp^{480} is protected from

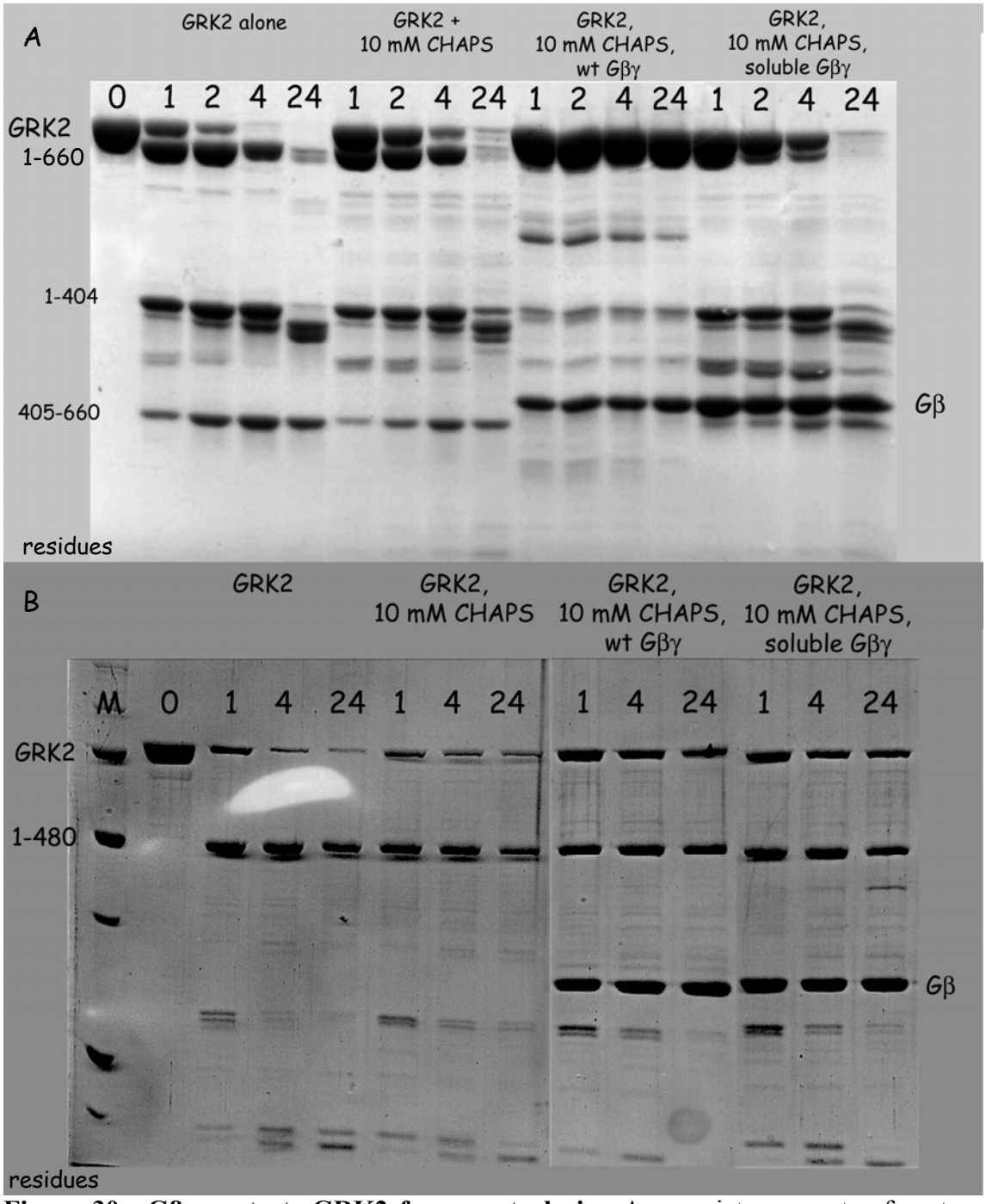

Figure 30. Gβγ protects GRK2 from proteolysis. Appropriate amounts of protease were determined by incubating GRK2 with serial dilutions of protease and choosing the smallest amount of protease that was sufficient to proteolyze GRK2 in an overnight digest. All digests containing Gβγ were done in a 2:1 molar excess of Gβγ over GRK2. A. Clostripain digest of GRK2. GRK2 was digested at 25° C and 1, 2, 4 and 24 time

points taken. Conditions consisted of GRK2 alone, GRK2 and 10 mM CHAPS, GRK2, 10 mM CHAPS and wild type Gβγ, or GRK2, 10 mM CHAPS, and a soluble mutant of Gβγ (C68S). Only the addition of wild type Gβγ is sufficient to protect both protease sensitive sites (Asp^{404} and Asp^{660}). The soluble mutant which is expected to associate with the PH domain protects the Arg^{660} at the Gβγ binding site but exerts no influence on the other site located in the kinase domain (Arg^{404}). Sites were assigned through a combination of N-terminal sequencing and MALDI-TOF mass spectroscopy. B. Endoprotease-Asp-N Digest of GRK2. GRK2 was digested at 30° C and 1, 4, and 24 hour time points taken. Conditions were the same as in the clostripain digests above. The addition of CHAPS was determined in activity assays to make Endo-Asp-N proteolyze a colorimetric substrate at an approximately 20% faster rate (data not shown). The addition of CHAPS plus wild type Gβγ partially protected GRK2 from proteolysis. The addition of CHAPS or CHAPS and soluble Gβγ partially protected GRK2 from proteolysis but to a lesser extent than wild type Gβγ.

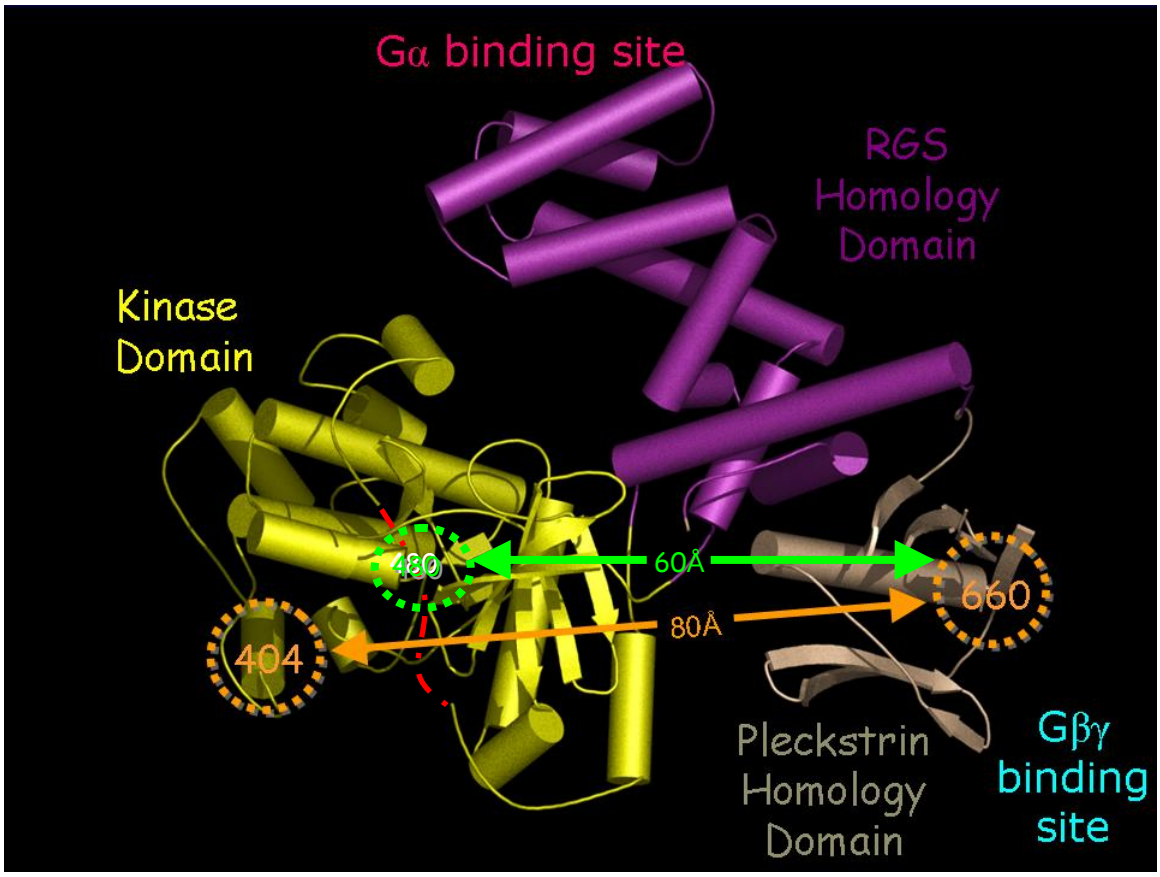

Figure 31. Protease sensitive sites within GRK2. Sites sensitive to proteolysis by clostripain are circled in orange. The disordered nucleotide gate region containing the Endo-Asp-N (Asp^{480}) site is shown in red. This site (circled in green) is partially protected by Gβγ binding although it is located ~60 Å from the Gβγ binding site. The clostripain sensitive site located at Arg^{404} is ~80Å away from the Gβγ binding site that protects it. The fact that protease sensitive sites distant to the Gβγ binding site can be protected by Gβγ suggests structural rearrangement upon binding Gβγ is occurring.

proteolysis by Gβγ and resides within a region known to be implicated in the activation of other kinases suggesting that the binding of Gβγ and interactions with the plasma membrane are able to influence the structure of the GRK2 kinase active site.

Sedimentation Equilibrium Analysis

To eliminate the possibility that the protease protection seen at residues 404 and 480 was due to the recruitment of GRK2 to a large detergent micelle similar to that seen in the NMR structure of E1F4E (Matsuo, Li et al. 1997; McGuire, Matsuo et al. 1998), a series of sedimentation equilibrium analysis experiments was performed upon GRK2, Gβγ and the GRK2·Gβγ complex in the presence of 10 mM CHAPS. Analysis was kindly performed by Dr. Rodolpho Ghirlando at NIH-NIDDK. In these experiments, the buoyant densities of each protein were calculated from equilibrium sedimentation runs done at various rotor speeds, and these buoyant densities were fitted to a formula to determine the molecular weight. Buoyant densities that were greater than the sum of the density of the individual components were assumed to be due to CHAPS detergent micelles. Results from the three experiments suggest that GRK2 on its own does not recruit CHAPS detergent. The geranylgeranylated Gβγ on the other hand was found to bind 24 ± 7 CHAPS detergent molecules. The GRK2·Gβγ complex is found to be associated with 35 ± 22 CHAPS detergent molecules. This amount of CHAPS is consistent with the amount found to be associated with Gβγ alone, and even a micelle containing 50 CHAPS molecules would not be able to span the distance between the geranylgeranyl group located on Gβγ and the clostripain and Endo-Asp-N sites within the kinase domain. This abrogates the possibility of an enormous detergent micelle

associated with the entire membrane proximal face of GRK2 being responsible for the protection seen upon binding Gβγ.

Implications of the GRK2 soluble structure

The high level of structural similarity between the GRK2·Gβγ and that of the GRK2 soluble structure suggests that the domains arrangement of GRK2 when found in the cytosol is quite similar to the arrangement seen upon binding Gβγ. This can further be extended to other GRK family members as a recently solved structure of GRK6 also has the same relative orientations for both its kinase and RH domains. This structure of GRK6 has nucleotide bound but the kinase domain is open to the same extent as in the GRK2 structures (Lodowski, unpublished data). So it is probable that some event such as the binding of both nucleotide and substrate is necessary to initiate the closure of the kinase domain, making it fully active and competent to phosphorylate substrate.

Now that the structure of GRK2 has in effect been solved five times (once in the complex structure and once for each monomer in the soluble structure), it is possible to make an informed assumption as to the flexibility of various regions within GRK2. When the differences in the structures of each of the GRK2 structures are combined with the proteolysis data, it becomes obvious that GRK2 must undergo structural changes within the kinase domain not captured in any of the GRK2 structures. These changes in the dynamic structure of GRK2 upon binding Gβγ could have implications in the regulation of the kinase activity of GRK2. The rotation of the RH domain seen in the structures suggests that the bundle subdomain is a mobile region which could be utilized for the control of GRK2 activity.

DISCUSSION AND CONCLUSIONS

Summary

A number of studies summarized within the introductory section indicate the importance of GRKs in the context of GPCR signaling. The GRKs represent a widespread mechanism allowing for the many levels of regulation of GPCR mediated signaling. The GRKs are necessary so that the signaling state within the cell can accurately reflect that of the environment outside of the cell. GRK2, the most widely studied member of the GRK family is fairly well characterized in terms of biochemistry. GRK2 contains a RH domain, a protein kinase domain and a PH domain, the interactions that these domains made with one another was largely unknown. The only structural data available was the NMR structure of the PH domain of GRK2 and the structures of homologs of various AGC kinase domains and RGS homology domains. The structural studies presented in this thesis reveal the structure of GRK2, its interactions with Gβγ, mechanisms by which the activity of GRK2 can be regulated by both proteins and phospholipids and mechanisms by which GRK2 acts to desensitize GPCR regulated signaling.

Roles of the RH domain in regulating kinase activity

The RH domain makes two contacts with the kinase domain of GRK2. The interactions of the terminal subdomain with small lobe of the kinase domain comprise a region that could be utilized to allosterically regulate kinase activity through these interactions. The α11 helix is positioned to interact with the plasma membrane and the membrane proximal residues are positively charged to interact with the anionic

headgroups of phospholipids. The α11 helix is intimately associated with the α10 helix which appears to function as an axle for the movment of the entire RH domain. The synergistic activation of GRK2 by both Gβγ and phospholipids suggests that in addition to recruiting GRK2 to the plasma membrane, the interactions with Gβγ and phospholipids are effecting changes in activity of the kinase domain that appear to be allosteric in nature. The charged residues on the α11 helix of the RH domain provide a mechanism by which proximity to the cell membrane can be detected by GRK2 and activation can occur.

The bundle subdomain also makes contact with the kinase domain. The interactions that the bundle subdomain makes with the large lobe of the kinase domain are capable of restricting the relative orientation of the two lobes of the kinase domain. That this region is flexible further supports that the interactions that the RH domain makes with the large lobe of the kinase domain may be responsible for regulating its activity. The RH domain could serve to cement the kinase domain in an open conformation (inactive) until it is released through some allosteric event much like the regulation of c-Src is modulated by interactions of its SH3 domain with that of the large lobe of its kinase domain (Xu, Doshi et al. 1999). The 5-7 º rotation of the RH domain that was seen in the five GRK2 structures would be capable of moving the bundle subdomain laterally away from the large lobe, freeing it to assume an alternate more active orientation.

The activation of GRK2 by Gβγ and the cell membrane

Structural changes upon binding Gβγ also serve to regulate the activity of GRK2. Prior to our protease protection assays and the determination of these five GRK2

structures, it was assumed that the interactions with Gβγ or simple recruitment to the membrane were responsible for the activation of GRK2 upon association with Gβγ (Pitcher, Inglese et al. 1992). The mechanism behind the ~six-fold synergistic activation of GRK2 by binding both Gβγ and anionic phospholipids was also not fully characterized (Pitcher, Touhara et al. 1995). The structure of the GRK2·Gβγ complex revealed that Gβγ also serves to orient GRK2 so that it may interact with the membrane as well as with GPCRs and Gα subunits. Although these processes are at work, the protease protection data suggests that some allosteric events occur upon association with the membrane by GRK2. When GRK2 is recruited to the plasma membrane by Gβγ it is recruited into an environment similar to that when it is bound to Gβγ and CHAPS detergent micelles. A similar role for the membrane to which Gβγ recruits GRK2 can easily be imagined, that upon binding to wild type (geranylgeranylated) Gβγ, GRK2 would be in the immediate vicinity of the plasma membrane which could then induce structural change within the kinase domain of GRK2, leading to an increase in the phosphorylation of activated GPCRs.

It is difficult to argue that it is just binding to Gβγ which is responsible for the structural changes within GRK2. Gel filtration studies of a complex between GRK2 and a soluble mutant of Gβγ have a lower apparent molecular weight than that of complexes prepared with wild type (geranylgeranylated) Gβγ. This indicates that the interactions between GRK2 and Gβγ are of a lower affinity and binding of Gβγ to GRK2 is partially mediated through the geranylgeranyl moiety attached to the Gβγ. Because the full amount of protease protection is only seen in the presence of wild type (geranylgeranylated) Gβγ, it is most likely that it is not just the Gβγ but also the geranylgeranyl group and its associated CHAPS detergent micelles which induce dynamic changes within the kinase domain GRK2 upon association with Gβγ (Fig. 31).

Furthermore, the membrane proximal surface of GRK2 is highly charged and these charged groups could be utilized by GRK2 to sense the proximity of the plasma membrane through interactions with phospholipid headgroups upon being recruited and oriented to the plasma membrane by Gβγ. Finally, the Endo-Asp-N sensitive site is partially protected in the presence of CHAPS which could conceivably interact with the charged groups on the membrane proximal surface of GRK2.

To extend the activation of GRK2 by Gβγ subunits in detergent micelles to the activation of GRK2 within the cell, the CHAPS detergent micelles although zwitterionic, make a detergent micelle that has anionic character much like that of the plasma membrane. CHAPS is a detergent which is a sulfobetaine derivative of cholic acid. When CHAPS detergent forms a micelle, a negatively charged sulfate bound to a carbon is most exposed to solvent. Upon recruitment to the plasma membrane by Gβγ, GRK2 is oriented such that it can interact with both activated GPCRs and membrane phospholipids. These interactions serve to fully activate GRK2 to quickly desensitize activated GPCRs at the cell membrane. By virtue of its triangular arrangement of binding sites and simultaneous binding of Gα, Gβγ and GPCRs (Fig. 23), GRK2 can very effectively attenuate GPCR signaling.

Possible routes for allosteric regulation of GRK activity

The core RH and kinase domains provide a framework for the allosteric regulation of the activity of GRK2. These include the allosteric activation of GRK2 through the interactions the PH domain makes with both Gβγ and phospholipids. A second possible route for the allosteric activation of GRK2 is mediated by interactions of proteins with the RH domain.

The interactions that Gβγ and phospholipids make with the PH domain are a promising mechanism for the allosteric regulation of GRK activity. When taken with the changes in structure upon binding Gβγ revealed by limited proteolytic digests and the biochemical evidence for synergistic activation of GRK2, the structural differences within GRK2 seen in both the complex and soluble structures suggest that the mobility of the RH domain provides a mechanism by which the kinase domain of GRK2 can be regulated. The interactions that the α10 helix makes with both the kinase domain and the terminal subdomain are extensive and upon a rotation of the RH domain due to the binding of both Gβγ and phospholipid, could act upon the hinge region of the kinase domain to modulate its activity.

The RH and kinase domain form a conserved core for all GRK family members. This core comprises a catalytic (protein kinase domain) and regulatory region (RH domain). The family of RGS proteins modulates levels of active signaling proteins. Their role in the GRK family members is no different, the binding of ligands such as Ca^{2+}/calmodulin (residues 20-39) and caveolin (residues 63-71) to regions within the terminal subdomain have been shown to inhibit GRK activity (Fig. 32) (Chuang, Paolucci et al. 1996; Carman, Lisanti et al. 1999). The regulation of kinase activity by Ca^{2+}/calmodulin can be explained by the position of its binding site; when GRKs are bound to Ca^{2+}/calmodulin, the calmodulin is sandwiched between the RH domain and membrane and this forcess the kinase domain away from the membrane and activated GPCRs. This agrees with the experimental results that Ca^{2+}/calmodulin can affect the levels of GRK5 at the plasma membrane (Chuang, Paolucci et al. 1996). Furthermore, when Ca^{2+}/calmodulin (or recoverin) binds to the RH domain of a GRK, this could manipulate the orientation of the terminal subdomain. This change in the orientation of the terminal subdomain could then be propagated to the kinase domain through the

contacts that the terminal subdomain makes with the small lobe. This mechanism could be shared among all members of the GRK family as the residues within the interface between the kinase and terminal subdomains are partially conserved among all GRK family members (Fig. 14A) and calmodulin or recoverin have been shown to regulate the activities of all GRK family members through their interactions with the terminal subdomain (Chuang, Paolucci et al. 1996).

Impact of the GRK2 structures

The determination of the structures of the GRK2·Gβγ complex and the GRK2 alone, has heightened the understanding of the processes of the desensitization of activated GPCRs. The GRK2·Gβγ complex structure corroborated biochemical evidence for the location of the Gβγ binding site and suggested that one function of Gβγ is to recruit the kinase to the site of active GPCRs, orient the kinase such that it can interact with and phosphorylate activated GPCRs tagging them for inactivation by arrestin. When GRK2 is in this orientation it is also capable of binding up a $G\alpha_q$ subunit in addition to the Gβγ subunit to which it is already bound, further attenuating the duration of the GPCR mediated signal.

The second structure of GRK2 (the soluble structure) and the protease protection and sedimentation equilibrium analysis answered several key questions raised by the complex structure. The flexibility seen in the five GRK2 structures reveals a possible mechanism by which GRK2 (and other GRK family members) may be regulated. The protease protection of GRK2 by wild type Gβγ corroborates data that both Gβγ and negatively charged phospholipid are a requirement for full activity of GRK2. This

reveals that it is the membrane to which GRK2 is recruited by Gβγ which is at least partially responsible for the activation of GRK2.

In conclusion, the structures of GRK2 which are presented in this thesis have elucidated many facets in the process of desensitization of GPCRs and in the function and activity of the GRK family of proteins. However many structural questions about GRK2 and other GRK family members still exist. A structure of any GRK family member bound to substrate and nucleotide in a closed, active conformation would demonstrate changes in the RH-kinase core upon full activation. A structure of GRK2 in complex with $G\alpha_q$ would also help to reveal the role that the RH domain plays in both the activation of the kinase and in the desensitization of the GPCR mediated signal. Mutational analysis of the charged residues that interact with the plasma membrane could further elucidate the mechanism of activation of GRK2 upon binding Gβγ and anionic phospholipids. Finally, the structure of a G protein coupled receptor in its agonist bound (activated) state bound to a GRK family member would reveal the mechanism by which activated GPCRs can regulate GRK activity and possibly the mechanism by which GRKs specifically recognize activated GPCRs.

Figure 32. Allosteric regulation of GRK2. All figures are as viewed from the plasma membrane. Sites within the RH domain of GRK2 which are implicated in the binding of Ca^{2+}/calmodulin and $G\alpha_q$ are colored in cyan (Chuang, Paolucci et al. 1996; Sterne-Marr, Tesmer et al. 2003). The α10 helix which might provide an axle upon which the RH domain can rotate, manipulating the interface with the kinase domain and regulating the activity of GRK2 is colored red. The RH, kinase and PH domains are colored in magenta, yellow and tan respectively. A. Binding sites for Ca^{2+}/calmodulin and $G\alpha_q$ are situated located at two distinct binding sites within the RH domain. Upon binding Ca^{2+}/calmodulin, the terminal subdomain can undergo a spatial or conformational change that can be passed on to the kinase domain through its interface with the small lobe of the kinase domain. Upon binding $G\alpha_q$, interactions that the bundle subdomain makes with the large lobe of the kinase domain can be utilized to regulate its activity (E^{96} and K^{465} denoted in green). The phospholipid binding site is partially disordered in both structures. The binding of calmodulin to the amino-terminus (residues 26-37) (Chuang, Paolucci et al. 1996; Krasel, Dammeier et al. 2001) could force the kinase domain away from the plasma membrane, prohibiting its interactions with activated GPCRs. B. Molecular surface representation of A. showing the calmodulin and $G\alpha_q$ distinct binding surfaces within the GRK2 RH domain. C. Gβγ bound to GRK2 site in same orientation as in A. Interactions with Gβγ could be transmitted through the PH domain to the terminal subdomain and from there to the hinge region of the kinase domain.

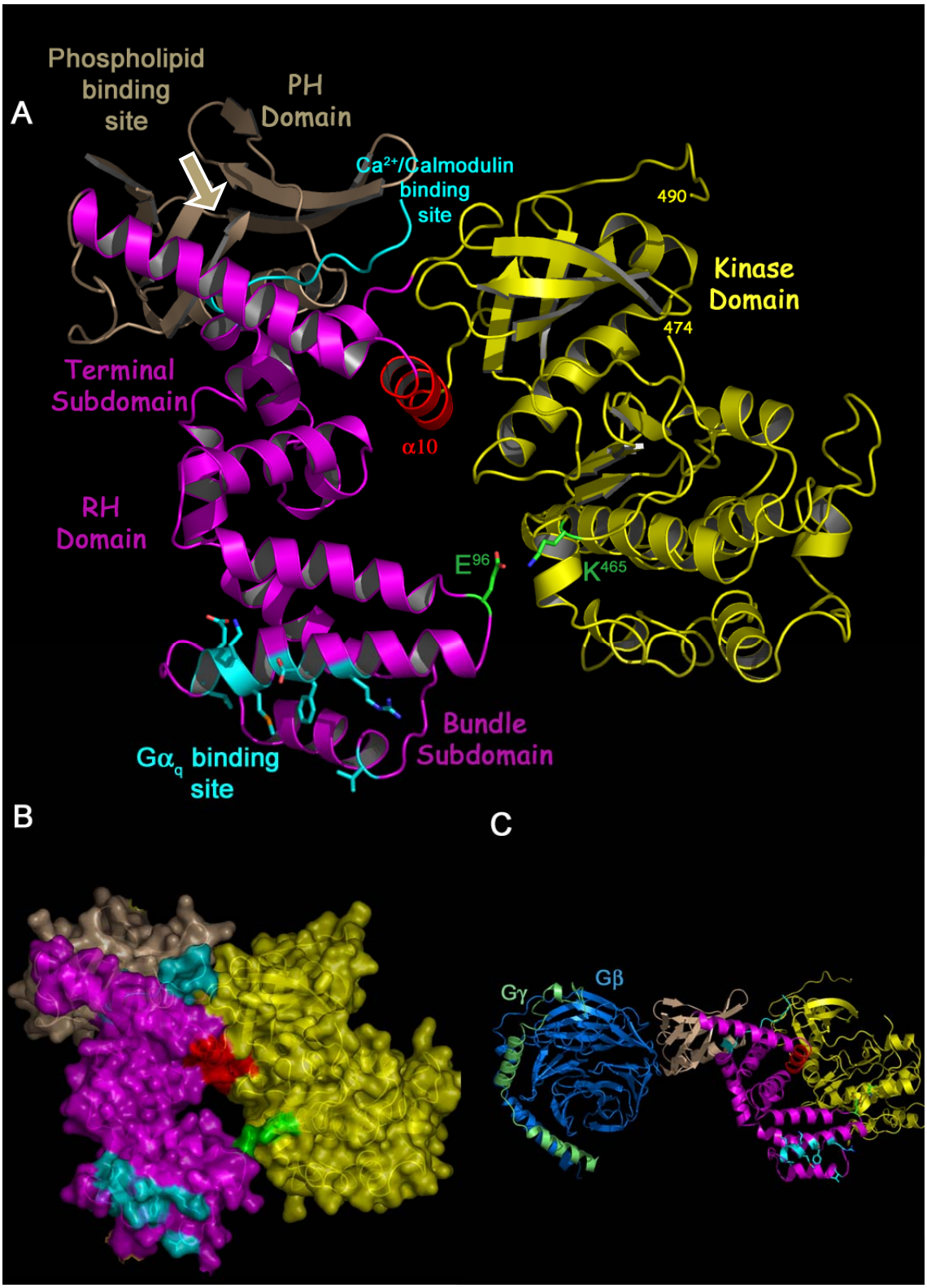
A
Phospholipid binding site
PH Domain
Ca2+/Calmodulin binding site
490
Kinase Domain
474
Terminal Subdomain
α10
RH Domain
E96
K465
Bundle Subdomain
Gαq binding site
B
C
Gγ
Gβ

Appendix: A Brief History of GPCR signaling

In 1950, Earl Sutherland and Carl Cori demonstrated that the addition of epinephrine to slices of rabbit liver had the ability to activate liver phosphorylase activity threefold (Sutherland and Cori 1951). This was the first time that phosphorylation activity was observed in response to an extracellular stimulus. Later, Sutherland was able to show that this activation of phosphorylase was due to a heat stable factor (Rall, Sutherland et al. 1957) which was later demonstrated to be 3'-5'-cyclic adenosine monophosphate (cAMP). Furthermore, he and his colleagues showed that an enzyme (adenylyl cyclase) was responsible for the formation of the cAMP and that glucagon and epinephrine had the ability to regulate cAMP production. (Klainer, Chi et al. 1962; Murad, Chi et al. 1962; Rall, Sutherland et al. 1962; Sutherland, Rall et al. 1962). He termed epinephrine and glucagon "first messengers" and the cAMP a "second messenger," terms that are still used today to describe the initiation and propagation stages in GPCR signaling.

In the late 1970's Alfred Gilman demonstrated that a GTP dependant protein was necessary for this activation of adenylyl cyclase. An attempt to restore adenylyl cyclase activity in a cell line that was thought to be deficient in AC by adding a detergent extract of membrane proteins led to the fortuitous discovery of heterotrimeric Gα subunits. It was thought that the adenylyl cyclase present in the membrane extract would reinsert into the membranes of the deficient cells thus rescuing AC activity upon stimulation with epinephrine. A control experiment in which the AC within this extract had been inactivated showed AC activation upon treatment with epinephrine, leading to the discovery that another protein that was present in the extract was in fact responsible for this activation. This protein extract was found to bind both guanosine triphosphate (GTP)

and non-hydrolysable analogs of GTP and upon its binding GTP, was able to stimulate adenylyl cyclase activity (Sternweis, Northup et al. 1981; Manning and Gilman 1983; Northup, Smigel et al. 1983; Northup, Sternweis et al. 1983). Because the binding of GTP activated the protein and that this protein stimulated AC activity this protein extract was termed N_s. Other researchers found homologous proteins which inhibited AC that were termed N_i.

Further analysis of these detergent extracts identified a complex of two proteins, which would later be termed heterotrimeric Gβ and Gα subunits, were in fact the proteins responsible for the activation of AC (Northup, Smigel et al. 1983; Northup, Sternweis et al. 1983). Later studies revealed the presence of the Gγ subunits within what was thought to be a "dimer" of Gα and Gβ. When SDS-PAGE was performed upon preparations of the two subunits, a third protein band was visible within the dye front. Further analysis revealed that this protein component had an apparent molecular weight of ~5,000 Da and was exclusively associated with the Gβ subunit (Hildebrandt, Codina et al. 1984). A similar βγ heterodimer was observed in the visual system complexed with transducin. Transducin would later be identified as being a Gα subunit as well (Fung 1983).

The first G protein coupled receptor to be sequenced and fully characterized was bovine rhodopsin (Nathans and Hogness 1983). However, it was not until the β2-adrenergic receptor (β_2AR) was sequenced, cloned and characterized that rhodopsin was a GPCR. The characterization of the β_2AR was integral to the understanding of the role GPCRs play in signal transduction. The characterization of β_2AR clarified the transmission of an agonist derived signal from GPCR, onto the heterotrimeric G proteins and then onto adenylyl cyclase (Kobilka, Dixon et al. 1987; Strader, Dixon et al. 1987). An *in vitro* complex containing purified β-Adrenergic receptor (βAR), N_s (Gαβγ heterotrimer), and adenylyl cyclase demonstrated the requirement for the heterotrimeric

G protein subunits in the activation of AC. This experiment demonstrated that both Gα and GTP were necessary for the cyclase activity of AC upon stimulation of βAR by isoprotenerol (agonist) (Cerione, Sibley et al. 1984).

REFERENCES

Barr, A. J., H. Ali, et al. (2000). "Identification of a region at the N-terminus of phospholipase C-beta 3 that interacts with G protein beta gamma subunits." Biochemistry **39**(7): 1800-6.

Benovic, J. L., A. DeBlasi, et al. (1989). "Beta-adrenergic receptor kinase: primary structure delineates a multigene family." Science **246**(4927): 235-40.

Benovic, J. L., F. Mayor, Jr., et al. (1986). "Light-dependent phosphorylation of rhodopsin by beta-adrenergic receptor kinase." Nature **321**(6073): 869-72.

Benovic, J. L., J. Onorato, et al. (1990). "Synthetic peptides of the hamster beta 2-adrenoceptor as substrates and inhibitors of the beta-adrenoceptor kinase." Br J Clin Pharmacol **30 Suppl 1**: 3S-12S.

Benovic, J. L., R. H. Strasser, et al. (1986). "Beta-adrenergic receptor kinase: identification of a novel protein kinase that phosphorylates the agonist-occupied form of the receptor." Proc Natl Acad Sci U S A **83**(9): 2797-801.

Berman, D. M., T. Kozasa, et al. (1996). "The GTPase-activating protein RGS4 stabilizes the transition state for nucleotide hydrolysis." J Biol Chem **271**(44): 27209-12.

Berman, D. M., T. M. Wilkie, et al. (1996). "GAIP and RGS4 are GTPase-activating proteins for the Gi subfamily of G protein alpha subunits." Cell **86**(3): 445-52.

Berstein, G., J. L. Blank, et al. (1992). "Phospholipase C-Beta-1 Is a Gtpase-Activating Protein for Gq/11, Its Physiological Regulator." Cell **70**(3): 411-418.

Biondi, R. M., D. Komander, et al. (2002). "High resolution crystal structure of the human PDK1 catalytic domain defines the regulatory phosphopeptide docking site." EMBO J. **21**(16): 4219-4228.

Bownds, D. and A. E. Brodie (1975). "Light-sensitive swelling of isolated frog rod outer segments as an in vitro assay for visual transduction and dark adaptation." J Gen Physiol **66**(4): 407-25.

Braganza, V. J. and W. H. Simmons (1991). "Tryptase from rat skin: purification and properties." Biochemistry **30**(20): 4997-5007.

Bromann, P. A., E. E. Boetticher, et al. (1997). "A single amino acid substitution in the pleckstrin homology domain of phospholipase C delta1 enhances the rate of substrate hydrolysis." J Biol Chem **272**(26): 16240-6.

Brown, N. G., C. Fowles, et al. (1992). "Mechanistic studies on rhodopsin kinase. Light-dependent phosphorylation of C-terminal peptides of rhodopsin." Eur J Biochem **208**(3): 659-67.

Brunger, A. T., P. D. Adams, et al. (1998). "Crystallography & NMR system: A new software suite for macromolecular structure determination." Acta Crystallogr D Biol Crystallogr **54 (Pt 5)**: 905-21.

Carman, C. V., L. S. Barak, et al. (2000). "Mutational analysis of Gbetagamma and phospholipid interaction with G protein-coupled receptor kinase 2." J Biol Chem **275**(14): 10443-52.

Carman, C. V., M. P. Lisanti, et al. (1999). "Regulation of G protein-coupled receptor kinases by caveolin." J Biol Chem **274**(13): 8858-64.

Carman, C. V., M. P. Lisanti, et al. (1999). "Regulation of G Protein-coupled Receptor Kinases by Caveolin." J. Biol. Chem. **274**(13): 8858-8864.
Carman, C. V., J.-L. Parent, et al. (1999). "Selective Regulation of Galpha q/11 by an RGS Domain in the G Protein-coupled Receptor Kinase, GRK2." J. Biol. Chem. **274**(48): 34483-34492.
CCP4 (1994). "The CCP4 suite: programs for protein crystallography." Acta Crystallographica Section D **50**(5): 760-763.
Cenni, V., H. Doppler, et al. (2002). "Regulation of novel protein kinase C epsilon by phosphorylation." Biochem J **363**(Pt 3): 537-45.
Cerione, R., D. Sibley, et al. (1984). "Reconstitution of a hormone-sensitive adenylate cyclase system. The pure beta-adrenergic receptor and guanine nucleotide regulatory protein confer hormone responsiveness on the resolved catalytic unit." J. Biol. Chem. **259**(16): 9979-9982.
Chambers, J. L. and R. M. Stroud (1979). "The accuracy of refined protein structures: comparison of two independently refined models of bovine trypsin." Acta Crystallographica Section B **35**(8): 1861-1874.
Chen, C., S. Dion, et al. (1993). "Beta-adrenergic receptor kinase. Agonist-dependent receptor binding promotes kinase activation." J. Biol. Chem. **268**(11): 7825-7831.
Chen, C. K., K. Zhang, et al. (2001). "Characterization of human GRK7 as a potential cone opsin kinase." Mol Vis **7**: 305-13.
Chen, Z., C. D. Wells, et al. (2001). "Structure of the rgRGS domain of p115RhoGEF." Nat Struct Biol **8**(9): 805-9.
Chuang, T. T., L. Paolucci, et al. (1996). "Inhibition of G protein-coupled receptor kinase subtypes by Ca2+/calmodulin." J Biol Chem **271**(45): 28691-6.
Claing, A., S. A. Laporte, et al. (2002). "Endocytosis of G protein-coupled receptors: roles of G protein-coupled receptor kinases and [ss]-arrestin proteins." Progress in Neurobiology **66**(2): 61-79.
Cong, M., S. J. Perry, et al. (2001). "Regulation of membrane targeting of the G protein-coupled receptor kinase 2 by protein kinase A and its anchoring protein AKAP79." J Biol Chem **276**(18): 15192-9.
Cruickshank, D. (1956). "The analysis of the anisotropic thermal motion of molecules in crystals." Acta Crystallographica **9**(9): 754-756.
Cruickshank, D. (1999). "Remarks about protein structure precision." Acta Crystallographica Section D **55**(3): 583-601.
Day, P. W., C. V. Carman, et al. (2003). "Differential interaction of GRK2 with members of the G alpha q family." Biochemistry **42**(30): 9176-84.
DebBurman, S. K., J. Ptasienski, et al. (1996). "G protein-coupled receptor kinase GRK2 is a phospholipid-dependent enzyme that can be conditionally activated by G protein betagamma subunits." J Biol Chem **271**(37): 22552-62.
DebBurman, S. K., J. Ptasienski, et al. (1995). "Lipid-mediated regulation of G protein-coupled receptor kinases 2 and 3." J Biol Chem **270**(11): 5742-7.
DeLano, W. L. (2002). The Pymol Molecular Graphics System. San Carlos, CA, USA, DeLano Scientific.

Dhami, G. K., L. B. Dale, et al. (2004). "G Protein-coupled receptor kinase 2 regulator of G protein signaling homology domain binds to both metabotropic glutamate receptor 1a and Galphaq to attenuate signaling." J Biol Chem **279**(16): 16614-20.
Eckhart, A. D., T. Ozaki, et al. (2002). "Vascular-targeted overexpression of G protein-coupled receptor kinase-2 in transgenic mice attenuates beta-adrenergic receptor signaling and increases resting blood pressure." Mol Pharmacol **61**(4): 749-58.
Elorza, A., P. Penela, et al. (2003). "MAPK-dependent Degradation of G Protein-coupled Receptor Kinase 2." J. Biol. Chem. **278**(31): 29164-29173.
Elorza, A., S. Sarnago, et al. (2000). "Agonist-Dependent Modulation of G Protein-Coupled Receptor Kinase 2 by Mitogen-Activated Protein Kinases." Mol Pharmacol **57**(4): 778-783.
Esnouf, R. M. (1997). "An extensively modified version of MolScript that includes greatly enhanced coloring capabilities." J Mol Graph Model **15**(2): 132-4, 112-3.
Esnouf, R. M. (1999). "Further additions to MolScript version 1.4, including reading and contouring of electron-density maps." Acta Crystallogr D Biol Crystallogr **55 (Pt 4)**: 938-40.
Ferguson, K. M., J. M. Kavran, et al. (2000). "Structural basis for discrimination of 3-phosphoinositides by pleckstrin homology domains." Mol Cell **6**(2): 373-84.
Ferguson, K. M., M. A. Lemmon, et al. (1995). "Structure of the high affinity complex of inositol trisphosphate with a phospholipase C pleckstrin homology domain." Cell **83**(6): 1037-46.
Ferguson, S. S. G., W. E. Downey, III, et al. (1996). "Role of beta-Arrestin in Mediating Agonist-Promoted G Protein-Coupled Receptor Internalization." Science **271**(5247): 363-366.
Ford, C. E., N. P. Skiba, et al. (1998). "Molecular Basis for Interactions of G Protein {beta} Subunits with Effectors." Science **280**(5367): 1271-1274.
Freeman, J. L., P. Gonzalo, et al. (2002). "Beta 2-adrenergic receptor stimulated, G protein-coupled receptor kinase 2 mediated, phosphorylation of ribosomal protein P2." Biochemistry **41**(42): 12850-7.
Freeman, J. L. R., J. A. Pitcher, et al. (2000). "[alpha]-Actinin is a potent regulator of G protein-coupled receptor kinase activity and substrate specificity in vitro." FEBS Letters **473**(3): 280-284.
Fung, B. (1983). "Characterization of transducin from bovine retinal rod outer segments. I. Separation and reconstitution of the subunits." J. Biol. Chem. **258**(17): 10495-10502.
Fushman, D., T. Najmabadi-Haske, et al. (1998). "The solution structure and dynamics of the pleckstrin homology domain of G protein-coupled receptor kinase 2 (beta-adrenergic receptor kinase 1). A binding partner of Gbetagamma subunits." J Biol Chem **273**(5): 2835-43.
Gainetdinov, R. R., R. T. Premont, et al. (2004). "Desensitization of G Protein-Coupled Receptors and Neuronal Functions." Annual Review of Neuroscience **27**(1): 107-144.
Gaudet, R., A. Bohm, et al. (1996). "Crystal structure at 2.4 angstroms resolution of the complex of transducin betagamma and its regulator, phosducin." Cell **87**(3): 577-88.

Gonfloni, S., J. C. Williams, et al. (1997). "The role of the linker between the SH2 domain and catalytic domain in the regulation and function of Src." EMBO J. **16**(24): 7261-7271.
Gros, R., J. L. Benovic, et al. (1997). "G-protein-coupled receptor kinase activity is increased in hypertension." J Clin Invest **99**(9): 2087-93.
Gros, R., J. Chorazyczewski, et al. (2000). "G-Protein-coupled receptor kinase activity in hypertension : increased vascular and lymphocyte G-protein receptor kinase-2 protein expression." Hypertension **35**(1 Pt 1): 38-42.
Gros, R., C. M. Tan, et al. (1999). "G-protein-coupled receptor kinase expression in hypertension." Clin Pharmacol Ther **65**(5): 545-51.
Harding, V. B., L. R. Jones, et al. (2001). "Cardiac beta ARK1 inhibition prolongs survival and augments beta blocker therapy in a mouse model of severe heart failure." Proc Natl Acad Sci U S A **98**(10): 5809-14.
Haslam, R. J., H. B. Koide, et al. (1993). "Pleckstrin domain homology." Nature **363**(6427): 309-10.
Hepler, J. R., D. M. Berman, et al. (1997). "RGS4 and GAIP are GTPase-activating proteins for Gqalpha and block activation of phospholipase Cbeta by gamma -thio-GTP-Gqalpha." PNAS **94**(2): 428-432.
Hildebrandt, J., J. Codina, et al. (1984). "Identification of a gamma subunit associated with the adenylyl cyclase regulatory proteins Ns and Ni." J. Biol. Chem. **259**(4): 2039-2042.
Hisatomi, O., S. Matsuda, et al. (1998). "A novel subtype of G-protein-coupled receptor kinase, GRK7, in teleost cone photoreceptors." FEBS Lett **424**(3): 159-64.
Huse, M. and J. Kuriyan (2002). "The conformational plasticity of protein kinases." Cell **109**(3): 275-82.
Iaccarino, G., J. R. Keys, et al. (2001). "Regulation of myocardial betaARK1 expression in catecholamine-induced cardiac hypertrophy in transgenic mice overexpressing alpha1B-adrenergic receptors." J Am Coll Cardiol **38**(2): 534-40.
Iaccarino, G., R. J. Lefkowitz, et al. (1999). "Myocardial G protein-coupled receptor kinases: implications for heart failure therapy." Proc Assoc Am Physicians **111**(5): 399-405.
Jaber, M., W. J. Koch, et al. (1996). "Essential role of beta-adrenergic receptor kinase 1 in cardiac development and function." Proc Natl Acad Sci U S A **93**(23): 12974-9.
James, S. R., A. Paterson, et al. (1995). "Kinetic analysis of phospholipase C beta isoforms using phospholipid-detergent mixed micelles. Evidence for interfacial catalysis involving distinct micelle binding and catalytic steps." J Biol Chem **270**(20): 11872-81.
Jancarik, J. and S.-H. Kim (1991). "Sparse matrix sampling: a screening method for crystallization of proteins." Journal of Applied Crystallography **24**(4): 409-411.
Jones, T. A., J.-Y. Zou, et al. (1991). "Improved methods for building protein models in electron density maps and the location of errors in these models." Acta Crystallographica Section A **47**(2): 110-119.
Kaplan, W. and T. G. Littlejohn (2001). "Swiss-PDB Viewer (Deep View)." Brief Bioinform **2**(2): 195-7.

Kemp, B. E., D. B. Bylund, et al. (1975). "Substrate specificity of the cyclic AMP-dependent protein kinase." Proc Natl Acad Sci U S A **72**(9): 3448-52.
Klainer, L. M., Y.-M. Chi, et al. (1962). "Adenyl Cyclase. IV. THE EFFECTS OF NEUROHORMONES ON THE FORMATION OF ADENOSINE 3',5'-PHOSPHATE BY PREPARATIONS FROM BRAIN AND OTHER TISSUES." J. Biol. Chem. **237**(4): 1239-1243.
Knighton, D. R., J. H. Zheng, et al. (1991). "Structure of a peptide inhibitor bound to the catalytic subunit of cyclic adenosine monophosphate-dependent protein kinase." Science **253**(5018): 414-20.
Kobilka, B. K., R. A. Dixon, et al. (1987). "cDNA for the human beta 2-adrenergic receptor: a protein with multiple membrane-spanning domains and encoded by a gene whose chromosomal location is shared with that of the receptor for platelet-derived growth factor." Proc Natl Acad Sci U S A **84**(1): 46-50.
Koch, W. J., J. Inglese, et al. (1993). "The binding site for the beta gamma subunits of heterotrimeric G proteins on the beta-adrenergic receptor kinase." J Biol Chem **268**(11): 8256-60.
Koch, W. J., H. A. Rockman, et al. (1995). "Cardiac function in mice overexpressing the beta-adrenergic receptor kinase or a beta ARK inhibitor." Science **268**(5215): 1350-3.
Koelle, M. R. (1997). "A new family of G-protein regulators - The RGS proteins." Current Opinion in Cell Biology **9**(2): 143-147.
Kozasa, T. (1999). Purification of Recombinant G protein alpha and beta gamma Subunits from Sf9 Cells. G proteins Techniques of Analysis. D. R. Manning. Boca Raton, FL, CRC Press**:** 22-38.
Krasel, C., S. Dammeier, et al. (2001). "Phosphorylation of GRK2 by Protein Kinase C Abolishes Its Inhibition by Calmodulin." J. Biol. Chem. **276**(3): 1911-1915.
Krebs, W. G. and M. Gerstein (2000). "SURVEY AND SUMMARY: The morph server: a standardized system for analyzing and visualizing macromolecular motions in a database framework." Nucl. Acids Res. **28**(8): 1665-1675.
Krupnick, J. G. and J. L. Benovic (1998). "THE ROLE OF RECEPTOR KINASES AND ARRESTINS IN G PROTEIN-COUPLED RECEPTOR REGULATION." Annual Review of Pharmacology and Toxicology **38**(1): 289-319.
Kuhn, H., J. H. Cook, et al. (1973). "Phosphorylation of rhodopsin in bovine photoreceptor membranes. A dark reaction after illumination." Biochemistry **12**(13): 2495-502.
Kuhn, H. and U. Wilden (1982). "Assay of phosphorylation of rhodopsin in vitro and in vivo." Methods Enzymol **81**: 489-96.
LaFevre-Bernt, M., F. Sicheri, et al. (1998). "Intramolecular Regulatory Interactions in the Src Family Kinase Hck Probed by Mutagenesis of a Conserved Tryptophan Residue." J. Biol. Chem. **273**(48): 32129-32134.
Lambright, D. G., J. Sondek, et al. (1996). "The 2.0 A crystal structure of a heterotrimeric G protein." Nature **379**(6563): 311-9.
Lander, E. S., L. M. Linton, et al. (2001). "Initial sequencing and analysis of the human genome." Nature **409**(6822): 860-921.

Langhans-Rajasekaran, S., Y. Wan, et al. (1995). "Activation of Tsk and Btk Tyrosine Kinases by G Protein {beta}{gamma} Subunits." PNAS **92**(19): 8601-8605.
Le Good, J. A., W. H. Ziegler, et al. (1998). "Protein Kinase C Isotypes Controlled by Phosphoinositide 3-Kinase Through the Protein Kinase PDK1." Science **281**(5385): 2042-2045.
Lemmon, M. A. and K. M. Ferguson (2001). "Molecular determinants in pleckstrin homology domains that allow specific recognition of phosphoinositides." Biochem Soc Trans **29**(Pt 4): 377-84.
Levay, K., D. K. Satpaev, et al. (1998). "Localization of the sites for Ca2+-binding proteins on G protein-coupled receptor kinases." Biochemistry **37**(39): 13650-9.
Li, Y., P. M. Sternweis, et al. (1998). "Sites for Galpha Binding on the G Protein beta Subunit Overlap with Sites for Regulation of Phospholipase Cbeta and Adenylyl Cyclase." J. Biol. Chem. **273**(26): 16265-16272.
Linder, M. E., I. H. Pang, et al. (1991). "Lipid modifications of G protein subunits. Myristoylation of Go alpha increases its affinity for beta gamma." J Biol Chem **266**(7): 4654-9.
Lodowski, D. T., J. A. Pitcher, et al. (2003). "Keeping G Proteins at Bay: A Complex Between G Protein-Coupled Receptor Kinase 2 and G{beta}{gamma}." Science **300**(5623): 1256-1262.
Loew, A., Y. K. Ho, et al. (1998). "Phosducin induces a structural change in transducin beta gamma." Structure **6**(8): 1007-19.
Longenecker, K. L., M. E. Lewis, et al. (2001). "Structure of the RGS-like Domain from PDZ-RhoGEF: Linking Heterotrimeric G Protein-Coupled Signaling to Rho GTPases." Structure **9**(7): 559-569.
Madhusudan, P. Akamine, et al. (2002). "Crystal structure of a transition state mimic of the catalytic subunit of cAMP-dependent protein kinase." Nat Struct Biol **9**(4): 273-7.
Mahadevan, D., N. Thanki, et al. (1995). "Structural studies on the PH domains of Db1, Sos1, IRS-1, and beta ARK1 and their differential binding to G beta gamma subunits." Biochemistry **34**(28): 9111-7.
Maiti, R., G. H. Van Domselaar, et al. (2004). "SuperPose: a simple server for sophisticated structural superposition." Nucleic Acids Res **32**(Web Server issue): W590-4.
Manning, D. and A. Gilman (1983). "The regulatory components of adenylate cyclase and transducin. A family of structurally homologous guanine nucleotide-binding proteins." J. Biol. Chem. **258**(11): 7059-7063.
Matsuo, H., H. Li, et al. (1997). "Structure of translation factor eIF4E bound to m7GDP and interaction with 4E-binding protein." Nat Struct Biol **4**(9): 717-24.
Matthews, B. W. (1968). "Solvent content of protein crystals." J Mol Biol **33**(2): 491-7.
Mayer, B. J., R. Ren, et al. (1993). "A putative modular domain present in diverse signaling proteins." Cell **73**(4): 629-30.
McGuire, A. M., H. Matsuo, et al. (1998). "Internal and overall motions of the translation factor eIF4E: cap binding and insertion in a CHAPS detergent micelle." J Biomol NMR **12**(1): 73-88.

Merritt, E. A. (1994). "Raster3D Version 2.0. A program for photorealistic molecular graphics." Acta Crystallogr D Biol Crystallogr **50**(Pt 6): 869-73.
Miller, J. A. and R. Paulsen (1975). "Phosphorylation and dephosphorylation of frog rod outer segment membranes as part of the visual process." J Biol Chem **250**(12): 4427-32.
Moore, G. L. (1969). "Use of azo-dye-bound collagen to measure reaction velocities of proteolytic enzymes." Anal Biochem **32**(1): 122-7.
Murad, F., Y.-M. Chi, et al. (1962). "Adenyl Cyclase. III. THE EFFECT OF CATECHOLAMINES AND CHOLINE ESTERS ON THE FORMATION OF ADENOSINE 3',5'-PHOSPHATE BY PREPARATIONS FROM CARDIAC MUSCLE AND LIVER." J. Biol. Chem. **237**(4): 1233-1238.
Narayana, N., S. Cox, et al. (1997). "A binary complex of the catalytic subunit of cAMP-dependent protein kinase and adenosine further defines conformational flexibility." Structure **5**(7): 921-35.
Narayana, N., S. Cox, et al. (1997). "Crystal structure of a polyhistidine-tagged recombinant catalytic subunit of cAMP-dependent protein kinase complexed with the peptide inhibitor PKI(5-24) and adenosine." Biochemistry **36**(15): 4438-48.
Nathans, J. and D. S. Hogness (1983). "Isolation, sequence analysis, and intron-exon arrangement of the gene encoding bovine rhodopsin." Cell **34**(3): 807-14.
Newton, A. C. (2002). "Analyzing protein kinase C activation." Methods Enzymol **345**: 499-506.
Newton, A. C. (2003). "Regulation of the ABC kinases by phosphorylation: protein kinase C as a paradigm." Biochem J **370**(Pt 2): 361-71.
Northup, J., M. Smigel, et al. (1983). "The subunits of the stimulatory regulatory component of adenylate cyclase. Resolution of the activated 45,000-dalton (alpha) subunit." J. Biol. Chem. **258**(18): 11369-11376.
Northup, J., P. Sternweis, et al. (1983). "The subunits of the stimulatory regulatory component of adenylate cyclase. Resolution, activity, and properties of the 35,000-dalton (beta) subunit." J. Biol. Chem. **258**(18): 11361-11368.
Obata, T., M. B. Yaffe, et al. (2000). "Peptide and protein library screening defines optimal substrate motifs for AKT/PKB." J Biol Chem **275**(46): 36108-15.
Ogawa, A., Y. Takayama, et al. (2002). "Structure of the carboxyl-terminal Src kinase, Csk." J Biol Chem **277**(17): 14351-4.
Okada, T., Y. Fujiyoshi, et al. (2002). "Functional role of internal water molecules in rhodopsin revealed by X-ray crystallography." Proc Natl Acad Sci U S A **99**(9): 5982-7.
Onorato, J. J., K. Palczewski, et al. (1991). "Role of acidic amino acids in peptide substrates of the beta-adrenergic receptor kinase and rhodopsin kinase." Biochemistry **30**(21): 5118-25.
Otwinowski, Z. a. M., W (1997). Processing of X-ray Diffraction Data Collected in Oscillation Mode. Methods in Enzymology. J. R. M. S. C.W. Carter. New York, Academic Press. **276:** p.307-326.
Palczewski, K., J. H. McDowell, et al. (1988). "Purification and characterization of rhodopsin kinase." J Biol Chem **263**(28): 14067-73.

Pao, C. S. and J. L. Benovic (2002). "Phosphorylation-independent desensitization of G protein-coupled receptors?" Sci STKE **2002**(153): PE42.
Penela, P., A. Elorza, et al. (2001). "Beta-arrestin- and c-Src-dependent degradation of G-protein-coupled receptor kinase 2." Embo J **20**(18): 5129-38.
Penela, P., C. Ribas, et al. (2003). "Mechanisms of regulation of the expression and function of G protein-coupled receptor kinases." Cell Signal **15**(11): 973-81.
Perry, S. J. and R. J. Lefkowitz (2002). "Arresting developments in heptahelical receptor signaling and regulation." Trends in Cell Biology **12**(3): 130-138.
Pierce, K. L., R. T. Premont, et al. (2002). "SEVEN-TRANSMEMBRANE RECEPTORS." Nature Reviews Molecular Cell Biology
Nat Rev Mol Cell Biol **3**(9): 639-650.
Pitcher, J., M. J. Lohse, et al. (1992). "Desensitization of the isolated beta 2-adrenergic receptor by beta-adrenergic receptor kinase, cAMP-dependent protein kinase, and protein kinase C occurs via distinct molecular mechanisms." Biochemistry **31**(12): 3193-7.
Pitcher, J. A., Z. L. Fredericks, et al. (1996). "Phosphatidylinositol 4,5-bisphosphate (PIP2)-enhanced G protein-coupled receptor kinase (GRK) activity. Location, structure, and regulation of the PIP2 binding site distinguishes the GRK subfamilies." J Biol Chem **271**(40): 24907-13.
Pitcher, J. A., N. J. Freedman, et al. (1998). "G PROTEIN-COUPLED RECEPTOR KINASES." Annual Review of Biochemistry **67**(1): 653-692.
Pitcher, J. A., J. Inglese, et al. (1992). "Role of beta gamma subunits of G proteins in targeting the beta-adrenergic receptor kinase to membrane-bound receptors." Science **257**(5074): 1264-7.
Pitcher, J. A., J. J. Tesmer, et al. (1999). "Feedback inhibition of G protein-coupled receptor kinase 2 (GRK2) activity by extracellular signal-regulated kinases." J Biol Chem **274**(49): 34531-4.
Pitcher, J. A., J. J. G. Tesmer, et al. (1999). "Feedback Inhibition of G Protein-coupled Receptor Kinase 2 (GRK2) Activity by Extracellular Signal-regulated Kinases." J. Biol. Chem. **274**(49): 34531-34534.
Pitcher, J. A., K. Touhara, et al. (1995). "Pleckstrin homology domain-mediated membrane association and activation of the beta-adrenergic receptor kinase requires coordinate interaction with G beta gamma subunits and lipid." J Biol Chem **270**(20): 11707-10.
Poilane, I., T. Karjalainen, et al. (1998). "Protease activity of Clostridium difficile strains." Can J Microbiol **44**(2): 157-61.
Pronin, A. N., D. K. Satpaev, et al. (1997). "Regulation of G protein-coupled receptor kinases by calmodulin and localization of the calmodulin binding domain." J Biol Chem **272**(29): 18273-80.
Pronin, A. N., D. K. Satpaev, et al. (1997). "Regulation of G Protein-coupled Receptor Kinases by Calmodulin and Localization of the Calmodulin Binding Domain." J. Biol. Chem. **272**(29): 18273-18280.
Rall, T. W., E. W. Sutherland, et al. (1957). "THE RELATIONSHIP OF EPINEPHRINE AND GLUCAGON TO LIVER PHOSPHORYLASE. IV. EFFECT OF EPINEPHRINE AND GLUCAGON ON THE REACTIVATION OF

PHOSPHORYLASE IN LIVER HOMOGENATES." J. Biol. Chem. **224**(1): 463-475.
Rall, T. W., E. W. Sutherland, et al. (1962). "Adenyl Cyclase. II. THE ENZYMATICALLY CATALYZED FORMATION OF ADENOSINE 3',5'-PHOSPHATE AND INORGANIC PYROPHOSPHATE FROM ADENOSINE TRIPHOSPHATE." J. Biol. Chem. **237**(4): 1228-1232.
Razzini, G., A. Brancaccio, et al. (2000). "The Role of the Pleckstrin Homology Domain in Membrane Targeting and Activation of Phospholipase Cbeta 1." J. Biol. Chem. **275**(20): 14873-14881.
Read, R. (1986). "Improved Fourier coefficients for maps using phases from partial structures with errors." Acta Crystallographica Section A **42**(3): 140-149.
Rebecchi, M. J. and S. Scarlata (1998). "PLECKSTRIN HOMOLOGY DOMAINS: A Common Fold with Diverse Functions." Annual Review of Biophysics and Biomolecular Structure **27**(1): 503-528.
Rockman, H. A., K. R. Chien, et al. (1998). "Expression of a beta-adrenergic receptor kinase 1 inhibitor prevents the development of myocardial failure in gene-targeted mice." Proc Natl Acad Sci U S A **95**(12): 7000-5.
Rockman, H. A., D. J. Choi, et al. (1998). "Control of myocardial contractile function by the level of beta-adrenergic receptor kinase 1 in gene-targeted mice." J Biol Chem **273**(29): 18180-4.
Rockman, H. A., W. J. Koch, et al. (2002). "Seven-transmembrane-spanning receptors and heart function." Nature **415**(6868): 206-12.
Rockman, H. A., W. J. Koch, et al. (1996). "Myocardial beta-adrenergic receptor signaling in vivo: insights from transgenic mice." J Mol Med **74**(9): 489-95.
Ross, E. M. and T. M. Wilkie (2000). "GTPASE-ACTIVATING PROTEINS FOR HETEROTRIMERIC G PROTEINS: Regulators of G Protein Signaling (RGS) and RGS-Like Proteins." Annual Review of Biochemistry **69**(1): 795-827.
Sarnago, S., A. Elorza, et al. (1999). "Agonist-dependent phosphorylation of the G protein-coupled receptor kinase 2 (GRK2) by Src tyrosine kinase." J Biol Chem **274**(48): 34411-6.
Schneider, T. (2000). "Objective comparison of protein structures: error-scaled difference distance matrices." Acta Crystallographica Section D **56**(6): 714-721.
Schneider, T. (2002). "A genetic algorithm for the identification of conformationally invariant regions in protein molecules." Acta Crystallographica Section D **58**(2): 195-208.
Schomaker, V. and K. N. Trueblood (1998). "Correlation of Internal Torsional Motion with Overall Molecular Motion in Crystals." Acta Crystallographica Section B **54**(5): 507-514.
Shi, W., S. Osawa, et al. (1995). "Rhodopsin Mutants Discriminate Sites Important for the Activation of Rhodopsin Kinase and G(t)." J. Biol. Chem. **270**(5): 2112-2119.
Shichi, H. and R. L. Somers (1978). "Light-dependent phosphorylation of rhodopsin. Purification and properties of rhodopsin kinase." J. Biol. Chem. **253**(19): 7040-7046.
Shichi, H. and R. L. Somers (1978). "Light-dependent phosphorylation of rhodopsin. Purification and properties of rhodopsin kinase." J Biol Chem **253**(19): 7040-6.

Sicheri, F. and J. Kuriyan (1997). "Structures of Src-family tyrosine kinases." Curr Opin Struct Biol **7**(6): 777-85.
Siderovski, D. P., A. Hessel, et al. (1996). "A new family of regulators of G-protein-coupled receptors?" Curr Biol **6**(2): 211-2.
Siderovski, D. P., S. P. Heximer, et al. (1994). "A Human Gene Encoding a Putative Basic Helix-Loop-Helix Phosphoprotein Whose Messenger-Rna Increases Rapidly in Cycloheximide-Treated Blood Mononuclear-Cells." DNA and Cell Biology **13**(2): 125-147.
Smith, C. M., E. Radzio-Andzelm, et al. (1999). "The catalytic subunit of cAMP-dependent protein kinase: prototype for an extended network of communication." Prog Biophys Mol Biol **71**(3-4): 313-41.
Smith, C. M., E. Radzio-Andzelm, et al. (1999). "The catalytic subunit of cAMP-dependent protein kinase: prototype for an extended network of communication." Progress in Biophysics and Molecular Biology **71**(3-4): 313-341.
Soisson, S. M., A. S. Nimnual, et al. (1998). "Crystal structure of the Dbl and pleckstrin homology domains from the human Son of sevenless protein." Cell **95**(2): 259-68.
Sondek, J., A. Bohm, et al. (1996). "Crystal structure of a G-protein beta gamma dimer at 2.1A resolution." Nature **379**(6563): 369-74.
Spink, K. E., P. Polakis, et al. (2000). "Structural basis of the Axin-adenomatous polyposis coli interaction." EMBO J. **19**(10): 2270-2279.
Stadel, J. M., P. Nambi, et al. (1983). "Catecholamine-induced desensitization of turkey erythrocyte adenylate cyclase is associated with phosphorylation of the beta-adrenergic receptor." Proc Natl Acad Sci U S A **80**(11): 3173-7.
Sterne-Marr, R., J. J. Tesmer, et al. (2003). "G protein-coupled receptor Kinase 2/G alpha q/11 interaction. A novel surface on a regulator of G protein signaling homology domain for binding G alpha subunits." J Biol Chem **278**(8): 6050-8.
Sterne-Marr, R., J. J. G. Tesmer, et al. (2003). "G Protein-coupled Receptor Kinase 2/Galpha q/11 Interaction. A NOVEL SURFACE ON A REGULATOR OF G PROTEIN SIGNALING HOMOLOGY DOMAIN FOR BINDING Galpha SUBUNITS." J. Biol. Chem. **278**(8): 6050-6058.
Sternweis, P., J. Northup, et al. (1981). "The regulatory component of adenylate cyclase. Purification and properties." J. Biol. Chem. **256**(22): 11517-11526.
Strader, C. D., R. A. Dixon, et al. (1987). "Mutations that uncouple the beta-adrenergic receptor from Gs and increase agonist affinity." J Biol Chem **262**(34): 16439-43.
Sutherland, E. W. and C. F. Cori (1951). "EFFECT OF HYPERGLYCEMIC-GLYCOGENOLYTIC FACTOR AND EPINEPHRINE ON LIVER PHOSPHORYLASE." J. Biol. Chem. **188**(2): 531-543.
Sutherland, E. W., T. W. Rall, et al. (1962). "Adenyl Cyclase. I. DISTRIBUTION, PREPARATION, AND PROPERTIES." J. Biol. Chem. **237**(4): 1220-1227.
Tanaka, T., T. Kohno, et al. (1998). "Alpha helix content of G protein alpha subunit is decreased upon activation by receptor mimetics." J Biol Chem **273**(6): 3247-52.
Tesmer, J. J., D. M. Berman, et al. (1997). "Structure of RGS4 bound to AlF4--activated G(i alpha1): stabilization of the transition state for GTP hydrolysis." Cell **89**(2): 251-61.

Tesmer, J. J., R. K. Sunahara, et al. (1997). "Crystal structure of the catalytic domains of adenylyl cyclase in a complex with Gsalpha.GTPgammaS." Science **278**(5345): 1907-16.
Thompson, P. and J. B. Findlay (1984). "Phosphorylation of ovine rhodopsin. Identification of the phosphorylated sites." Biochem J **220**(3): 773-80.
Touhara, K. (1995). "[PH domain: a new functional domain]." Nippon Yakurigaku Zasshi **106**(1): 1-9.
Touhara, K. (1997). "Binding of multiple ligands to pleckstrin homology domain regulates membrane translocation and enzyme activity of [beta]-adrenergic receptor kinase." FEBS Letters **417**(2): 243-248.
Touhara, K., B. E. Hawes, et al. (1995). "G protein beta gamma subunits stimulate phosphorylation of Shc adapter protein." Proc Natl Acad Sci U S A **92**(20): 9284-7.
Touhara, K., J. Inglese, et al. (1994). "Binding of G protein beta gamma-subunits to pleckstrin homology domains." J Biol Chem **269**(14): 10217-20.
Touhara, K., W. J. Koch, et al. (1995). "Mutational analysis of the pleckstrin homology domain of the beta-adrenergic receptor kinase. Differential effects on G beta gamma and phosphatidylinositol 4,5-bisphosphate binding." J Biol Chem **270**(28): 17000-5.
Venter, J. C., M. D. Adams, et al.
Vries, L., M. Mousli, et al. (1995). "GAIP, a Protein that Specifically Interacts with the Trimeric G Protein G{alpha}i3, is a Member of a Protein Family with a Highly Conserved Core Domain." PNAS **92**(25): 11916-11920.
Wall, M. A., D. E. Coleman, et al. (1995). "The structure of the G protein heterotrimer Gi alpha 1 beta 1 gamma 2." Cell **83**(6): 1047-58.
Weiss, E. R., D. Raman, et al. (1998). "The cloning of GRK7, a candidate cone opsin kinase, from cone- and rod-dominant mammalian retinas." Mol Vis **4**: 27.
Winn, M. D., M. N. Isupov, et al. (2001). "Use of TLS parameters to model anisotropic displacements in macromolecular refinement." Acta Crystallographica Section D **57**(1): 122-133.
Wise, A., S. C. Jupe, et al. (2004). "THE IDENTIFICATION OF LIGANDS AT ORPHAN G-PROTEIN COUPLED RECEPTORS." Annual Review of Pharmacology and Toxicology **44**(1): 43-66.
Xu, W., A. Doshi, et al. (1999). "Crystal Structures of c-Src Reveal Features of Its Autoinhibitory Mechanism." Molecular Cell **3**(5): 629-638.
Xu, W., S. C. Harrison, et al. (1997). "Three-dimensional structure of the tyrosine kinase c-Src." Nature **385**(6617): 595-602.
Yang, J., P. Cron, et al. (2002). "Crystal structure of an activated Akt/protein kinase B ternary complex with GSK3-peptide and AMP-PNP." Nat Struct Biol **9**(12): 940-4.
Yang, J., P. Cron, et al. (2002). "Molecular mechanism for the regulation of protein kinase B/Akt by hydrophobic motif phosphorylation." Mol Cell **9**(6): 1227-40.
Yang, J., P. Cron, et al. (2002). "Molecular Mechanism for the Regulation of Protein Kinase B/Akt by Hydrophobic Motif Phosphorylation." Molecular Cell **9**(6): 1227-1240.

Zetterqvist, O., U. Ragnarsson, et al. (1976). "The minimum substrate of cyclic AMP-stimulated protein kinase, as studied by synthetic peptides representing the phosphorylatable site of pyruvate kinase (type L) of rat liver." Biochem Biophys Res Commun **70**(3): 696-703.

Zhang, P., S. Talluri, et al. (1995). "Solution structure of the pleckstrin homology domain of Drosophila beta-spectrin." Structure **3**(11): 1185-95.

Zheng, J., D. R. Knighton, et al. (1993). "Crystal structures of the myristylated catalytic subunit of cAMP-dependent protein kinase reveal open and closed conformations." Protein Sci **2**(10): 1559-1573.

Zhong, H. and R. R. Neubig (2001). "Regulator of G Protein Signaling Proteins: Novel Multifunctional Drug Targets." J Pharmacol Exp Ther **297**(3): 837-845.

VITA

David Thomas Lodowski was born in Dallas, Texas on April 21, 1975, the son of Marie Chambers Lodowski and Robert Thomas Lodowski. After completing his work at Episcopal High School in Bellaire, Texas, in 1994 he entered Tulane University in New Orleans, Louisiana. He received the degree of Bachelor of Science from Tulane University in May 1998. During the following year he was employed in a glass factory producing art glass for the artist, Gene Koss. He married Kerrie Lynn Hall, April 26, 2003, and in August of 1999, he entered The Graduate School of the University of Texas at Austin as a student in the molecular biology program.

Permanent address: 6142 Ella Lee Lane, Houston, Texas 77057

This dissertation was typed by the author.